Spring 4-29-2019

Extreme Altitude Search and Rescue Helicopter

Matthew J. De Sieno
Kennesaw State University

Anthony Chavarria
Kennesaw State University

David Stuver
Kennesaw State University

Zach Boss
Kennesaw State University

Extreme Altitude Mountain Rescue Helicopter:

Final Design Review

Matthew De Sieno, Zach Boss, David Stuver & Anthony Chavarria

Kennesaw State University

Department of Industrial and Systems Engineering

Marietta, Georgia

Aerospace Senior Design

ISYE 4803

Dr. Adeel Khalid

Executive Summary

The goal of this design was to develop an extreme altitude rescue helicopter capable of retrieving hikers stranded on top of Mount Everest. Using the Eurocopter AS350 as a baseline, a conceptual model was produced that is fully capable of hovering and delivering forward flight at the desired altitude of 8,848 meters. Combined blade element momentum theory, proper airfoil selection, and forward flight calculations were utilized in order to optimize the rotor for the given flight conditions on top of Mount Everest. Conceptual fluid dynamics and CAD modeling aided in the process of visually designing the fuselage and rotor. Not only are these visual aids available, but they also produced data on how the fuselage and rotor will react to the environment around them. Other analyses were introduced in order to accurately calculate the economic feasibility, the reliability, and the efficiency of the overall system.

Table of Contents:

Executive Summary 1
Table of Contents: 2
List of Figures: 5
List of Tables 10
List of Equations 10
Chapter 1: Introduction 12

Introduction 12
System Overview 12
Objectives 13
Justification 13
Project Background 13
Problem Statement 14
Chapter 2: : Literature Review 15

Chapter 3: : Problem Solution 18

Problem Solving Approach 18
Requirements 18
UML Use Case Diagram 19
GANTT Chart 19
Mission Profile 20
Responsibilities 21
Resources Available 21
Chapter 4: Blade and Hover Performance 22

Airfoil Selection 22
Rotor Sizing 23
Blade Design 24
Disk Loading and Power Loading 25
Figure of Merit 26
Chapter 5: Performance 27

Forward Flight 27
Rate of Climb 31
Rotor Trade Studies 33
Chapter 6: Fluid Analysis 36
Flow Analysis Setup 36
Hover Simulations: 38
Cruise Simulations 41
Chapter 7: Helicopter Architecture 45
Fuselage Design 45
Engine Selection 49
Weight Calculations 51
Failure Mode & Effect Analysis 53
Hoist 54
Avionics 56
Transmission 56
Materials 58
Chapter 8: Cost Analysis 62
Chapter 9: Conclusion 64
Overall Evaluation Criteria 64
Chapter 10: References 66
Appendix A: Acknowledgements 67
Appendix B: Contact Information 68
Appendix C: Reflections 69
Appendix D: BEMT Figures 70
Blade Design One: 70
Blade Design Two 76

Blade Design Three 82

Appendix E: Airfoil Graphs 88

Appendix F: Other Graphs and Figures 93

List of Figures:

Figure 2-1. SA315B Lama helicopter [3]. 16

Figure 2-2. SA135B Lama Helicopter technical details [3]. 16

Figure 2-3. AS350B3 helicopter [4]. 17

Figure 3-1. Gantt Chart. 19

Figure 3-2. Mission Profile. 20

Figure 4-1. ONERA OA209 Airfoil [6] 22

Figure 4-2. NACA 63-015A Airfoil [6] 22

Figure 4-3. SIKORSKY SC2110 Airfoil [6]. 22

Figure 4-4. Stall or no stall figure. 23

Figure 5-1. Forward flight at 4600 ft. 29

Figure 5-2. Forward flight at 12400 ft. 29

Figure 5-3. Forward flight at 29527 ft. 30

Figure 5-4. Rate of climb at 4600 ft. 31

Figure 5-5. Rate of climb at 12400 ft. 32

Figure 5-6. Rate of climb at 29527 ft. 32

Figure 5-7. Rotor trade studies (Power) 33

Figure 5-8. Rotor trade studies (Max Speed) 34

Figure 5-9. Rotor Trade Studies (Cruise Speed) 34

Figure 5-10. Trade Studies (Range Speed) 35

Figure 5-11. Rotor Trade Studies (RoC) 35

Figure 6-1. Sample SolidWorks Setup. 37

Figure 6-2. Rotational Frame Setup. 37

Figure 6-3. Airflow During Hover at Sea Level 38

Figure 6-4. Airflow During Hover at Everest 38

Figure 6-5. Pressure Across vs. Rotor Length During Hover Sea Level 39

Figure 6-6. Pressure Across vs. Rotor Length During Hover Summit 40

Figure 6-7. Induced Air Velocity vs Rotor Length During Hover Sea Level 40

Figure 6-8. Induced Air Velocity vs Rotor Length During Hover Summit 41

Figure 6-9. Airflow During Cruise at Sea Level. 42

Figure 6-10. Airflow During Cruise at Summit. 42

Figure 6-11. Pressure During Cruise at Sea Level 43

Figure 6-12. Pressure During Cruise at Sea Level 43

Figure 6-13. Induced Air Velocity vs Rotor Length During Cruise at Sea Level 44

Figure 6-14. Induced Air Velocity vs Rotor Length During Cruise at Summit 44

Figure 7-1. Conceptual Sketch 46

Figure 7-2. Conceptual layout Sketch 46

Figure 7-3. Sketch view from top 47

Figure 7-4. Front Sketch view 47

Figure 7-5. Side View 47

Figure 7-6. Isometric View. 48

Figure 7-7. Internal View 48

Figure 7-8. Required power at different heights 49

Figure 7-9. Service Ceiling 50

Figure 7-10. GE CT7-8A 50

Figure 7-11. Weight Estimates. 52

Figure 7-12 Diagram. 53

Figure 7-13. Reliability 54

Figure 7-14. Hoist 55

Figure 7-15. Hoist Specifications 55

Figure 7-16. Avionics 56

Figure 7-17. Transmission sketch 57

Figure 7-18. Transmission CAD 57

Figure 7-19. Transmission CAD side view 58

Figure 7-20. Transmission CAD complete view 58

Figure 7-21. Density vs price 59

Figure 7-22. FRacture toughness vs Tensile Strength 59

Figure 7-23. Yield vs Fatigue 60

Figure 7-24. Max Temperature 60

Figure D -1. Inflow vs Nondimensional R (sea level) 70

Figure D-2. Cl loss vs Nondimensional flow (sea level) 70

Figure D-3. Ct vs Nondimensional R (sea level) 71

Figure D-4. inflow loss vs nondimensional r (1402.08) 71

Figure D-5 Cl Loss vs Non-dimensional Radial Position, r (1402.08 meters) 72

Figure D-6 Ct Loss vs Non-dimensional Radial Position, r (1402.08 meters) 72

Figure D-7 Inflow Loss vs Non-dimensional Radial Position, r (3779.52 meters) 73

Figure D-8 Cl Loss vs Non-dimensional Radial Position, r (3779.52 meters) 73

Figure D-9 Ct Loss vs Non-dimensional Radial Position, r (3779.52 meters)..... 74

Figure D-10 Inflow Loss vs Non-dimensional Radial Position, r (8869.68 meters) 74

Figure D-11 Cl Loss vs Non-dimensional Radial Position, r (8869.68 meters)..... 75

Figure D-12 Ct Loss vs Non-dimensional Radial Position, r (8869.68 meters)..... 75

Figure D-13 Inflow Loss vs Non-dimensional Radial Position, r (Sea Level) 76

Figure D-14 Cl Loss vs Non-dimensional Radial Position, r (Sea Level)..... 76

Figure D-15 Ct Loss vs Non-dimensional Radial Position, r (Sea Level)..... 77

Figure D-16 Inflow Loss vs Non-dimensional Radial Position, r (1402.08 meters) 77

Figure D-17 Cl Loss vs Non-dimensional Radial Position, r (1402.08 meters)..... 78

Figure D-18 Ct Loss vs Non-dimensional Radial Position, r (1402.08 meters)..... 78

Figure D-19 Inflow Loss vs Non-dimensional Radial Position, r (3779.52 meters) 79

Figure D-20 Cl Loss vs Non-dimensional Radial Position, r (3779.52 meters)..... 79

Figure D-21 Ct Loss vs Non-dimensional Radial Position, r (3779.52 meters)..... 80

Figure D-22 Inflow Loss vs Non-dimensional Radial Position, r (8869.68 meters) 80

Figure D-23 Cl Loss vs Non-dimensional Radial Position, r (8869.68 meters)..... 81

Figure D-24 Ct Loss vs Non-dimensional Radial Position, r (8869.68 meters)..... 81

Figure D-25 Inflow Loss vs Non-dimensional Radial Position, r (Sea Level) 82

Figure D-26 Cl Loss vs Non-dimensional Radial Position, r (Sea Level)..... 82

Figure D-27 Ct Loss vs Non-dimensional Radial Position, r (Sea Level)..... 83

Figure D-28 Inflow Loss vs Non-dimensional Radial Position, r (1402.08 meters) 83

Figure D-29 Cl Loss vs Non-dimensional Radial Position, r (1402.08 meters)..... 84

Figure D-30 Ct Loss vs Non-dimensional Radial Position, r (1402.08 meters)..... 84

Figure D-31 Inflow Loss vs Non-dimensional Radial Position, r (3779.52 meters) 85

Figure D-32 Cl Loss vs Non-dimensional Radial Position, r (3779.52 meters)..... 85

Figure D-33 Ct Loss vs Non-dimensional Radial Position, r (3779.52 meters)..... 86

Figure D-34 Inflow Loss vs Non-dimensional Radial Position, r (8869.68 meters) 86

Figure D-35 Cl Loss vs Non-dimensional Radial Position, r (8869.68 meters)..... 87

Figure D-36 Ct Loss vs Non-dimensional Radial Position, r (8869.68 meters)..... 87

Figure E-37. Cl/Cd vs Alpha and Cd vs Alpha 88

Figure E-38. Cl v Cd and Cl v Alpha..... 88

Figure E-39. Cm v alpha 89

Figure E-40. Cl v Cd and Cl v alpha 89

Figure E-41. Cl/Cd v Alpha and Cd v alpha 90

Figure E-42. Cm v alpha 90

Figure E-43. Cl/Cd v Alpha and Cd v alpha 91

Figure E-44. Cl v Cd and Cl v alpha 91

Figure E-45. Cm v alpha 92

Figure F-46 UML Case Diagram 93

List of Tables

Table 4-1. Power Loading at different altitudes 26

Table 4-2. Figure of merit at different altitudes..... 27

Table 5-1. Speeds at different altitudes..... 30

Table 7-1. Fuel estimates 51

Table 9-1: Overall Evaluation Criteria 65

List of Equations

Equation 1 24

Equation 2 24

Equation 3 24

Equation 4 25

Equation 5 25

Equation 6 25

Equation 7 25

Equation 8 25

Equation 9 27

Equation 10 27

Equation 11 27

Equation 12 27

Equation 13 28

Equation 14 28

Equation 15 28

Equation 16 28

Equation 17 28

Equation 18 49

Equation 19 62

Equation 20 63

Equation 21 65

Equation 22 65

Equation 23 65

Chapter 1: Introduction

Introduction

Located in Nepal, Mount Everest is one of the tallest mountains in the world that is summited by many hikers each year. Even though summiting Everest is a very impressive feat, there are very high risks involved because of how remote and how tall the mountain is. If hikers ever run into any issues that require urgent medical attention, they must be escorted down the mountain by foot. If time is of the essence, evacuating hikers by foot may cost lives if dire medical attention is needed. The next best option would be to life flight hikers off the mountain, but that option is currently unavailable because most rotorcraft are not designed to operate at an altitude where the density of air is so thin. Due to these unique design challenges, the Vertical Flight Society has tasked students to overcome these design challenges in the form of a competition sponsored by Airbus.

System Overview

When tackling a rotorcraft design of this nature, the system must be designed with major components in mind. This means that it is important to optimize the components within the rotorcraft with the entire system in mind and not each individual component. To ensure that the rotorcraft being designed is functional, it will often be compared to the Airbus H125.

Objectives

The goal and main objective for this project and the competition is to develop a conceptual design for a rotorcraft capable of performing rescue missions up to the highest altitudes in the world.

Justification

Today serial helicopters, based on multi-purpose design trade-offs, with known good high-altitude performance are somewhat adapted to allow high altitude mountain rescue operations in extreme conditions. However, no rotorcraft model is available today that has been specifically designed for this specific task.

Project Background

On May 14, 2005, the Airbus H125 (then called the AS350 B3) piloted by Didier Delsalle, was recorded as completing the highest helicopter landing and takeoff at 8,848 meters (29,029 feet) on Mount Everest – the highest point on earth – an unbeatable title it still holds alone today.

However, evacuating people during helicopter rescue missions in such extreme altitudes is not possible today and remains an immense challenge, for the rotorcraft as well as for the crew, even in lower altitudes. Freezing temperatures, thin air and hostile weather conditions with oftentimes degraded visual environment all contribute to making rescue work in high-altitude environments particularly dangerous.

As the environment changes very rapidly, getting relevant information for mission preparation and possible mission adjustments can be of similar importance as rotorcraft performance.

Problem Statement

What would a rotorcraft look like when specifically designed to perform emergency medical services up to the highest peaks of the planet? What technologies could enable such a vehicle? Could it be used for other purposes as well?

Chapter 2: : Literature Review

Mount Everest is the tallest mountain of the world; it summits at 8850 m. (29035 ft.) [1]. Many people climb this mountain every year. In 2018, about 347 permits were given by the Nepali government to climbers. A total 261 of these climbers got to the summit along with 302 Sherpas, while on the north side an estimated 239 people made it to the summit [2]. This accounts for a total of 802 people making the summit out of an approximate 888 climbers.

Climbing Mount Everest is a very difficult task, many factors have to be considered like the weather which changes dramatically and the extreme lack of oxygen. All of these cause many problems for climbers with death being the worst case scenario. The overall death rate for Mount Everest is about 1.2 percent. From 1923 to 1999, 1169 people made it to the summit and 170 died for a death rate of about 14.5 percent. During the years of 2000 and 2018 there were 7990 summits with a total of 123 deaths for a rate of 1.5 percent [2]. Even though the rate has dropped through the years, it is still a very dangerous climb and accidents happen leading to the need of a helicopter that can go to the top to save or help people.

The task taken was to make a helicopter that could fly all the way to the top of the mountain. There have been little to none helicopters that can reach high altitudes. The highest altitude flight in a helicopter was done on June 21st of 1972 by Pilot Jean Bulet. The helicopter used was a SA315B Lama helicopter and it was flown to approximately 12442 m. (40820 ft.) [3]. This helicopter is shown in the following figures:

Figure 2-1. SA315B Lama helicopter [3].

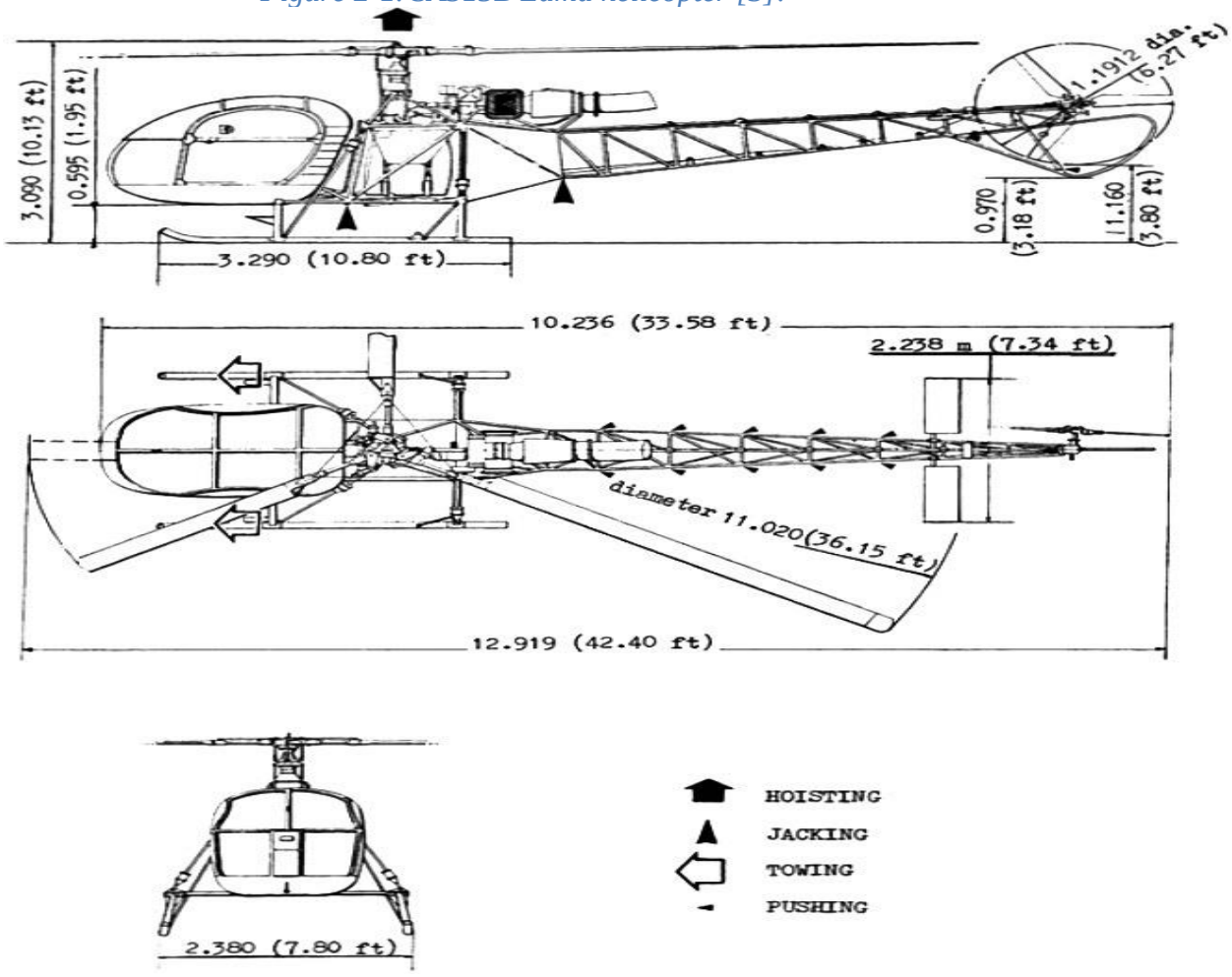

Figure 2-2. SA135B Lama Helicopter technical details [3].

The highest helicopter rescue was done by an AS350B3 from Eurocopter [4]. This helicopter can be seen in the following figure:

Figure 2-3. AS350B3 helicopter [4].

The rescue occurred at about 23000 feet in the year 2014 [4]. This helicopter also was able to get to the summit of Mount Everest in the year 2005 piloted by Didier Delsalle [5]. Since this is the only helicopter that could fly at the required altitudes, we used it as the baseline of our design.

Chapter 3: : Problem Solution

Problem Solving Approach

In order to design this helicopter to satisfy the design competition the helicopter will need to be designed in three parts: Main Rotor, Tail Rotor, and Fuselage. Mathematical models will be the first step in verification of the design and solving the problem. Simple momentum theory and then blade element theory will be conducted to ensure the validity of initial designs. Once initial designs are completed Blade Element Momentum Theory will be done to refine the vehicle along with CFD analysis via SolidWorks. All mathematical and computer models will need to be calculated at the various flight conditions and mission requirements as detailed in Design Requirements. Finally, physical 3D modeling and production will be made to showcase final design.

Requirements

The rotorcraft must have an internal or external hoist system that is weighed at 300 kg (661.4 lbs.). The rotorcraft must also be controllable at all flight conditions. Due to the strong winds of the mountains, the control systems must be capable of maintaining a controllable hover with wind up to 74 km/h at 8870m. The rotor must also be configured with an avionics system that meets the FAA requirements for day and night operations. A cruise speed that is above 259 km/h for leg one is also recommended in order to complete the mission in the given time.

UML Use Case Diagram

UML is a way to visualize functionality within a system. Usually, functions stem from a specific “actor” or object. In this case, the pilot can be the actor. Communications, navigation, and control systems all branch off the pilot as you can see in Figure F-1, which is located in Appendix F. This gives us a high-level overview of the complete system regarding the pilot of the helicopter. Use case diagrams can also help us debug our existing system and plan for overall requirements and objectives [13].

GANTT Chart

Figure 3-1. Gantt Chart.

Mission Profile

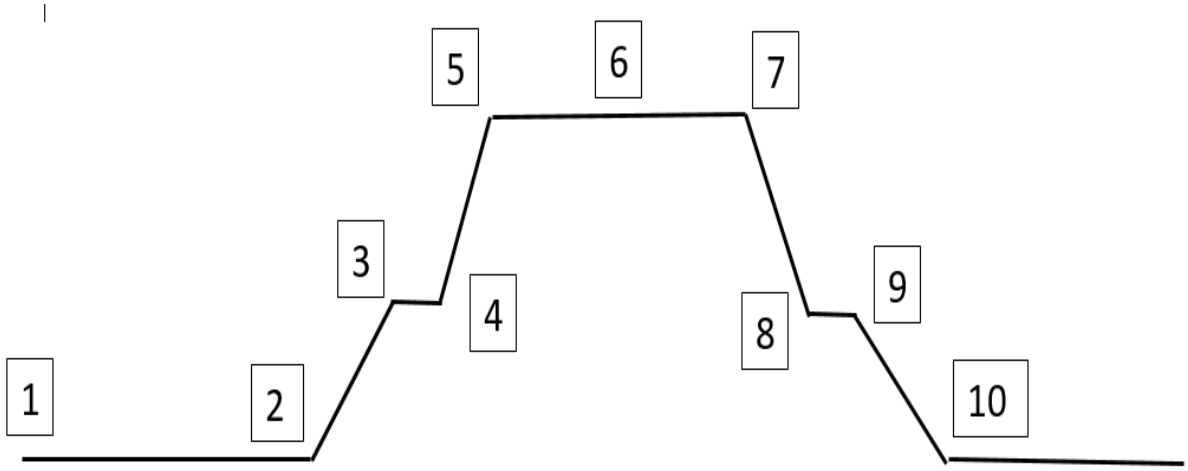

Figure 3-2. Mission Profile.

Leg 1: Transfer flight from international to smaller airport for refueling

Atmosphere: International Standard Atmosphere + 20

Payload: 3 crew + 330.693 lbs EMS equipment (892.872 lbs)

Take off from 4,600 ft, duration 2 minutes in hover

Climb to 12,400 ft & cruise for 73 nautical miles

Landing at 12,400 ft, duration 2 minutes in hover with 10% fuel margin

20 minutes of refueling

Leg 2: Take off from smaller airport, rescue mission, and return to smaller airport

- Takeoff at 12,400 ft, duration 2 minutes in hover
- Climb to 29,100 ft and level cruise for 15 nautical miles
- Hover out of ground effect @ 29,100 ft for 30 minutes
- Payload increases: 3 crew + 2 Passengers + 330.693 lbs EMS equipment (1267.66 lbs)
- Descent to 12,400 ft and level cruise for 15 nautical miles
- Landing at 12,400 ft, duration 2 minutes in hover with 10% fuel margin

Leg 3: Refueling and return with passengers to larger airport

- 20 minutes of refueling
- Takeoff at 12,400 ft, duration 2 minutes in hover
- Descent to 4,600 ft and level cruise for 73 nautical miles
- Landing at 4,600 ft, duration 2 minutes in hover with 10% fuel margin

Responsibilities

All the members of the group will work together to achieve the main objective of the project. The following are the team assignments:

- Matthew De Sieno – Project Manager, Systems Engineer
- Zach Boss – Systems Engineer, Avionics Specialist
- David Stuver – Aerodynamics & CAD Specialist
- Anthony Chavarria - Aerodynamic & Propulsion Specialist

Resources Available

Below are the required software packages used in the design of the vehicle:

1) Arena
2) Autodesk: AutoCAD 2019
3) Lingo/Lindo v17
4) MathWorks: MATLAB ver. R2018a
5) Microsoft Office 2019
6) SolidWorks 2019

Chapter 4: Blade and Hover Performance

Airfoil Selection

The airfoil of a rotor blade of a helicopter is an important factor in its performance. For the H125, the rotors have the OA209 airfoil which can be seen in the following picture:

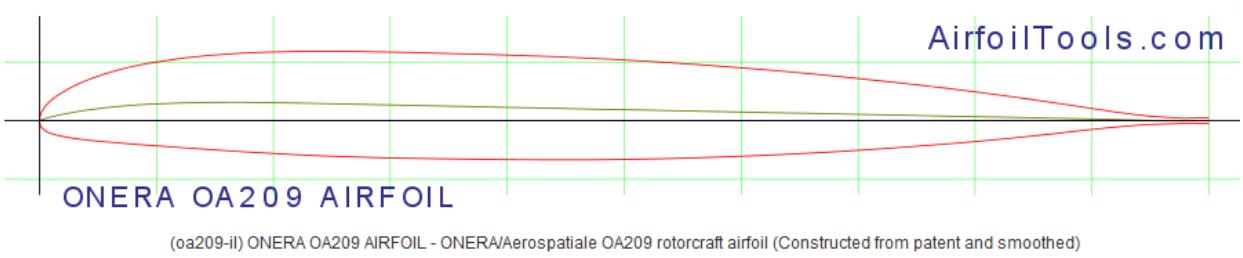

Figure 4-1. ONERA OA209 Airfoil [6].

The main characteristic of this airfoil is that it has 0.008 zero lift drag coefficient. The smaller the zero lift drag coefficient of an airfoil, the less parasitic drag the helicopter will have. With this said, the team looked for other airfoils used in rotorcraft that could have less zero lift drag coefficient and two were found. They are the Sikorsky SC2110 and the NACA 63-015A. They can be seen in the following figures [6]:

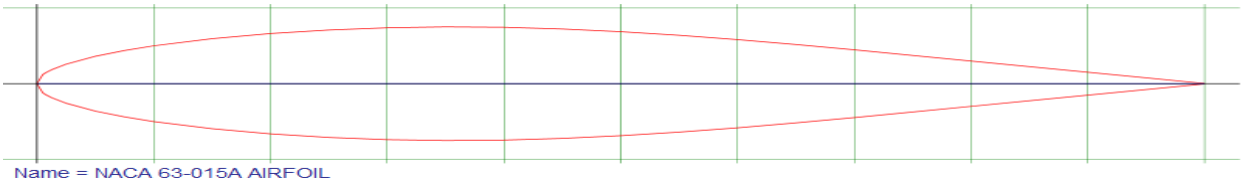

Figure 4-2. NACA 63-015A Airfoil [6]

Figure 4-3. SIKORSKY SC2110 Airfoil [6].

These two airfoils have the main characteristic of having a value of 0.005 for their zero lift drag coefficient. The Sikorsky airfoil was chosen since it is thinner and requires less weight. The corresponding Cl/Cd. Drag polar and other important airfoil graphs are in appendix E.

Rotor Sizing

For rotor sizing, a spreadsheet was made to calculate the average lift coefficient depending on the radius of the main rotor. Power, tip speed, thrust coefficient and solidity were all calculated to determine and select a rotor size. The following figure shows these calculations:

Rotor Radius (m)	3.8	4	4.2	4.4	4.6	4.8	4.876	5	5.2	5.4	5.6	5.8	6
Area (m^2)	45.3646	50.26548	55.41769	60.82123	66.4761	72.38229	74.69255	78.53982	84.94867	91.60884	98.52035	105.6832	113.0973
Power (W)	525212.9	498952.3	475192.6	453593	433871.5	415793.6	409312.8	399161.8	383809.4	369594.3	356394.5	344105	332634.8
Power (kW)	525.2129	498.9523	475.1926	453.593	433.8715	415.7936	409.3128	399.1618	383.8094	369.5943	356.3945	344.105	332.6348
tip speed (m/s)	155.1947	163.3628	171.531	179.6991	187.8672	196.0354	199.1393	204.2035	212.3717	220.5398	228.7079	236.8761	245.0442
Ct	0.047016	0.038295	0.031505	0.026156	0.021895	0.018468	0.017343	0.015686	0.013408	0.011529	0.009968	0.008663	0.007564
Solidity	0.217948	0.207051	0.197191	0.188228	0.180044	0.172543	0.169853	0.165641	0.15927	0.153371	0.147894	0.142794	0.138034
Cl average	1.29432	1.109717	0.958616	0.833747	0.729657	0.642198	0.612634	0.568175	0.505106	0.451036	0.404416	0.364006	0.328805
Stall	Yes	No	No	No	No	No	No	No	No	No	No	No	No
k	1.22	1.22	1.22	1.22	1.22	1.22	1.22	1.22	1.22	1.22	1.22	1.22	1.22
Induced Power (kW)	640.7598	608.7218	579.735	553.3834	529.3233	507.2681	499.3616	486.9774	468.2475	450.905	434.8013	419.8081	405.8145
Profile Power (W)	9924.715	12184.95	14810.88	17839.98	21311.55	25266.71	26905.34	29748.41	34801.43	40472.38	46809.69	53863.63	61686.29
Total Power (MR) (kW)	650.6845	620.9067	594.5459	571.2234	550.6348	532.5348	526.2669	516.7258	503.0489	491.3774	481.611	473.6718	467.5008

Figure 4-4. Stall or no stall figure.

It can be seen that the lower the radius, the higher the average lift coefficient. The minimum radius that can be chosen was 4 meters. It can also be seen that as the radius is smaller, the induced power increases while the tip speed decreases.

Three main rotor designs were chosen. The first design was using a radius of 4.876 m. (16 ft.), a chord of 0.67056 m. (2.2 ft.), and four blades. The second design was using a radius of 5 m. (16.4042 ft.), a chord of 0.33528 m. (1.1 ft.), and three blades. The third design was using a radius of 5.2 m. (17.0604 ft.), a chord of 0.9 m. (2.95276 ft.), and four blades.

Blade Design

To help out with the blade design calculations, we used the combined blade element momentum theory. It combines the basic principles of the blade element theory and momentum theory. With assumptions, BEMT allows the inflow distribution across the blade to be estimated. According to the theory, the rotor blade will no longer have a uniform inflow. The goal is to minimize total power and maximize the figure of merit. The rotor blade will also have a very high pitch angle near the root, which in turn causes the rotor to stall near the root.

To make our calculations even more accurate, we decided to incorporate Prandtl's Tip-loss Function to accommodate for the loss of lift near the tips, which is shown below [11]:

$$F = \left(\frac{2}{\pi}\right) cos^{-1}(\exp(-f))$$

Equation 1

where "f" is:

$$f = \frac{N_b}{2}\left(\frac{1-r}{r\phi}\right)$$

Equation 2

In our analysis, we essentially solved for the total inflow velocity at different altitudes (sea level, 1402.08 meters, 3779.52 meters, and 8868.68 meters) with the following equation [11]:

$$\lambda(r) = \frac{\sigma C_{l_\alpha}}{16F}\left(\sqrt{1 + \frac{32F}{\sigma C_{l_\alpha}}\theta r} - 1\right.$$

Equation 3

Once the inflow ratio is calculated, we then used it to calculate the coefficient of thrust over the blade and the coefficient of lift. While comparing different degrees of twist (0°, 5°, 10°, and 20°), we were able to represent the effect of altitude on inflow, thrust, and lift across different sections of the blade. The coefficient of thrust steadily increases as you go across the blade and

then it rapidly decreases at the tip. The coefficient of lift is the highest near the root of the blade and then it decreases across the blade. As we added twist to the blade, the inflow, Ct and Cl increased near the root of the blade and then decreased the near the tip. These results can be seen in Appendix D. Some other major equations that we used can be seen below:

$$\lambda_{r_n} = \frac{\sigma C_{l_\alpha}}{16}\left(\sqrt{1 + \frac{32}{\sigma C_{l_\alpha}}\theta(r_n) r_n} - 1\right)$$

Equation 4

$$\theta_0 = \frac{6C_T}{\sigma C_{l_\alpha}} - \frac{3}{4}\theta_{tw} + \frac{3}{2}\sqrt{\frac{C_T}{2}}$$

Equation 5

$$\frac{dC_T}{dr} = 4F\lambda^2 r$$

Equation 6

$$\phi = tan^{-1}\left(\frac{U_p}{U_t}\right) \approx \frac{U_p}{U_t}\ for\ small\ angles$$

Equation 7

$$\alpha = \theta - \phi = \theta - \frac{U_p}{U_t}$$

Equation 8

Disk Loading and Power Loading

Disk Loading and power loading are two parameters normally used for helicopters. Disk Loading is T/A where T stands for the thrust and A is the area of the main rotor. Power loading is defined as T/P where T Is also thrust and P is the power required at hover. The following figure shows normal trends for helicopters [7]:

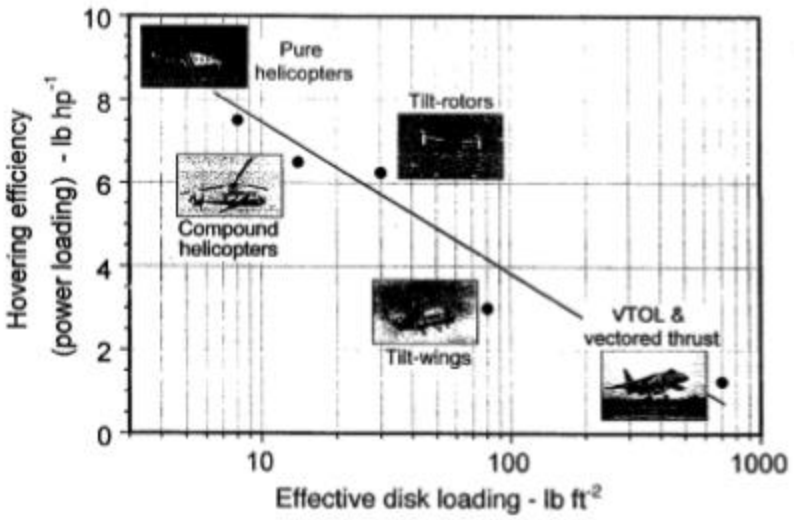

Figure 4-5. Power loading vs disk loading [11]

For our helicopter, the thrust is 4960 lbs. while the area of the rotor is 804 ft^2. This gives us a disk loading of 6.16 lbs./ft^2. Power Loading can be calculated at 4 heights, and can be seen in the following table:

Table 4-1. Power Loading at different altitudes

Height (ft)	**Power (hp)**	**Thrust (lbs.)**	**Power Loading (lbs./hp)**
Sea Level	551	4960	9
4600	561	4960	8.8
12400	607	4960	8.2
29527	785	4960	6.31

As can be seen from the table, the higher the altitude, the more power is required hence power loading drops.

Figure of Merit

The figure of merit of a helicopter is another measure used to see the efficiency at hover the following equation is used to find the FoM:

$$FM = \frac{Ideal\ power\ required\ to\ hover}{Actual\ power\ required\ to\ hover} < 1$$

Equation 9

In the case of our helicopter, the FoM is presented in the following table:

Table 4-2. Figure of merit at different altitudes

Altitude	Figure of Merit
SL	0.809018568
4600	0.838461538
12400	0.883054893
29527	0.948669202

It can be seen that the higher the altitude the better FoM at hover the helicopter has.

Chapter 5: Performance

Forward Flight

With the hover performance calculations completed, the next step is calculating how fast the rotorcraft can move and how much power it will require. The equations used to calculate these curves are the following:

$$\mu = \frac{V_\infty}{\Omega R}$$

Equation 10

$$T sin\alpha_{TPP} = D$$

Equation 11

$$T cos\alpha_{TPP} = W$$

Equation 12

$$T = 2\rho A v \sqrt{(V_\infty cos\alpha_{TPP})^2 + (V_\infty sin\alpha_{TPP} + v)^2}$$

Equation 13

$$P_i = Tv$$

Equation 14

$$P_o = \frac{\sigma C_{d0}}{8}[1 + 4.6\mu^2]$$

Equation 15

$$P_d = \frac{1}{2}\rho {V_\infty}^3 f$$

Equation 16

$$DV_\infty = \left[\frac{1}{2}\rho {V_\infty}^2 C_D S\right] V_\infty$$

Equation 17

There are three main altitudes that are important, 4600 ft, 12400 ft and 29100 ft which is the summit of Mount Everest. For our purposes, we are making our rotorcraft be able to hover at a higher altitude than the summit which would be around 29527 ft (9000 m). The following power curves were obtained:

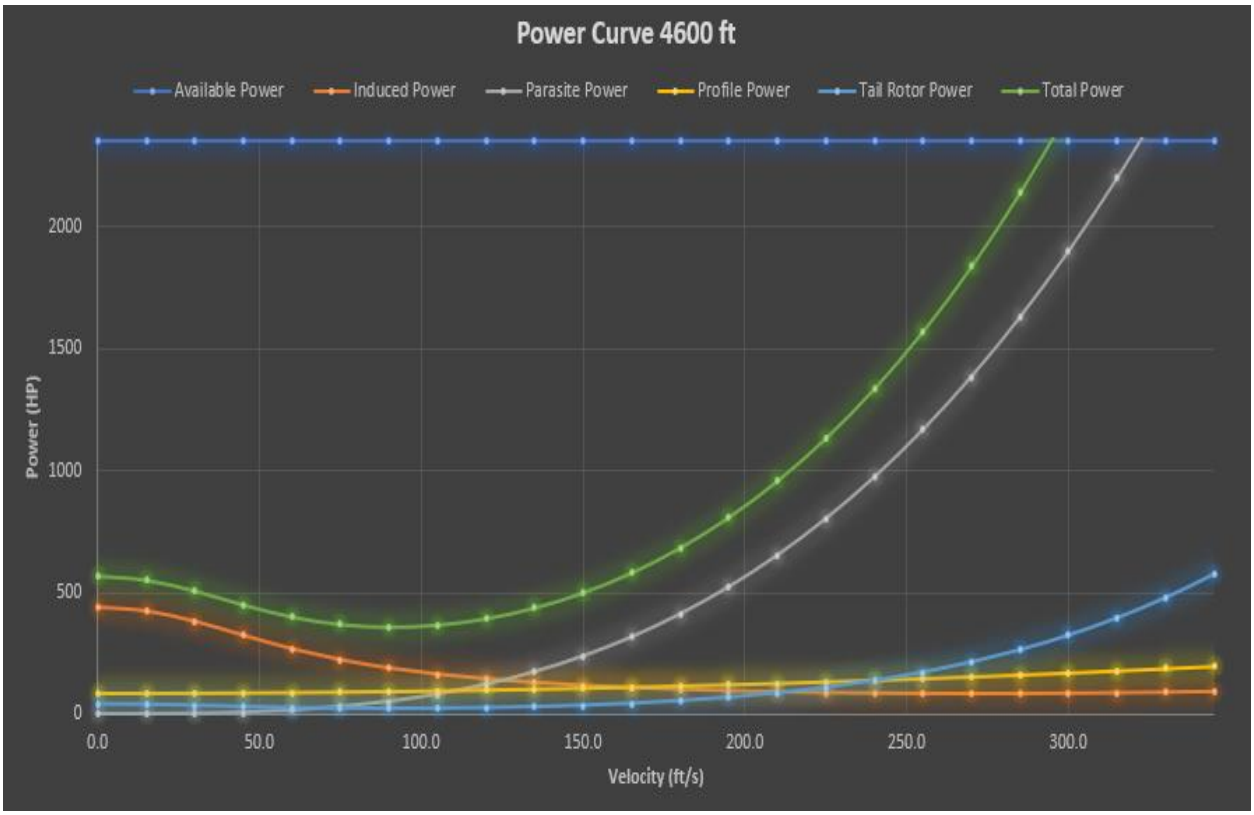

Figure 5-1. Forward flight at 4600 ft.

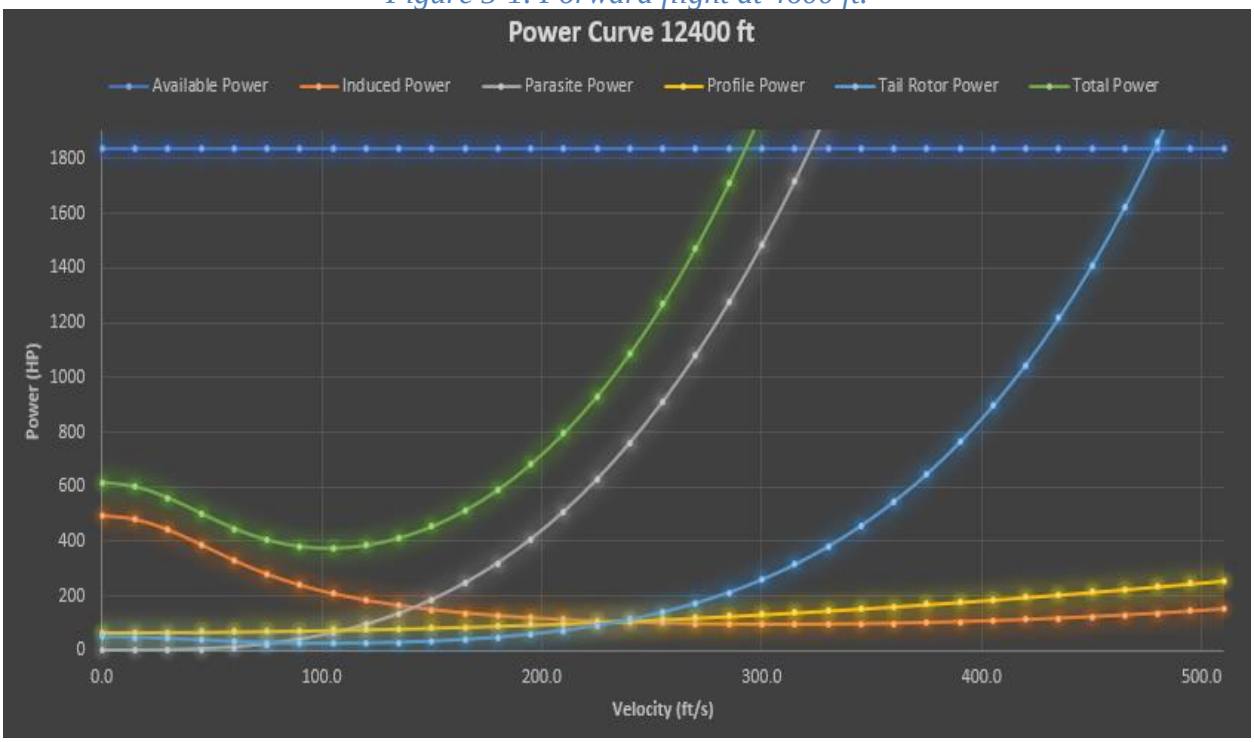

Figure 5-2. Forward flight at 12400 ft.

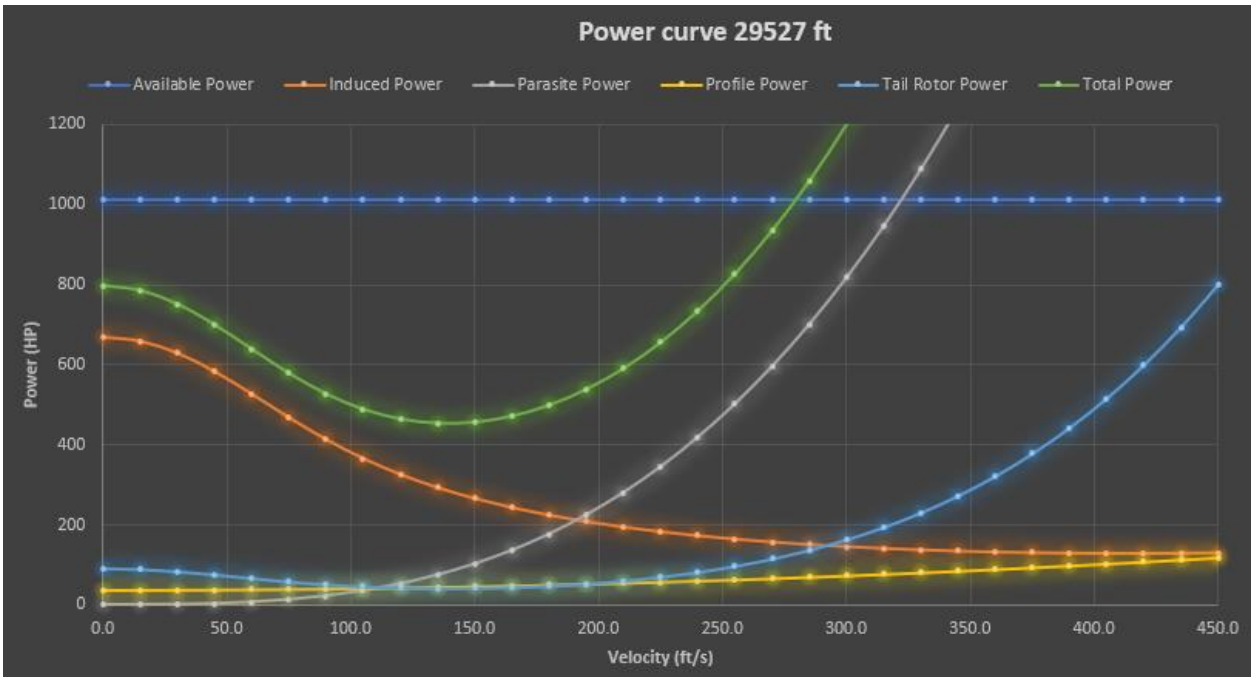

Figure 5-3. Forward flight at 29527 ft.

The power curves show that the power required for hover rises as altitude goes up. For hover at 4600 ft., power required is 567 HP, at 12400 ft., the power needed is 615 HP while at max altitude the power required is 798 Hp. Other variables like max speed, best cruise speed and best range speed are different, and these changes can be seen in the following figure:

Table 5-1. Speeds at different altitudes

Altitude (ft)	Best Cruise Speed (ft/s)	Best Range Speed (ft/s)	Max Speed (ft/s)
4600	90	135	295
12400	105	135	295
29527	135	180	280

Rate of Climb

Another aspect that can be looked at is the rate of climb. The rate of climb is important in a helicopter because it tells us how fast it can climb. The following figures show the rate of climb at each height:

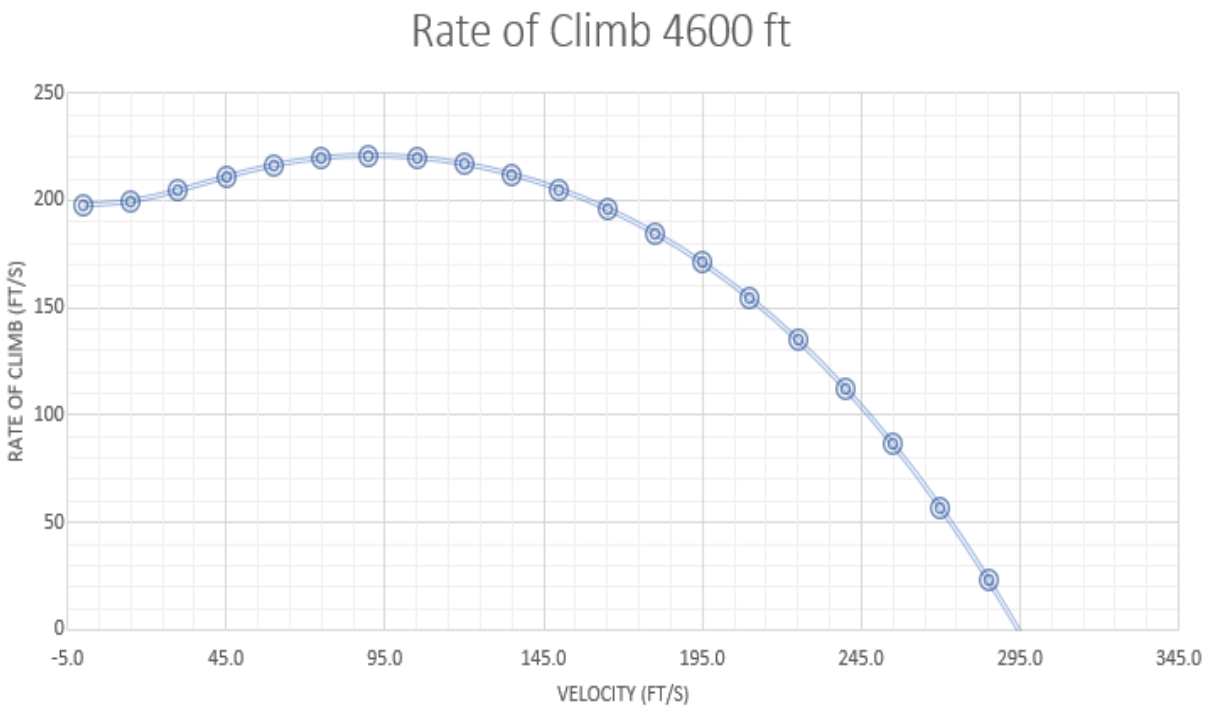

Figure 5-4. Rate of climb at 4600 ft.

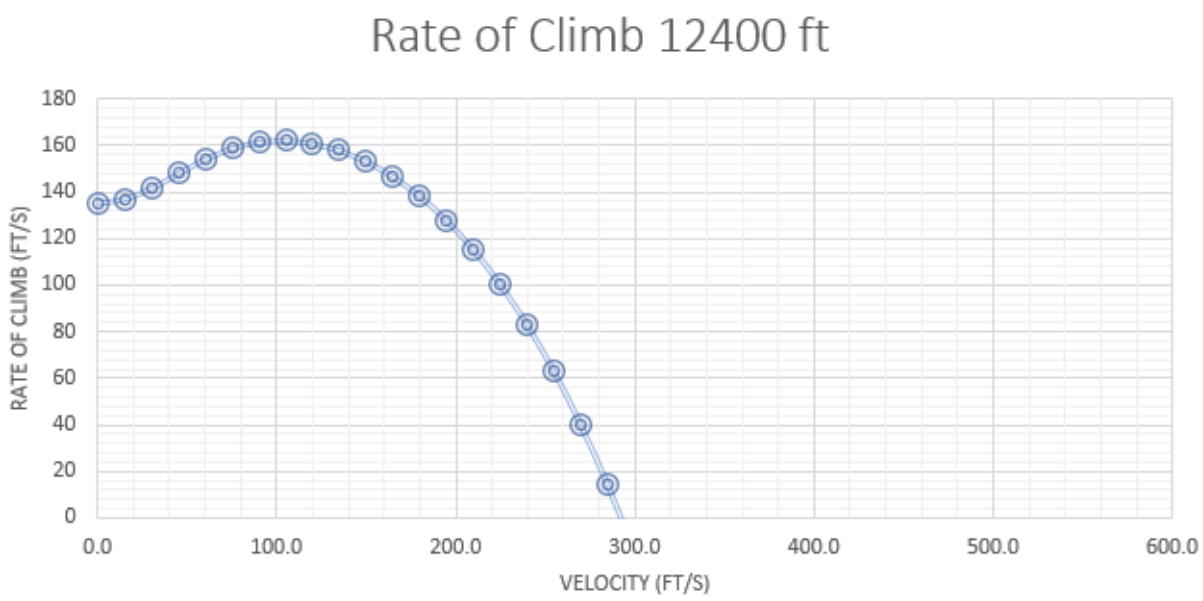

Figure 5-5. Rate of climb at 12400 ft.

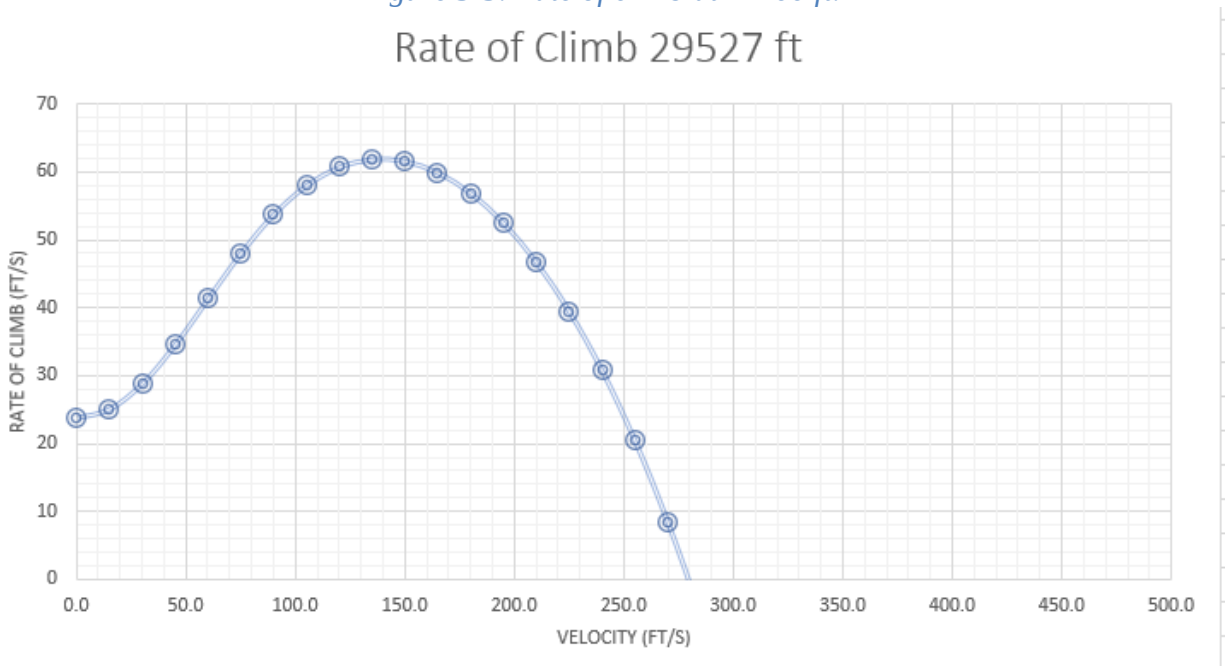

Figure 5-6. Rate of climb at 29527 ft.

As can be seen, at higher altitudes the climb rate is smaller because the power available is less than at lower altitudes.

Rotor Trade Studies

Rotor trade Studies were done to compare different designs and pick the best one. The following rotor parameters were used in this comparison:

1) Rotor Diameter of 32 feet and a chord of 2.2 feet with 4 blades.
2) Rotor Diameter of 32.8 feet and a chord of 2.6 feet with 5 blades.
3) Rotor Diameter of 34.1 feet and a chord of 3 feet with 4 blades.

The following figures were obtained to compare these rotors in aspects like rate of climb, power at hover, max speed, best cruise speed and best range speed:

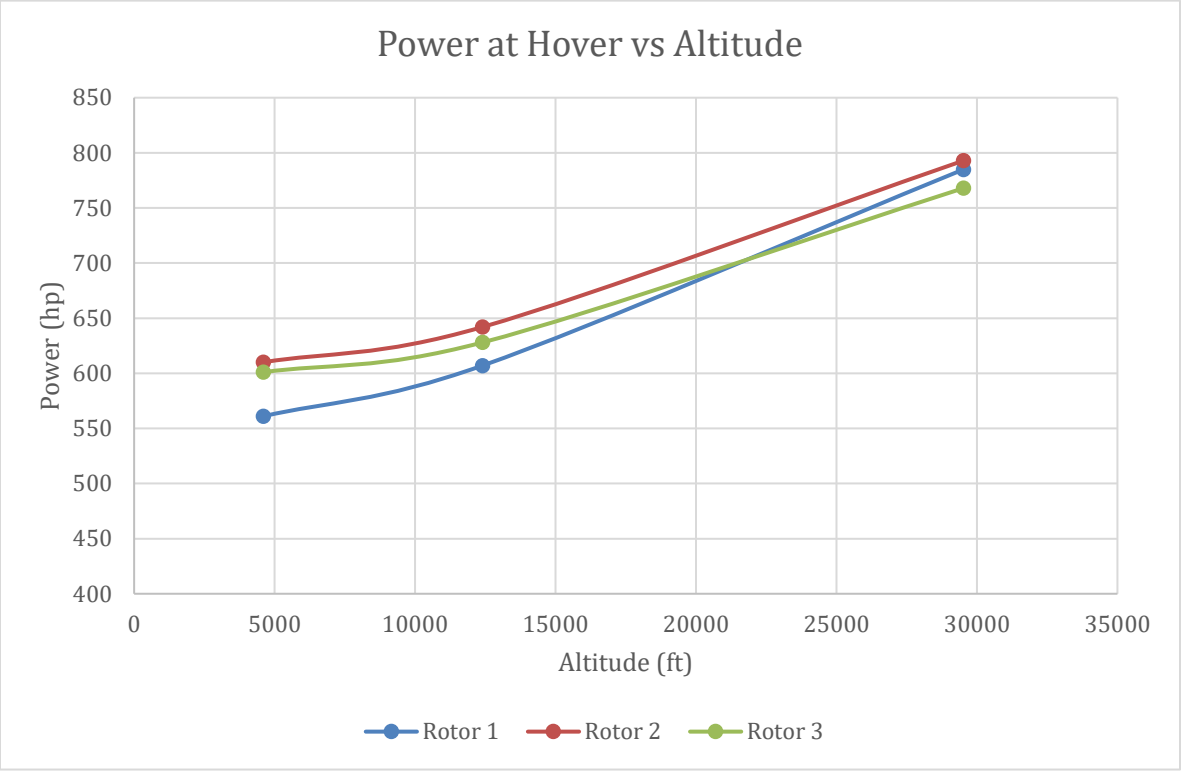

Figure 5-7. Rotor trade studies (Power)

Figure 5-8. Rotor trade studies (Max Speed)

Figure 5-9. Rotor Trade Studies (Cruise Speed)

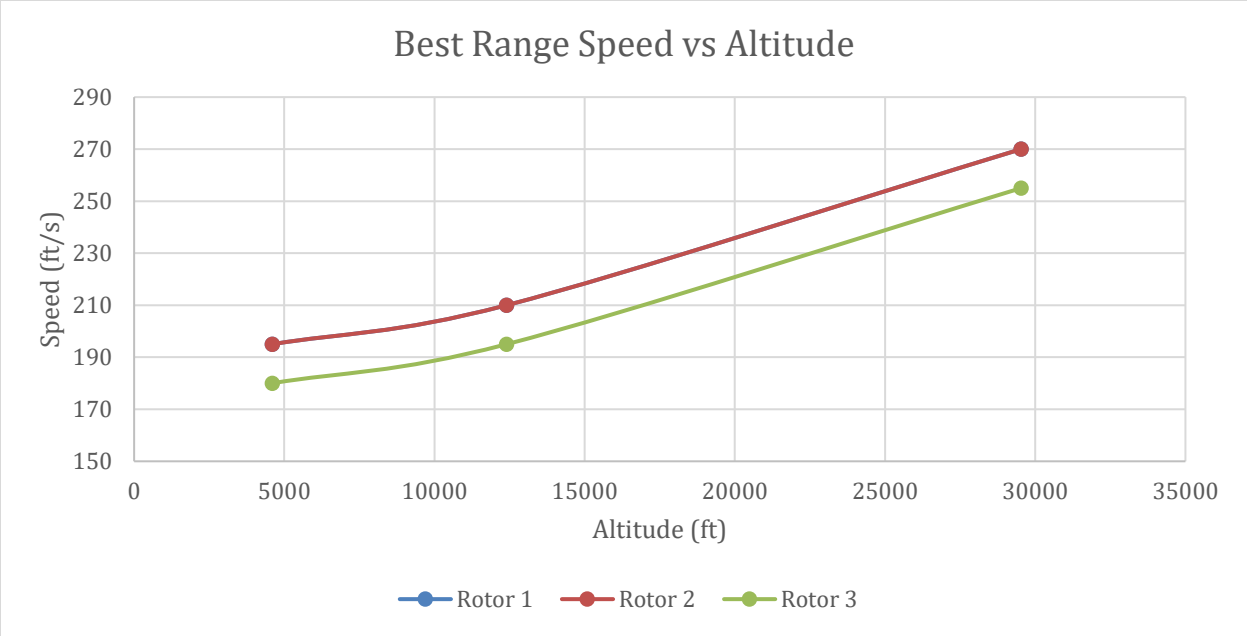

Figure 5-10. Trade Studies (Range Speed)

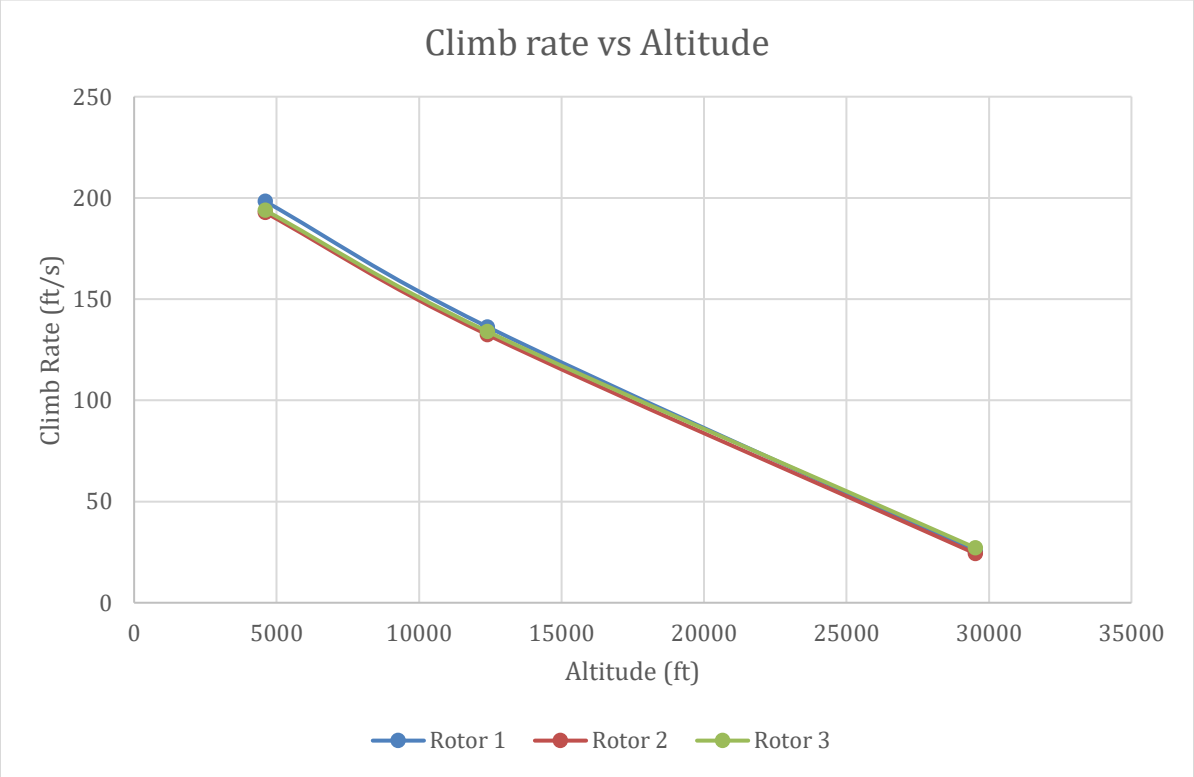

Figure 5-11. Rotor Trade Studies (RoC)

Looking at these graphs, the rotor 1 design is better in respects to max speed, power at hover and cruise speed. It is also tied for best in climb rate and best range speed.

Chapter 6: Fluid Analysis

As part of the requirements of the project, a 3D modeling of fluid analysis needed to be completed. In order to do this the helicopter was modeled within Solid Works 2018 and then a flow simulation conducted. The goal of these calculations is twofold, one to double check the hand calculations, and two to locate any points of failure in the helicopter design. By utilizing the built in flow simulation module, a rough verification of the hand calculations could be made via analysis of the pressure and velocity of the flow around the aircraft. These calculations were done ISA +0 and ISA + 20 at Sea Level and at 29,527ft at both hover and at cruise speeds.

Flow Analysis Setup

The first round of simulations was set during hover using a simplified model of the aircraft. Figures 6- 1 shows an example setup of the simulations using SolidWorks Flow Simulation 2018.

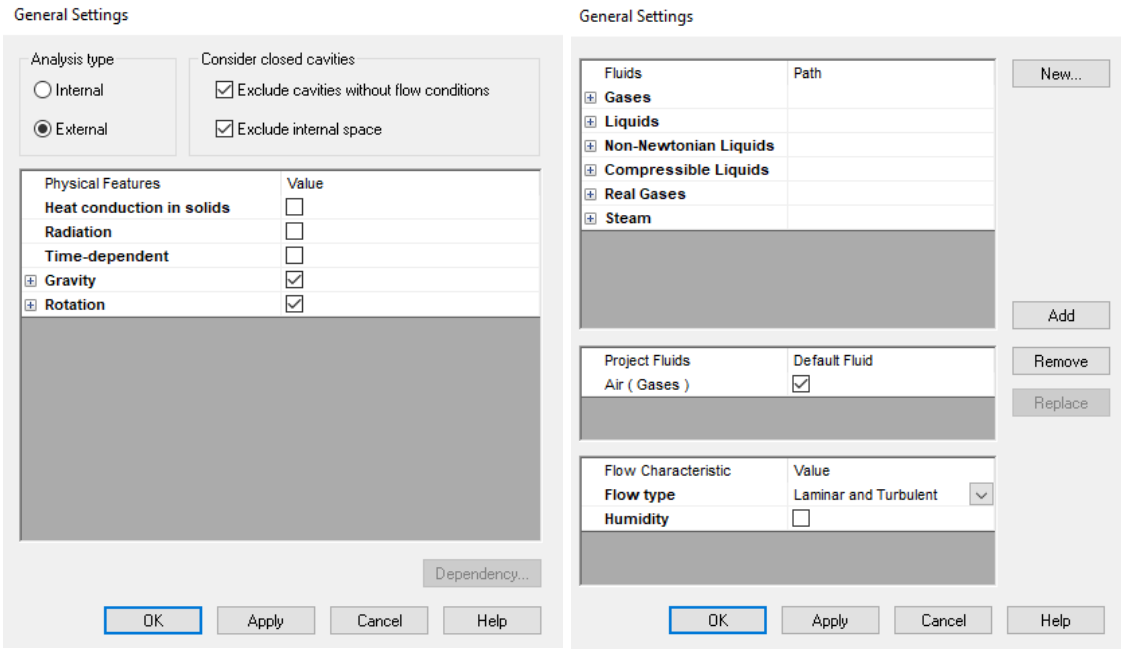

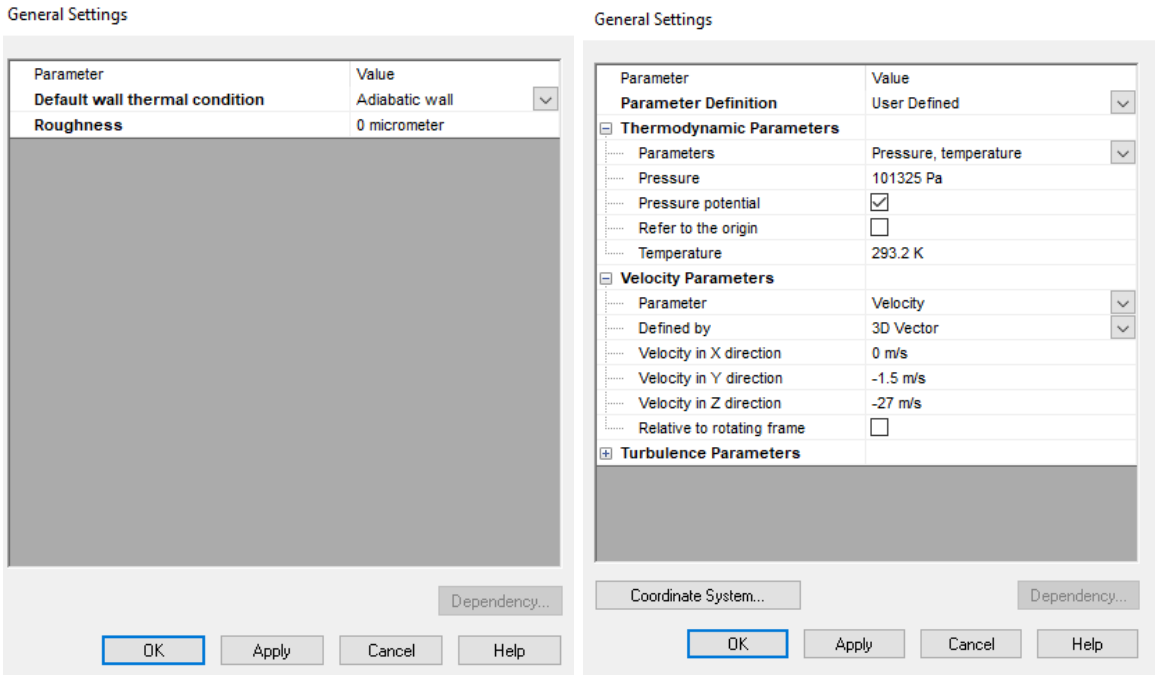

Figure 6-1. Sample SolidWorks Setup.

After setup a rotational fluid zone was set around the rotor blades in order to simulate the rotating region of the blades as shown in Figure 6-2.

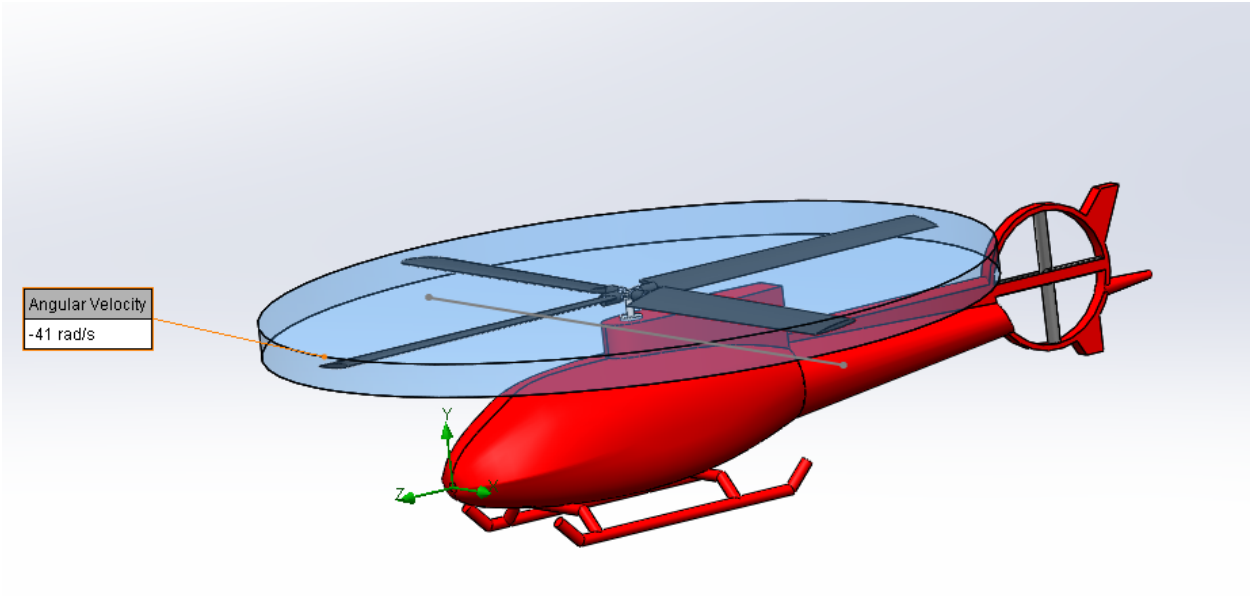

Figure 6-2. Rotational Frame Setup.

Computational domain was set to automatic and the data for each situation was collected.

Hover Simulations:

For simulating the conditions of hover, the x, y, and z components of flows was set to zero in the general flow settings. Then the atmospheric pressures and densities were set to 101325 Pa and Temperatures to 288.15°K.

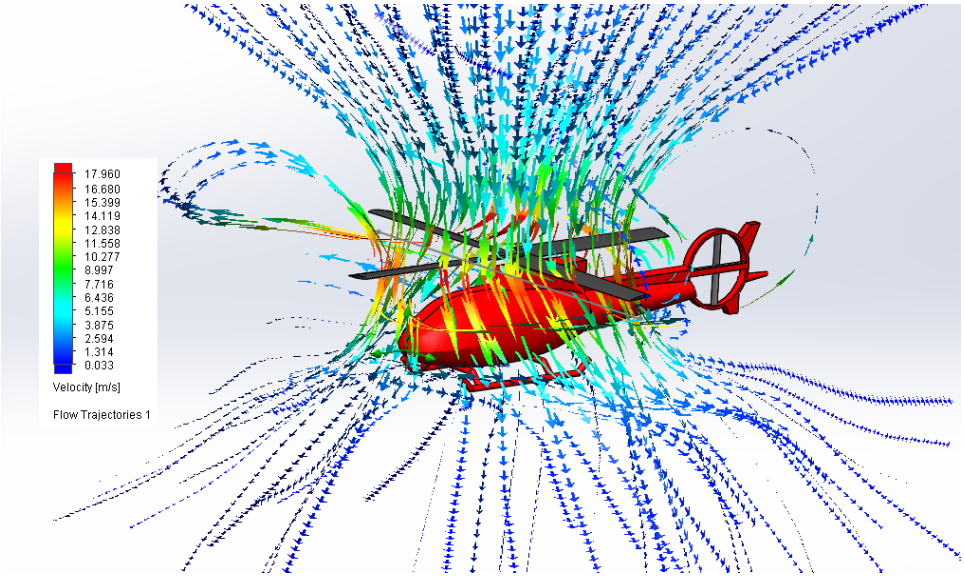

Figure 6-3. Airflow During Hover at Sea Level

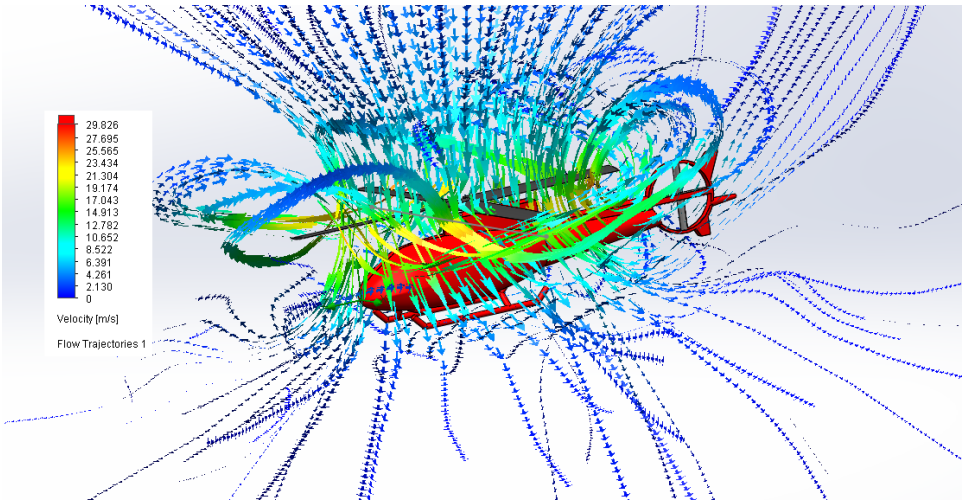

Figure 6-4. Airflow During Hover at Everest

Here the simulations show that with the increase of altitude the flow induced by the blades will increase substantially in order to account for the lower air density. This is consistent with the BEMT Calculations and Performance calculations as noted previously in the paper. However, SolidWorks Flow Simulation 2018 is not properly designed for rotating blade systems and cannot be used for accurate simulation of thrusts and drag on the rotor blades.

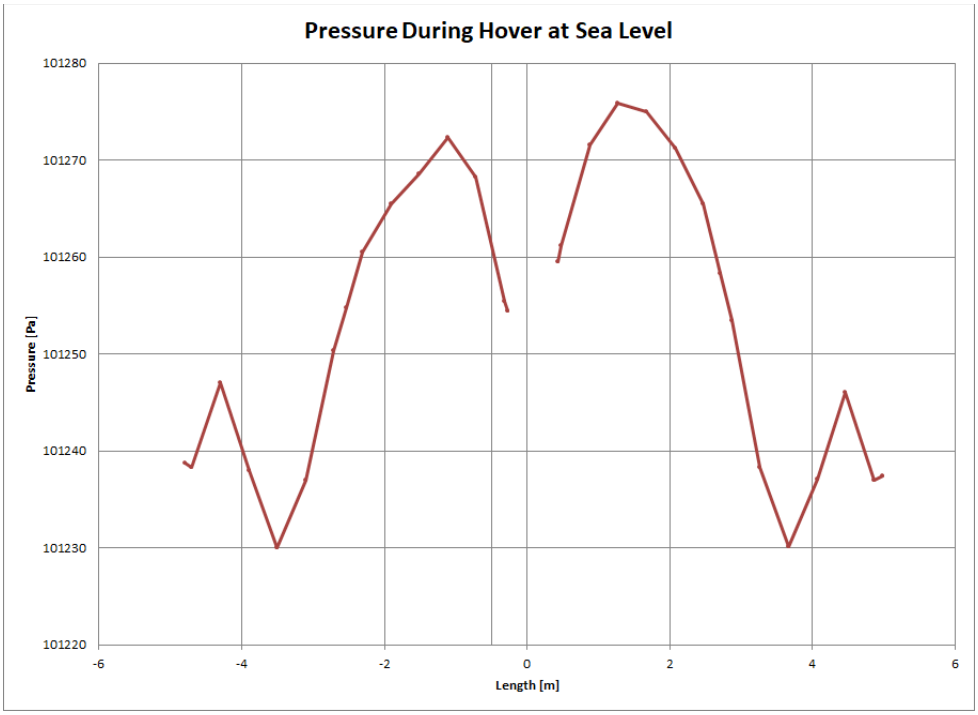

Figure 6-5. Pressure Across vs. Rotor Length During Hover Sea Level

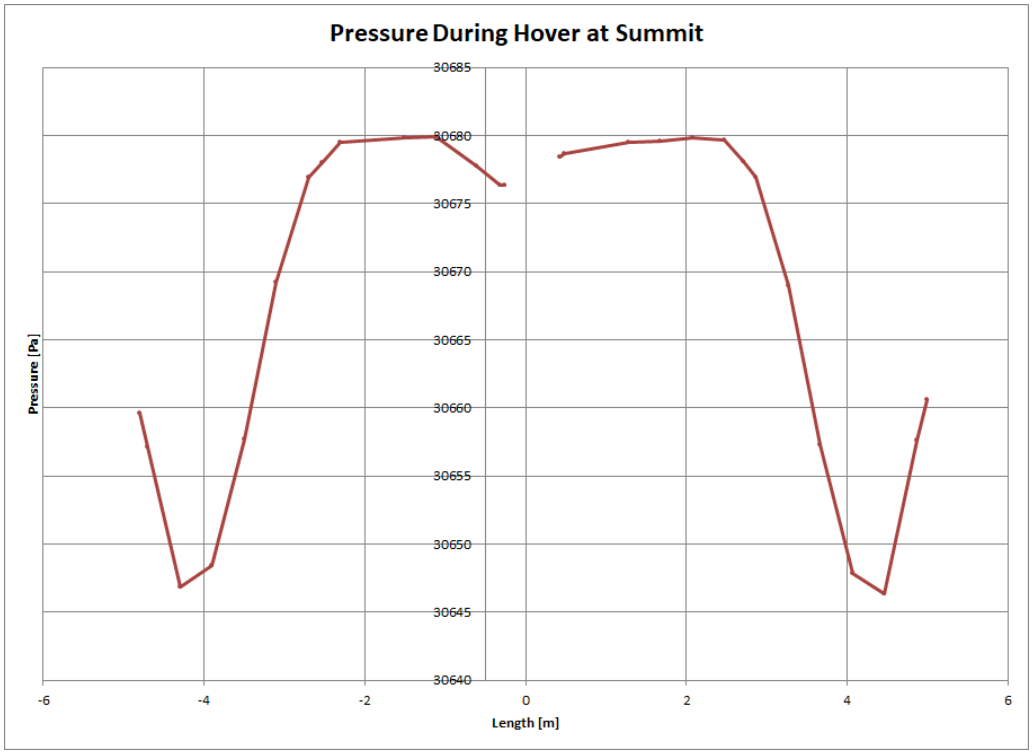

Figure 6-6. Pressure Across vs. Rotor Length During Hover Summit

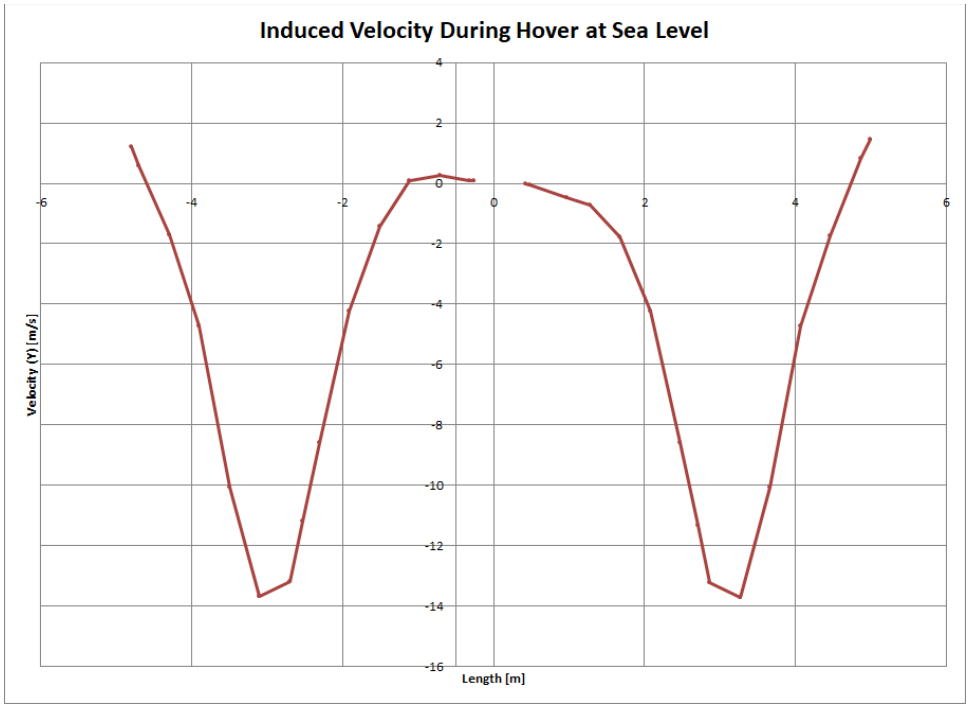

Figure 6-7. Induced Air Velocity vs Rotor Length During Hover Sea Level

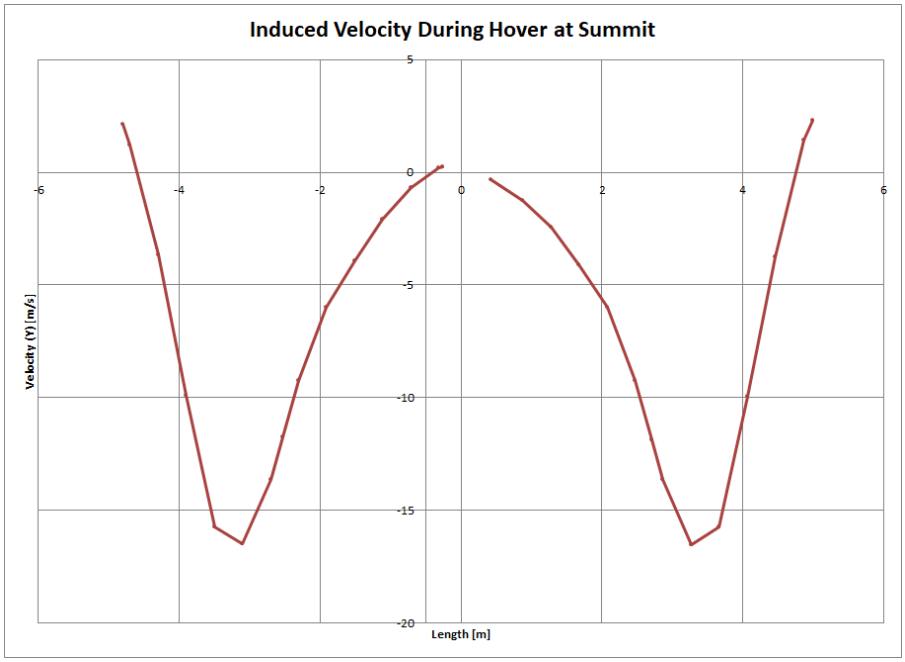

Figure 6-8. Induced Air Velocity vs Rotor Length During Hover Summit

The graphical representations of pressure and induced velocity experienced along the blade axis were made to ensure that the flow generated by the SolidWorks Flow Simulation was indeed correct in direction. As shown in Figures 6-5 and 6-6, the pressures greater than the ambient pressure thus generating lift. However, much of the lift is lost due to tip losses and vortex shedding. Figures 6-7 and 6-8 shows the velocity across the span of both the blades at the advancing and retreating side. During hover these should remain similar in shape with a majority of induced velocity occurring at around 80% the blade length while dropping off significantly toward the hub and tip of the blades. This is proven in the simulations.

Cruise Simulations

The next part of the simulations measured the pressure and velocities during cruise conditions. Setup was similar to hover conditions however the Y-axis was set to -1.5 m/s flow

direction and the Z-axis was set to -27 m/s flow velocity in order to simulate the freestream velocity during cruise conditions.

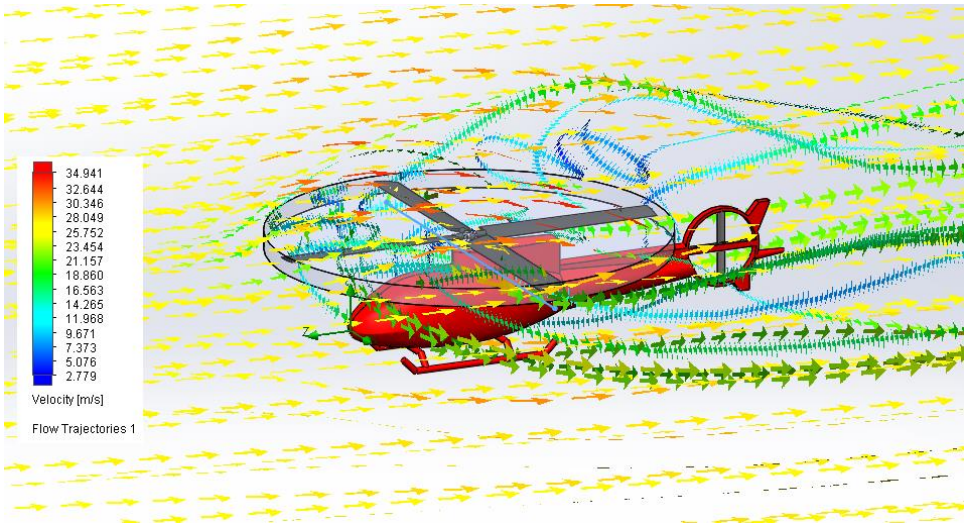

Figure 6-9. Airflow During Cruise at Sea Level.

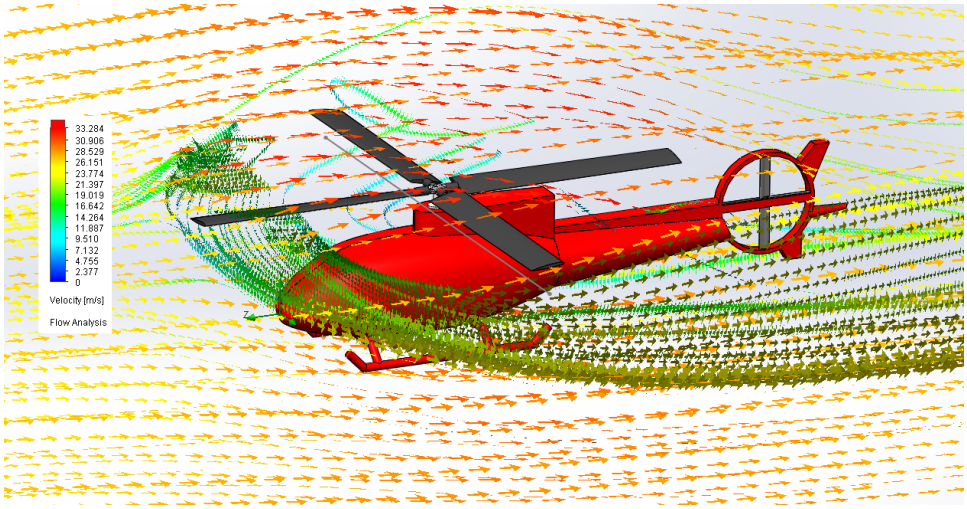

Figure 6-10. Airflow During Cruise at Summit.

As shown in the Figures 6-9 and 6-10, the airflow around the rotors creates some votexes along the tip of the blades, however it is much more diminished in comparison to the hover conditions. This is because the blades are able to rotate through clean air during its cruise speed.

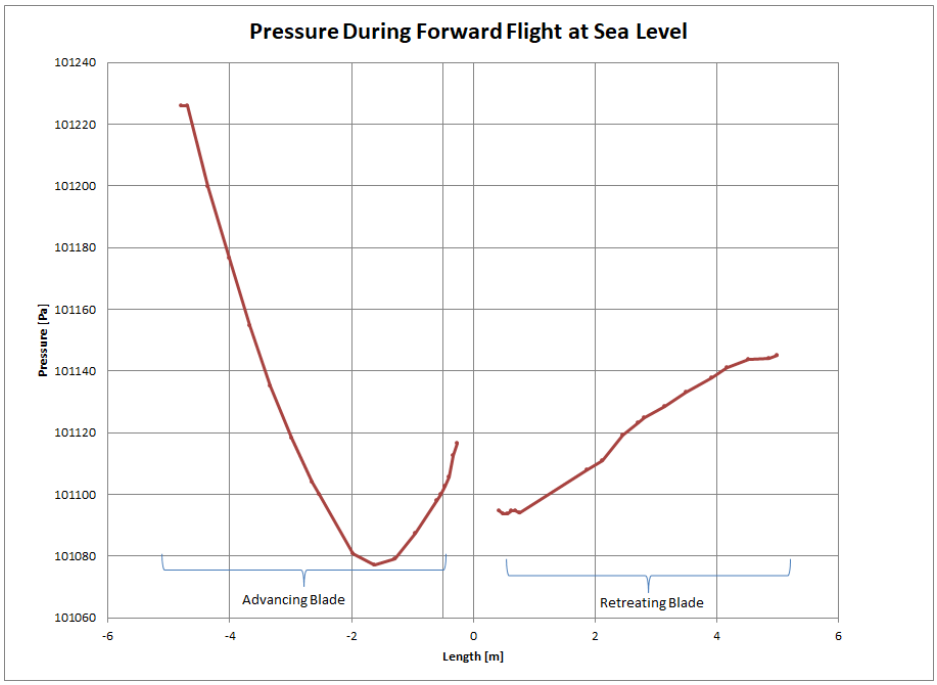

Figure 6-11. Pressure During Cruise at Sea Level

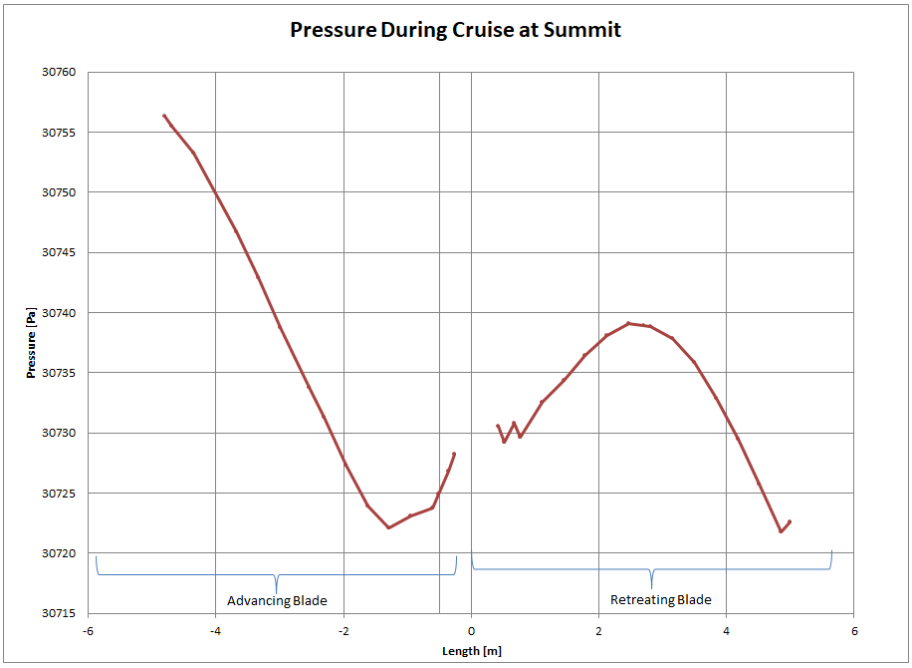

Figure 6-12. Pressure During Cruise at Sea Level

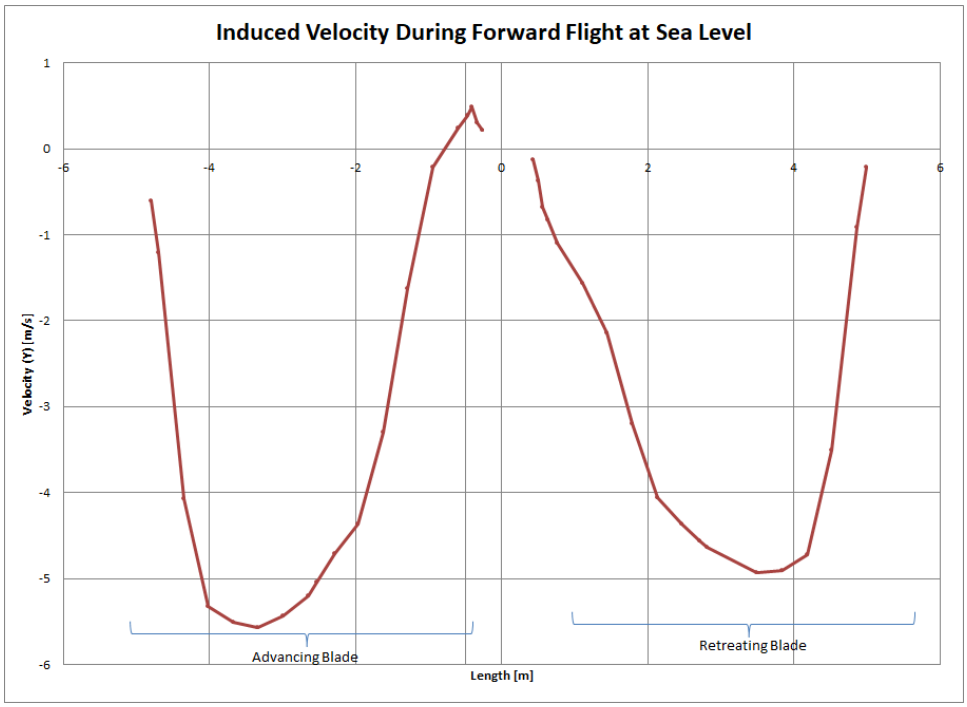

Figure 6-13. Induced Air Velocity vs Rotor Length During Cruise at Sea Level

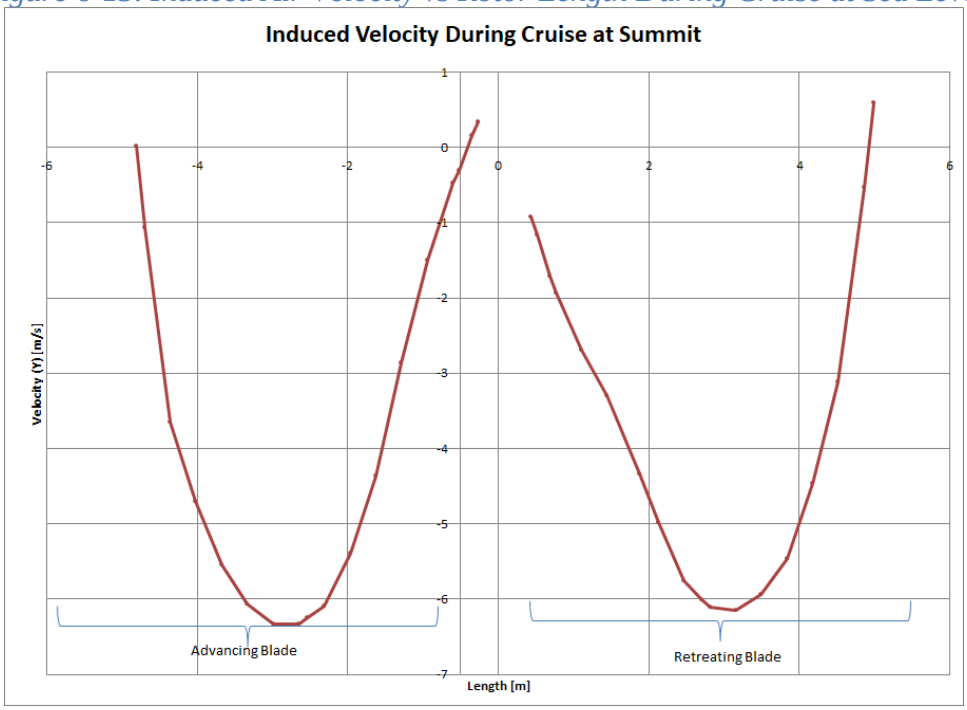

Figure 6-14. Induced Air Velocity vs Rotor Length During Cruise at Summit

The pressure and velocity graphs show an interesting facet of forward flight in that the retreating blade experiences less lift than the advancing blade because of the rotational component of the blades. This can cause some major disturbances under extreme conditions but both simulations show that the helicopter still produces lift at both sea level and operating altitude. The dissymmetry of lift can be most clearly seen in the sea level calculations, while the high-altitude simulations have a much less dissymmetry. This is most likely because the helicopter has a much higher angle of attack at high altitude thus limiting the effects of the dissymmetry, however in future work high level analysis will need to be conducted in order to verify these results.

Chapter 7: Helicopter Architecture

Fuselage Design

The base cabin size of the H125 is not optimized for the mission. We decided to stretch it in order to fit the semi-large stretchers for the hikers. The stretchers measure out to about 7.5 ft. We also had to accommodate for the doctor's seat and the medical supplies. Unfortunately, the feet of the stretchers will be against the back wall of the cabin. Also, there is space in between the stretchers for the doctor to tend to both hikers at once. During the design phase of the aircraft, we played around with the placement of the access door for the cabin. We eventually decided on having on the side of the cabin with the hoist system on the edge. The door will also slide to the side for easy access.

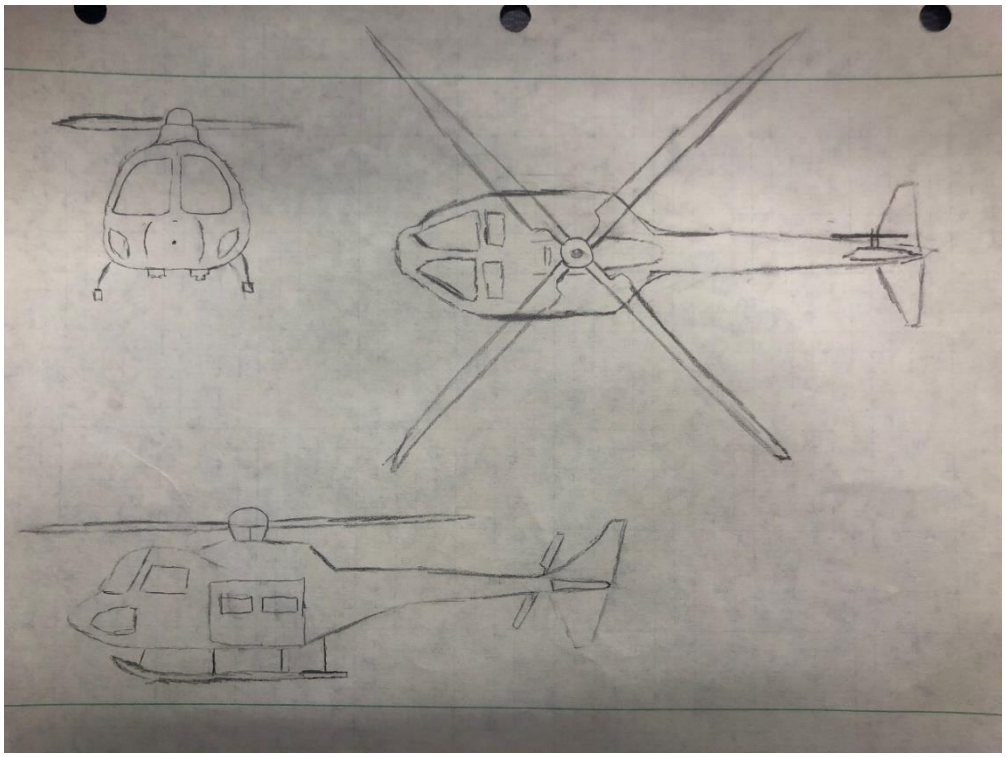

Figure 7-1. Conceptual Sketch

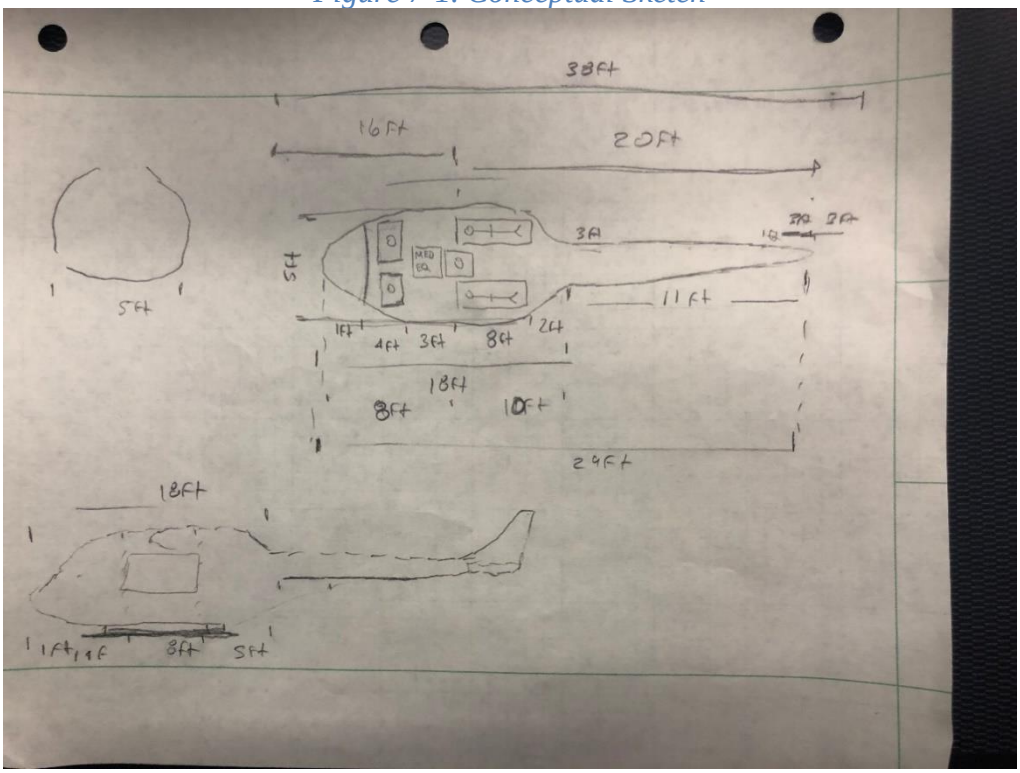

Figure 7-2. Conceptual layout Sketch

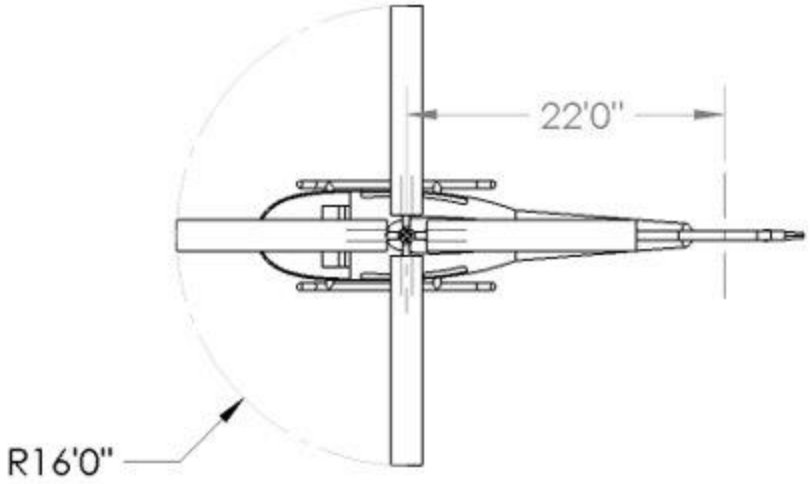

Figure 7-3. Sketch view from top

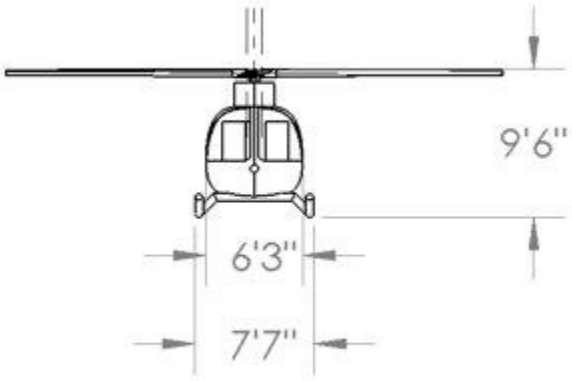

Figure 7-4. Front Sketch view

Figure 7-5. Side View

Figure 7-6. Isometric View.

The fuselage also had to accommodate the crew, two stretchers and injured personnel, and medical supplies and finally a hoist system. This meant that the internals of the helicopter had to be increased to a size of 17’ by 6.5’ with a 11.5’ rear bay for ease of loading stretchers as shown in Figure 7-7.

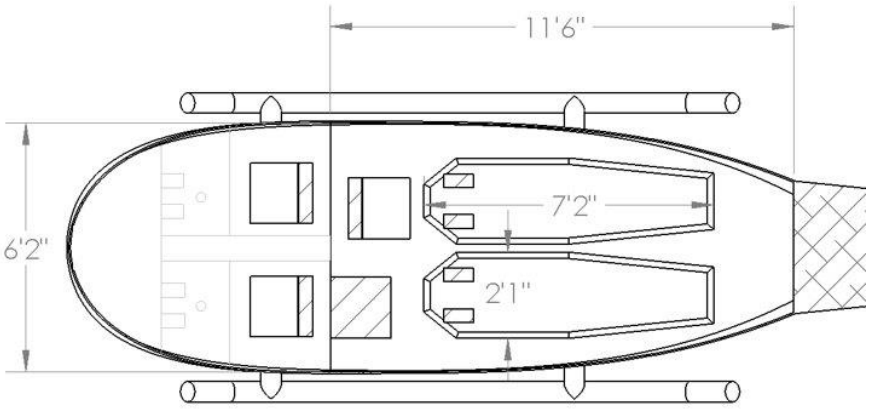

Figure 7-7. Internal View

Engine Selection

To find what engine was needed that can have enough power at those high altitudes, a spreadsheet was made to find the service ceiling where several values were calculated like density, power at hover for main rotor and tail rotor as well as power of the engine at those densities. We also used the following relationship to obtain the engine power:

$$\frac{P}{P_{sea-level}} = \frac{\rho}{\rho_{sea-level}}$$

Equation 18

The following is an extract of the spreadsheet with the three altitudes:

h, ft	4599.7377	12401.58	29527.56
rho (slugs/ft^3)	0.0019345	0.001512	0.000834
A MR (ft^2)	804.24772	804.2477	804.2477
A TR (ft^2)	29.224666	29.22467	29.22467
v MR (ft/s)	39.924978	45.15657	60.81713
sigma MR	0.1750704	0.17507	0.17507
sigma TR	0.2087278	0.208728	0.208728
Vtip MR (ft/s)	653.45127	653.4513	653.4513
Vtip TR (ft/s)	652.8439	652.8439	652.8439
P MR (lbs*ft/s^2)	289094.15	310382.9	388487.3
Q MR (lbs*ft/s)	7078.579	7599.842	9512.258
T TR (lbs)	352.16811	378.1016	473.2466
v TR (ft/s)	55.808327	65.40402	98.54827
P TR (lbs*ft/s)	26029.93	31774.02	57782.32
P req (hp)	572.95288	622.1035	811.3993
P avail (hp)	2350.0138	1837.037	1012.763
R/C (ft/min)	11823.187	8083.229	1339.72

Figure 7-8. Required power at different heights

Using the spreadsheet, it was found that to be able reach a service ceiling of 29527 ft, the power required of the engine is of 2550 hp. After extensive search, there was no engine that had that amount of power, the engines were either lower or higher. Two options were considered, having our rotorcraft have one engine with high power or two engines each with low power. Two engines normally bring too much weight, for this reason we selected one engine that had higher power. At the end, the selection was the CT7-8A7 engine from the General Electric Aero Engine company it gives 3000 hp total power. The calculations were done again using this engines power and including an installation loss of 10%. The following graph was what was obtained:

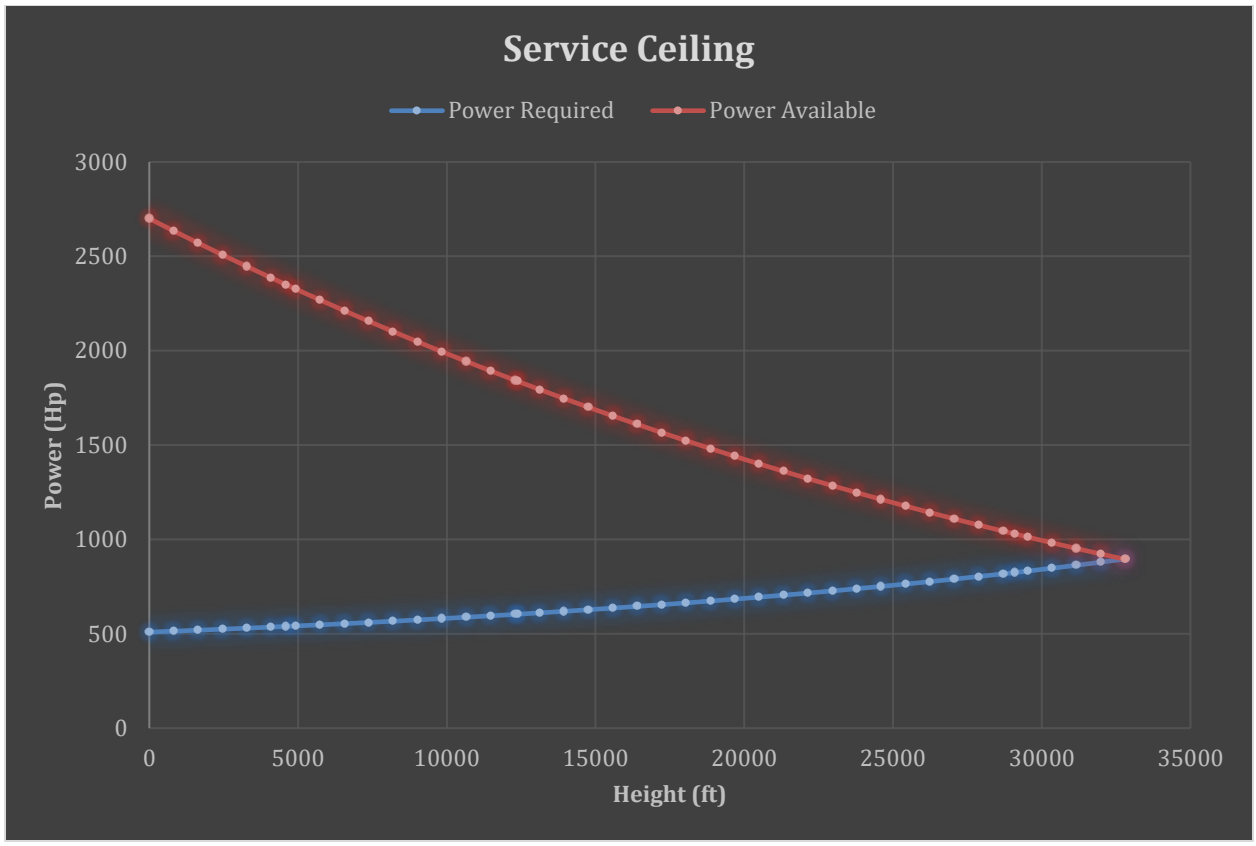

Figure 7-9. Service Ceiling

It can be seen that the service ceiling for this engine and our rotor is at about 32000 feet.

The following is a picture of the engine selected:

Figure 7-10. GE CT7-8A

The CT7-8 family of engines is described by the GE company as the following: “The highest reliability of any engines in its class, the CT7-8 engine provides maximum mission performance. Certified by the FAA in April 2004, the CT7-8 combines advanced, state-of-the-art technology with mission proven T700 design architecture. Designed for increased durability with commercially proven components, these powerful engines feature Full Authority Digital Electrical Control (FADEC) for better cockpit information and reduced pilot workload. The CT7-8 proudly powers a variety of multi role aircraft including the S92, AW101, and NH90.”

The most important aspects of the CT7-8A7 is that it weighs 537 lbs. and has a specific fuel consumption of 0.45 lb./h/hp.

Weight Calculations

With the engine selected and the forward flight power curve made, weight estimations were made. The following tables give us an idea of the weight available for several parts of the helicopter:

Table 7-1. Fuel estimates

Leg 1	Time (hours)	Power Needed (hp)	Fuel Needed (lbs)
Hover (TO)	0.033333333	567	8.505
Climb	0.009803922	355	1.566176471
Cruise	0.675	676	205.335
Hover (Land)	0.033333333	607	9.105
Total	0.751470588		224.5111765
Leg 2			
Hover (TO)	0.033333333	615	9.225
Climb	0.029367284	374	4.942513889

Cruise	0.189189189	454	38.65135135
Hover	0.5	798	179.55
Cruise	0.243478261	374	40.9773913
Hover (Land)	0.033333333	615	9.225
Total	1.028701401		282.5712565
Leg 3			
Hover (TO)	0.033333333	607	9.105
Cruise	0.675	676	205.335
Hover (Land)	0.033333333	567	8.505
Total	0.741666667		222.945

Item	Weight (kg)	Weight (lbs)
3 Crew + Payload + 2 PAX	575	1265
Hoist Jenoptix	53	116.6
fuel	159.0909091	350
Engine	244.0909091	537
Fuselage and rotors	1218.818182	2681.4
Total	2250	4950

Figure 7-11. Weight Estimates.

In table 6.1, the fuel consumption was calculated based on each leg of the mission. The second leg of the mission is the one that requires the most amount of fuel. Since there is refueling before each leg, the fuel tank should be capable of carrying at least 282 lbs. of fuel. For this matter, it was decided that a fuel tank that could carry 350 lbs. of fuel to have some reserve would be adequate.

In the second figure the itemization of the weight can be seen. The payload which includes the crew members, equipment and patients is of 575 kg, the hoist is 53 kg, fuel is 159 kg, engine is 244 kg and that leaves 1218 kg for the fuselage and rotors. All of this amounts to a grand total of 2250 kg. Once final fuselage weight calculations are done and total weight is found, all calculation can be remade to the required weight.

Failure Mode & Effect Analysis

Largely used when analyzing a system, the failure mode and effect analysis (FMEA) allows engineers to identify the modes in which a system will fail and the effects that these failures will have on said system. In order to accurately conduct this analysis, the system must be broken down into specific components in order to identify where specific failures may occur.

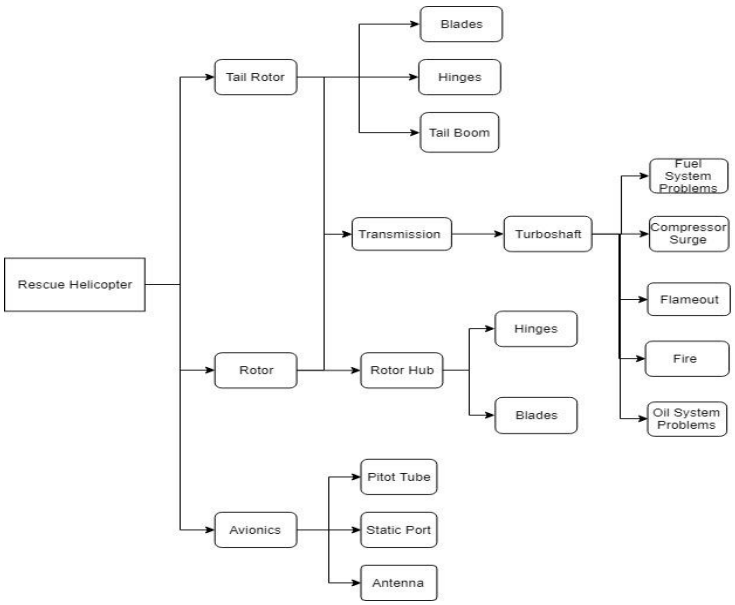

Figure 7-12 Diagram.

Referencing the system breakdown above, the rescue helicopter is broken down into three main components. These components include the avionics, rotor, tail rotor, and their various subsystems. Combining this breakdown with empirical data, the reliability of the helicopter can be calculated. According to the FAA, not only do most crashes occur during takeoff and landing but they are often caused by human error. Other sources of information, including the National Transportation & Safety Board, also point in the direction that human error is the likely cause of most incidents. As seen below, the calculations produced an extremely high reliability for the current design of our system.

Fuel System Problems	0.8
Compressor Surge	0.95
Flameout	0.9
Fire	0.98
Oil System Problems	0.9
Turboshaft/Transmission	0.999998

Blades	0.995
Hinges	0.85
Tail Boom	0.96
Tail Rotor	0.9999999999

Hinges	0.9
Blades	0.97
Rotor Hub	0.997
Rotor	0.999999994

Pitot Tube	0.998
Static Port	0.9
Antenna	0.99
Avionics	0.999998

Rescue helicopter
1

Figure 7-13. Reliability

Hoist

The hoist system that was chosen for our helicopter is the Skyhoist 800 by JENOPTIX. It can be seen in the following figure:

Figure 7-14. Hoist

The SkyHoist 800 is a light weight hoist system that can carry more than the minimum required 300 kg of weight. The following figure gives a summary of the hoist's specifications:

Technical specifications	
Max. lifting load capacity	760 lbs (@ 197 ft/min) 350 kg (@ 1.0 m/s)
Max. lifting speed	390 ft/min (@ < 330 lb) 2.0 m/s (@ < 150 kg)
System target weight	max. 110 lb max. 50 kg
Cable length	max. 390 ft max. 120 m
Power supply	28 V DC, 150 A (or 115 V AC)
Power consumption	approx. 4.2 kW

Figure 7-15. Hoist Specifications

Avionics

When considering the conditions of Everest, top of the line flight control systems and avionics must be incorporated in order to give pilots the best chance possible in order to complete the mission at hand. To meet these conditions, an integrated flight deck must be utilized in order to supply all the information he or she needs. A Garmin 3000H is a good example of the flight deck which can be seen to the right. Integrated flight decks remove all the clutter of conventional avionics and incorporate all the instruments needed into a few touch screen displays.

Figure 7-16. Avionics

From a human machine system aspect, an integrated flight deck is one of the better choices because it provides a high reliability under the given local operating conditions.

Transmission

The transmission of the helicopter will consist of a main gear box that will reduce the RPM's of the engine in two different speeds. It will have a top part with a gear ratio of 56.26:1 to reduce the speed of the engine from 21945 RPM to 390 RPM for the main rotor. It will also have a bottom part that will have a reduction ratio of 3.57:1 to the tail drive shaft for a speed of 6132 RPM. The tail rotor drive shaft will be separated into 8 sections and go down to the tail gear box that changes the direction of the shaft to 90 degrees and have a gear reduction ratio of 3:1 for a tail rotor speed of 2044 RPM. The following is a rough schematic of the transmission architecture.

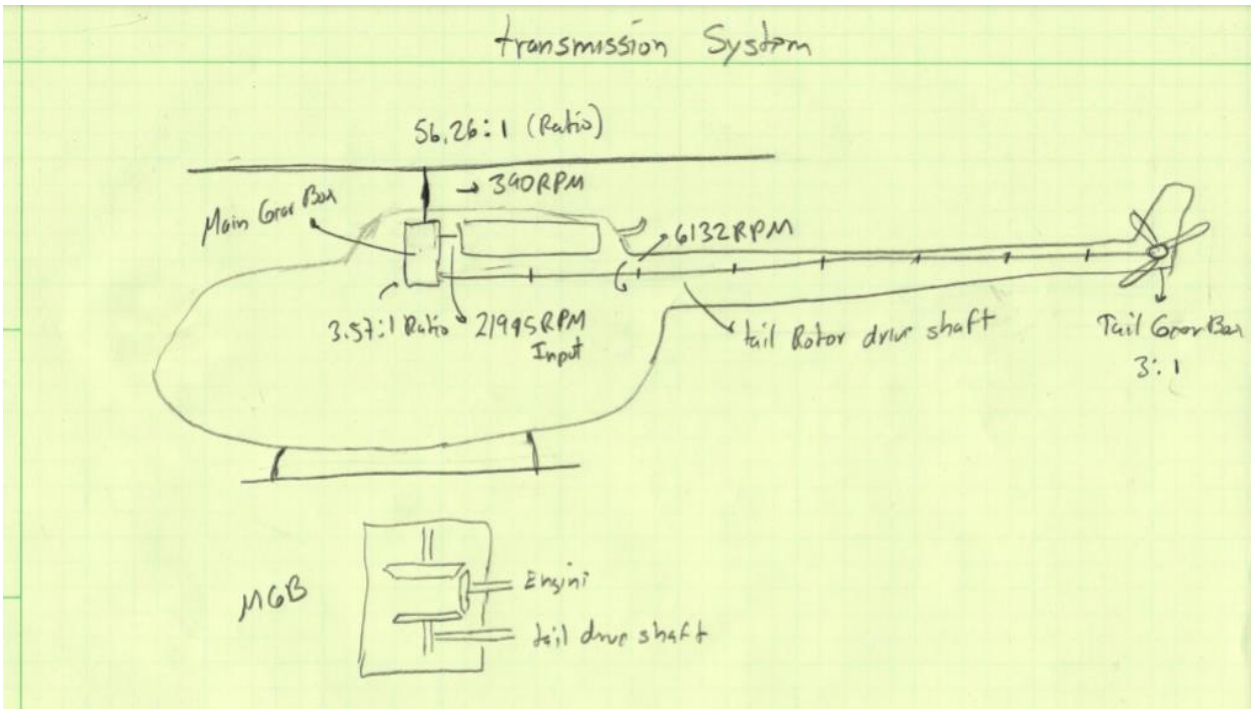

Figure 7-17. Transmission sketch

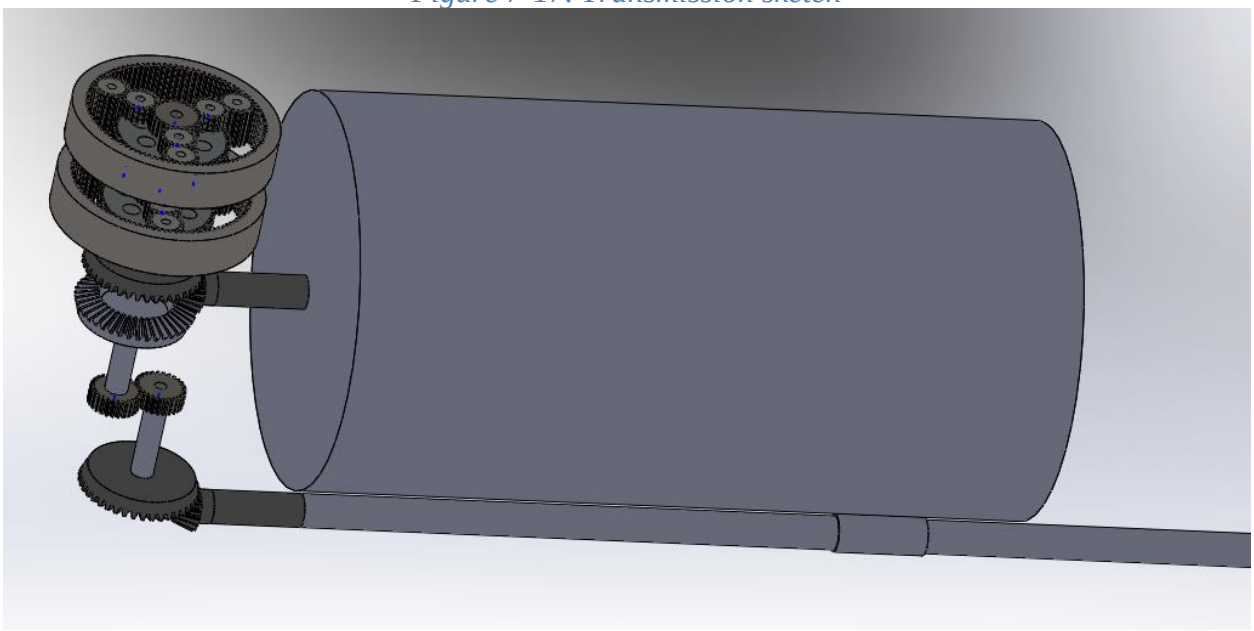

Figure 7-18. Transmission CAD

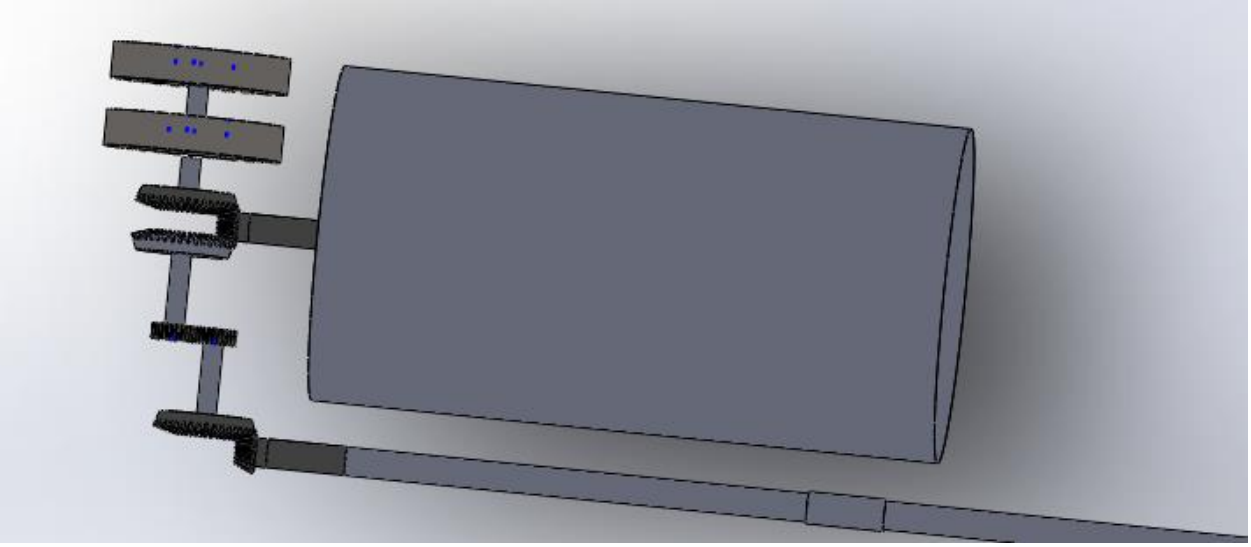

Figure 7-19. Transmission CAD side view

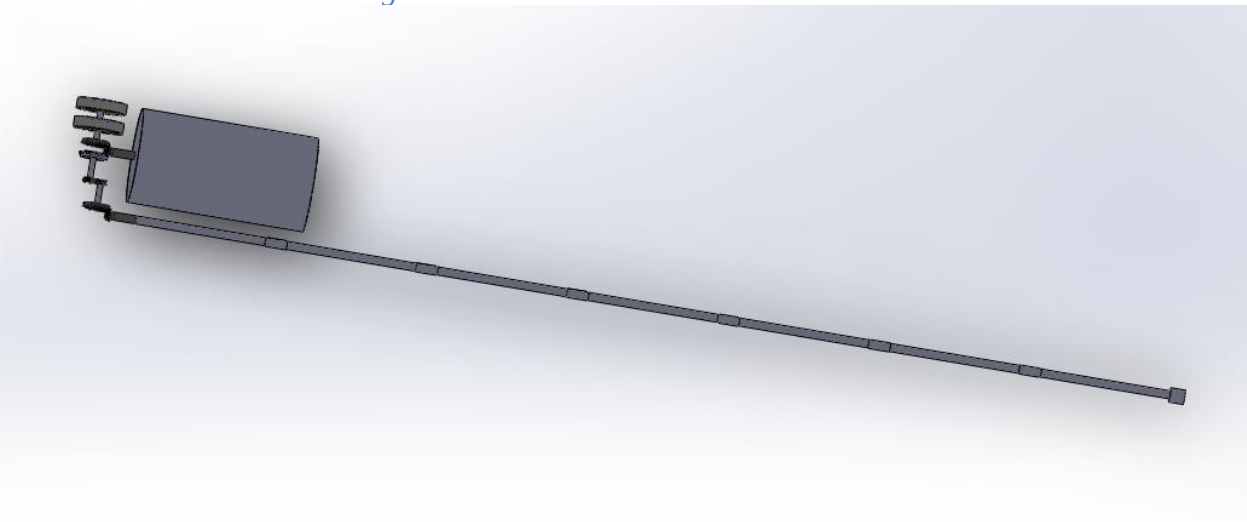

Figure 7-20. Transmission CAD complete view

Materials

Material selection is also an important process in making a helicopter. For aircraft there are various materials that can be used to build the fuselage and other parts, some of these are titanium alloys, aluminum alloys, carbon fiber and metallic composites. All of these materials vary with density, price and other aspect. The following graphs show a comparison of these materials:

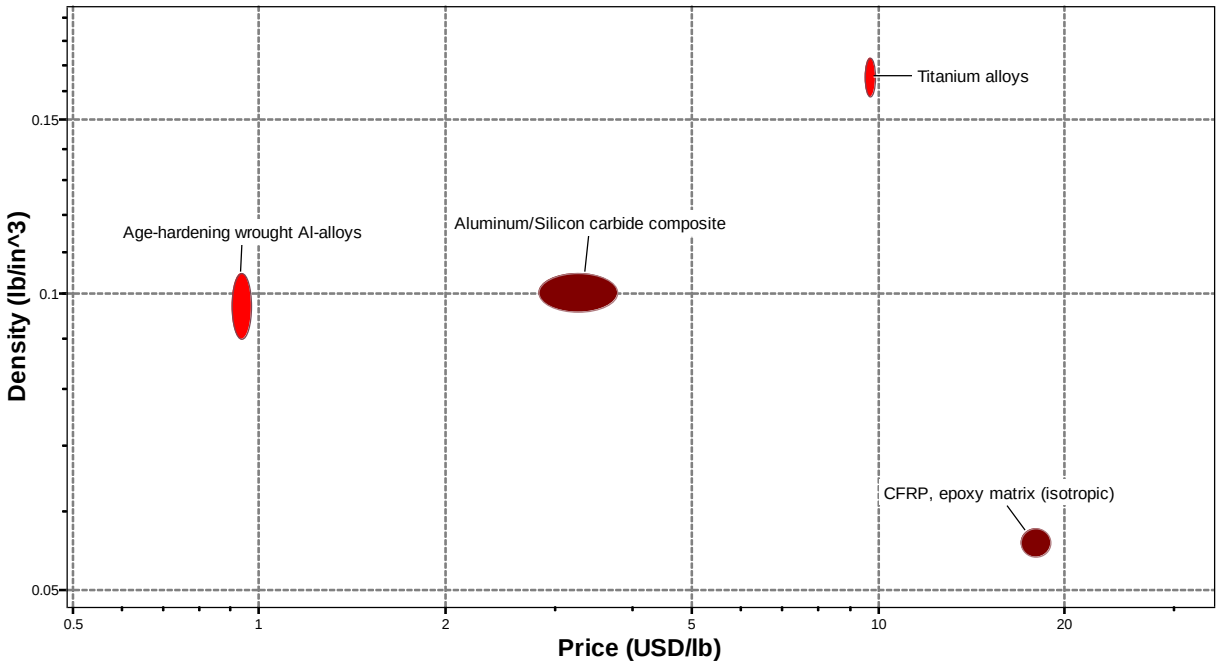

Figure 7-21. Density vs price

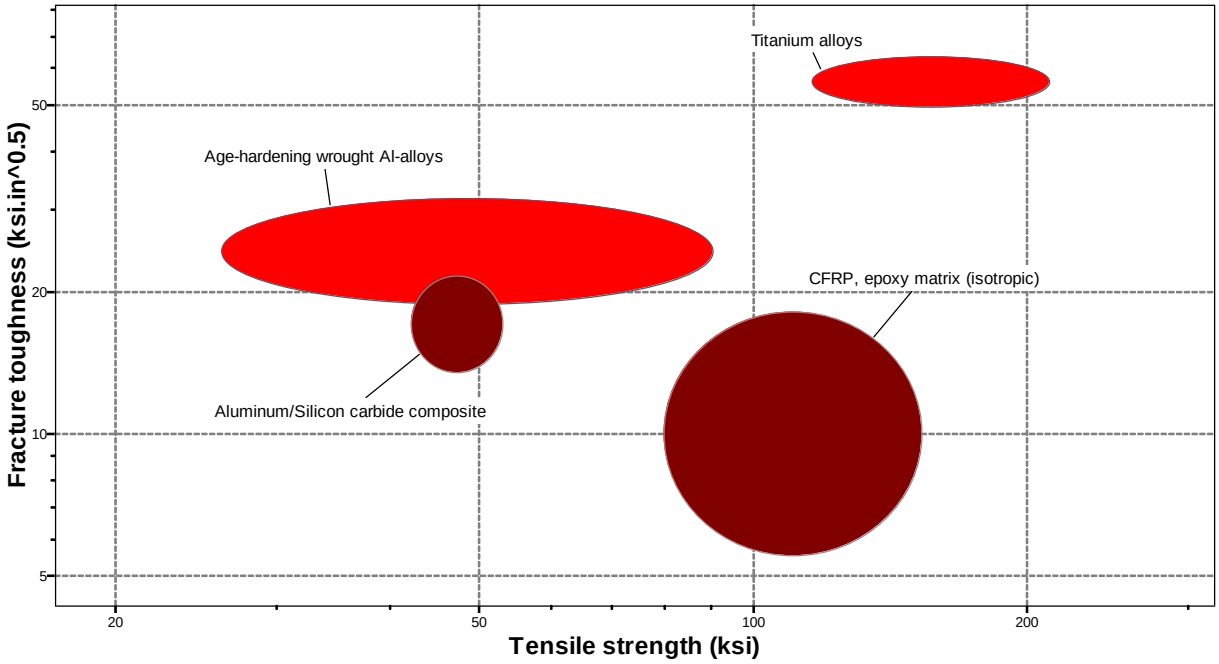

Figure 7-22. FRacture toughness vs Tensile Strength

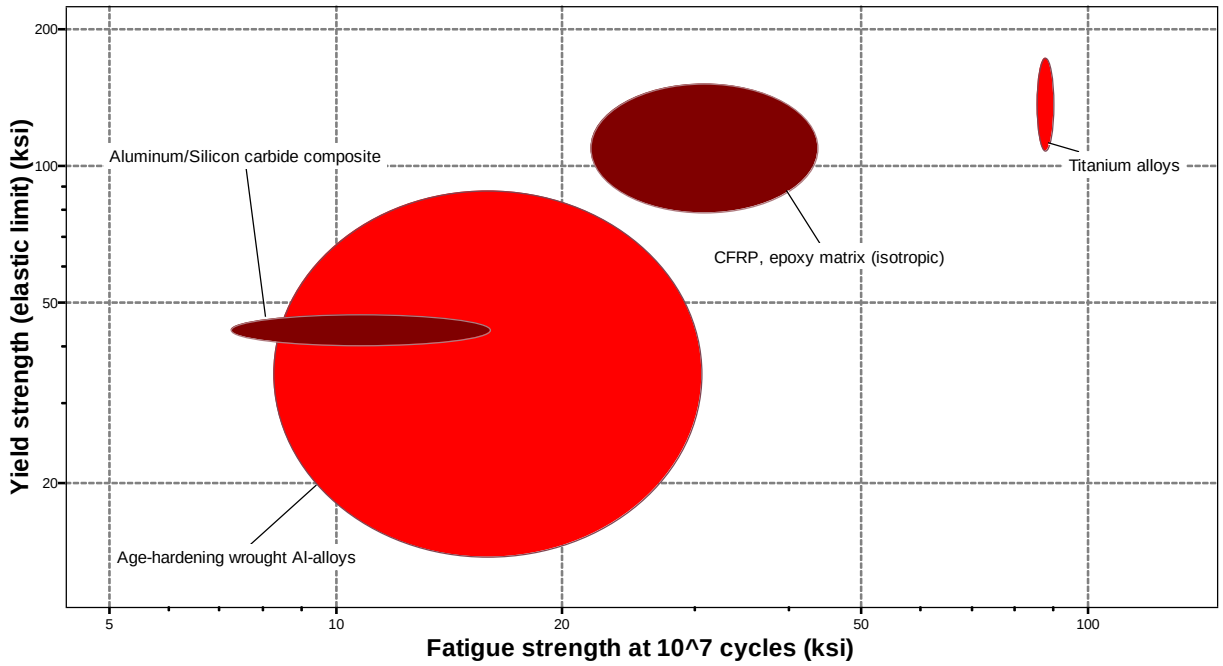

Figure 7-23. Yield vs Fatigue

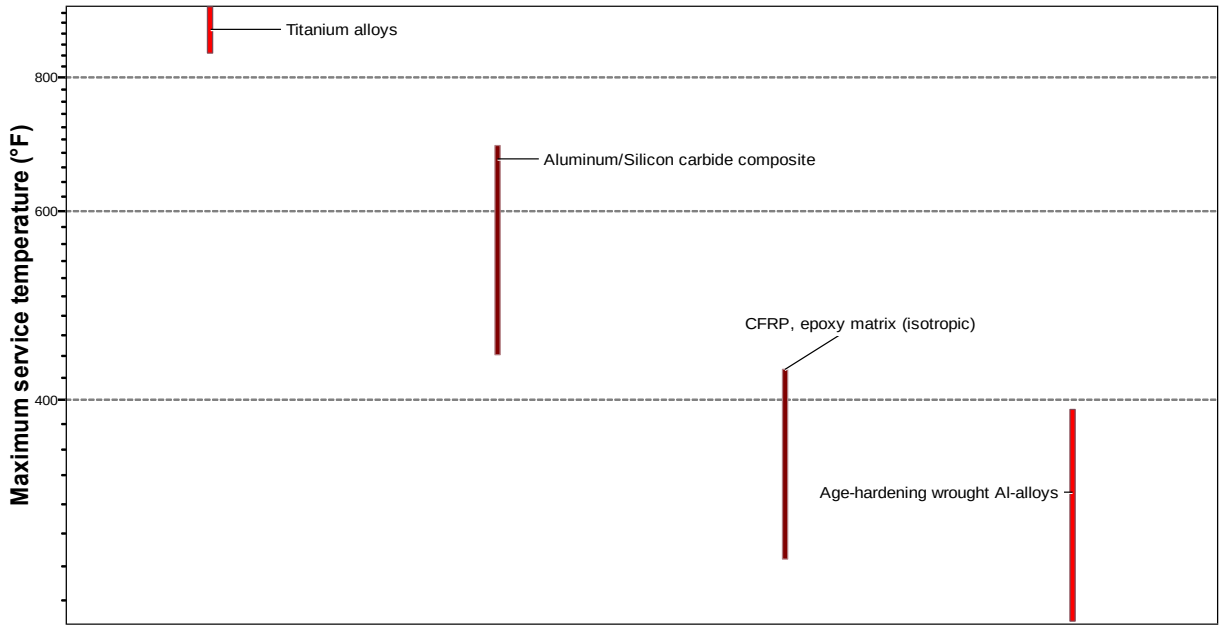

Figure 7-24. Max Temperature

These graphs show various properties of the materials that are important to consider when building a helicopter. In the first graph we can see that the titanium alloys have higher densities and are somewhat expensive while carbon fiber has really low density but is the most expensive.

In the second and third graphs it can be seen that titanium alloys have higher strength and fatigue strength while the others are a bit lower. In the last graph we can see that titanium alloys have better temperature resistance than the rest. With these aspects, we could consider that the part where the engine is located can be made with titanium alloys since it is hotter. The rotor can be made of a carbon fiber composite since it is less likely to fracture from stresses and the fuselage can be made of aluminum alloys or a metal composite with graphite epoxy. The important parts like gears, etc. will be made of steel.

Chapter 8: Cost Analysis

In our cost analysis, we decided to use the "RAND DAPCA IV Model." This model estimates the hours required for RDT&E and production by the engineering, manufacturing, and quality groups. These are then multiplied by the corresponding hourly rates to give estimated costs [10]. The total cost can then be calculated by using the following equation:

$$RDT\&E + flyaway = H_E R_E + H_T R_T + H_M R_M + H_Q R_Q + C_D + C_F + C_M + C_{eng} N_{eng} + C_{avionics}$$

Equation 19

$$H_E = Eng\ Hours, \quad R_E = Eng.hourly\ rate, \quad H_T = Tooling\ Hours,$$
$$R_T = Tooling\ Hour\ rate, \quad H_M = Mfg\ hours,$$
$$R_M = Manufacturing\ Hourly\ rate, \quad H_Q = QC\ hours,$$
$$R_Q = Quality\ Control\ hourly\ Rate, \quad C_D = Devel\ support\ cost,$$
$$C_F = Flt\ Test\ Cost, \quad C_M = Mfg\ Materials\ Cost,$$
$$C_{eng} = Eng\ Production\ Cost,$$
$$N_{eng} = total\ production\ quantity\ times\ number\ of\ engines\ per\ aircraft,$$
$$C_{avionics} = cost\ of\ avionics$$

The results showed if we produced more of the new helicopter, the less it will cost. If we produced one unit, then it will roughly come out to be $100,000,000. However, if we produced 40-50 units, then it will be in the $2,000,000 range. Realistically, 2-5 units will be manufactured for production on top of the 10 units that will be used for testing purposes. The next step would be to estimate the crew costs. This is done by using the equation seen below:

$$Three - man\ crew\ cost = 94.5\left(V_c \frac{W_0}{10^5}\right)^{0.3} + 237.2$$

Equation 20

$$V_c = cruise\ velocity, W_0 = Take\ off\ gross\ weight$$

By using this equation, we were able to determine that it will roughly cost $375 per block hour ($1125 for the entire three-hour mission) for a three-man crew to operate the hovercraft [10].

Chapter 9: Conclusion

The final conceptual design of the helicopter meets all the needs required for it to complete the overall mission profile. The final weight of the rotorcraft is at 4960 lbs. (2250 kg.) and has enough space to carry three crew members, two patients and the required medical equipment. The helicopter comes with a hoist that can carry a rated weight of 660 lbs. (300 kg.) and a reliable avionics system. The GE CT7-8AF engine selected will have enough power to take the helicopter to the top of Mount Everest considering the loss of power because of low air density. Theoretical analysis showed that it has max speeds of almost 300 ft/s (91.4 m/s) and will be able to complete the mission in the required three-hour timeframe. This analysis also showed that it can withstand the crosswinds of 67 ft/s (20 m/s) that are present at the top of the mountain. CFD analysis using SolidWorks showed that it can produce enough thrust to carry the helicopter to the top. And finally, cost analysis showed that with the production of about 50 units in five years, the helicopter would cost around two million dollars which is comparable to other helicopters. This helicopter would be of great support to all the mountain climbers of Mount Everest and other highest peaks of the world while being able to save the lives of those that need it.

Overall Evaluation Criteria

To effectively evaluate our design, we needed to create an overall evaluation criteria system. This system allowed us to evaluate multiple objectives that our helicopter was set out to do by using a single numerical index. In our table, we gave our six main objectives (speed, weight, height, time, power, and passengers) a worst and best value. Sense of the Quality Characteristic (QC) indicates the desire of the specific objective. This ranges from “Bigger,”

"Nominal," and "Smaller." The OEC column is an overall grade for the objective [14]. The equations can be seen below:

$$Bigger\ OEC = \frac{Final\ Results - Worst\ Value}{Best\ Value - Worst\ Value} * Weighted\ \%$$

Equation 21

$$Nominal\ OEC = (1 - \left|\frac{Final\ Results - Best\ Value}{Best\ Value - Worst\ Value}\right| * Weighted\ \%$$

Equation 22

$$Smaller\ OEC = (1 - \left|\frac{Final\ Results - Best\ Value}{Best\ Value - Worst\ Value}\right| * Weighted\ \%$$

Equation 23

Table 9-1: Overall Evaluation Criteria

Objectives	Worst Value	Best Value	QC	Weighting	Final Results	OEC
Speed (ft/s)	100	461.83	Bigger	30	290	15.75325
Weight (lbs)	12000	2000	Smaller	5	4960	3.52
Height (ft)	10000	30000	Bigger	40	29527	39.054
Time of Mission (hrs)	3	2	Smaller	10	2.5	5
Power Output (HP)	5000	900	Smaller	5	3000	2.439024
Passenger Capability	2	5	Nominal	10	5	10
Total				100		75.76628

Chapter 10: References

[1] The route. (n.d.). Retrieved from https://www.mounteverest.net/expguide/route.htm

[2] Veillette, P. (n.d.). World's Highest Helicopter Rescue. Retrieved from https://aviationweek.com/business-aviation/world-s-highest-helicopter-rescue

[3] 17 March 1969. (2019, March 16). Retrieved from https://www.thisdayinaviation.com/17-march-1969/

[4] Airbus. (2017, November 02). Landing on Everest: Didier Delsalle Recalls his Record Flight. Retrieved from https://www.verticalmag.com/features/landing-everest-didier-delsalle-recalls-record-flight/

[5] Wilkinson, F. (2019, March 15). Want to climb Mount Everest? Here's what you need to know. Retrieved from https://www.nationalgeographic.com/adventure/everest/reference/climbing-mount-everest/

[6] Airfoil Tools. (n.d.). Retrieved from http://airfoiltools.com/

[7] Bourdelot, N. (n.d.). HELICOPTERS. Retrieved from https://www.airbushelicoptersinc.com/products/H125-specifications.asp

[8] Rescue Hoists for Helicopters: Extremely Reliable and Safe. (n.d.). Retrieved from https://www.jenoptik.us/products/aviation-subsystems/rescue-hoists-cargo-winches

[9] The CT7 Engine. (n.d.). Retrieved from https://www.geaviation.com/commercial/engines/ct7-engine

[10] Raymer, Daniel P. Aircraft Design: a Conceptual Approach. Fifth ed., American Institute of Aeronautics and Astronautics, 2006

[11] Leishman, J. Gordon. Principles of Helicopter Aerodynamics. Second ed., Cambridge University Press, 2017.

[12] "NTSB Aviation Accident Database & Synopses." *National Transportation Safety Board (NTSB)*, ntsb.gov/_layouts/ntsb.aviation/index.aspx.

[13] "Different UML Diagrams - Purpose and Usage." Different UML Diagrams - Purpose and Usage, www.edrawsoft.com/uml-introduction.php.

[14] "Overall Evaluation Criteria." *Nutek*, nutek-us.com/QITT07%20-%20Overall%20Evaluation%20Criteria%20(OEC)%20Strategy.pdf.

Appendix A: Acknowledgements

We would like to acknowledge the following people and entities:

- Our Senior Design Advisor Professor Adeel Khalid for the help provided throughout all the semester.
- Airbus and the Vertical Flight Society for providing the project.
- Kennesaw State University and the Department of Systems and Industrial Engineering.

Appendix B: Contact Information

Anthony Chavarria

Email: Legendlink@gmail.com

Phone:404-528-8276

Matthew De Sieno

Email: mttdsn1@gmail.com

Phone: 770-315-4099

David Stuver

Email: stuver.david.k@gmail.com

Phone: 952-657-8022

Zach Boss

Email: zboss23@gmail.com

Phone: 404-435-0281

Appendix C: Reflections

Although projects of this caliber can be incredibly tough and time consuming, it was a great learning experience for everyone involved. The most challenging portion of the project was transitioning the conceptual model into a working CAD model. After completing the CAD portion, the model was refined and stressed using many flow simulations provided by Solid Works. Once the CAD model was complete, a 3D printer was utilized in order to give us a physical model. The rotor and tail rotor were printed separately from the fuselage and assembled once they were complete. Moving forward with the project, the CAD model will be refined until it exceeds our expectations.

Appendix D: BEMT Figures

Blade Design One:

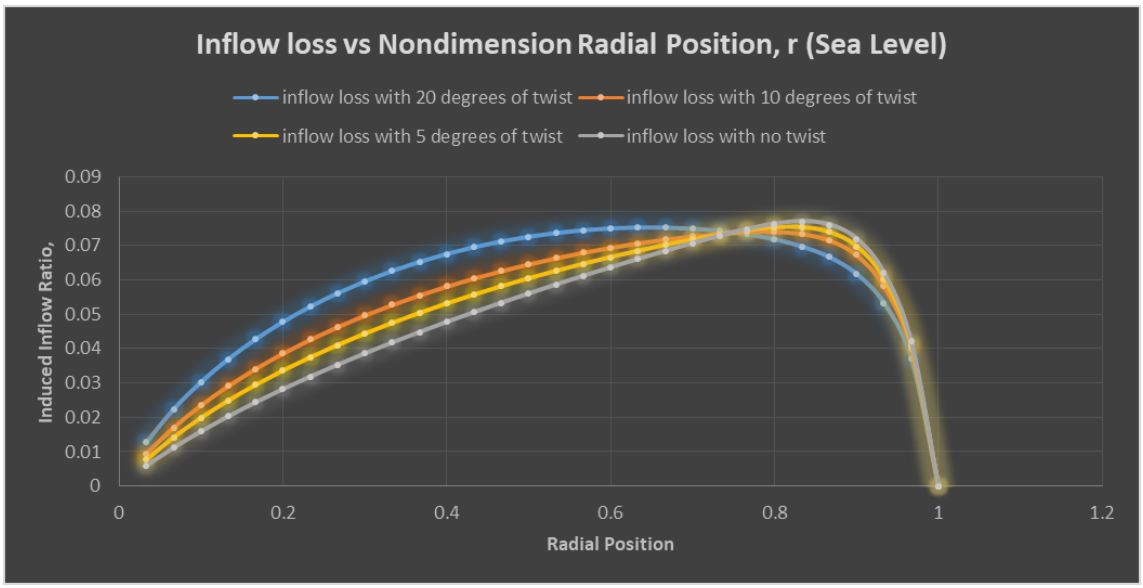

Figure D -1. Inflow vs Nondimensional R (sea level)

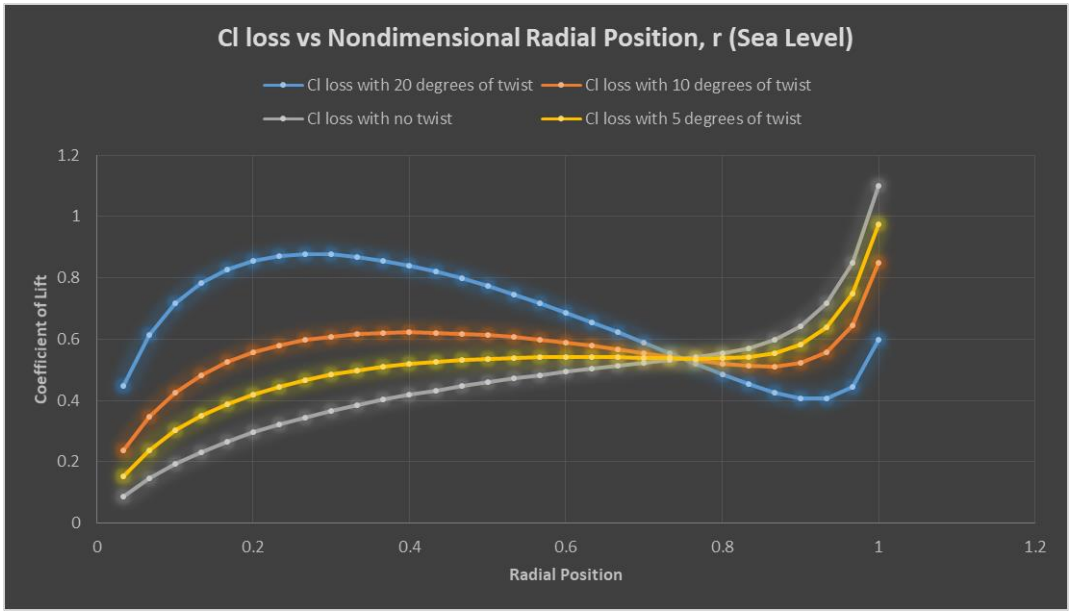

Figure D-2. Cl loss vs Nondimensional flow (sea level)

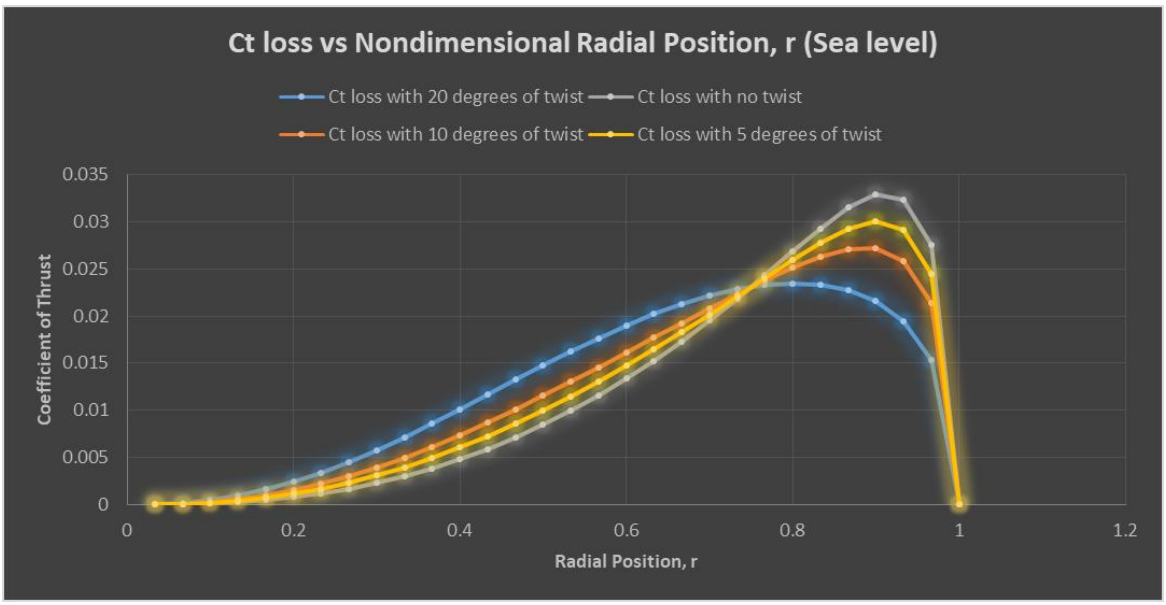

Figure D-3. Ct vs Nondimensional R (sea level)

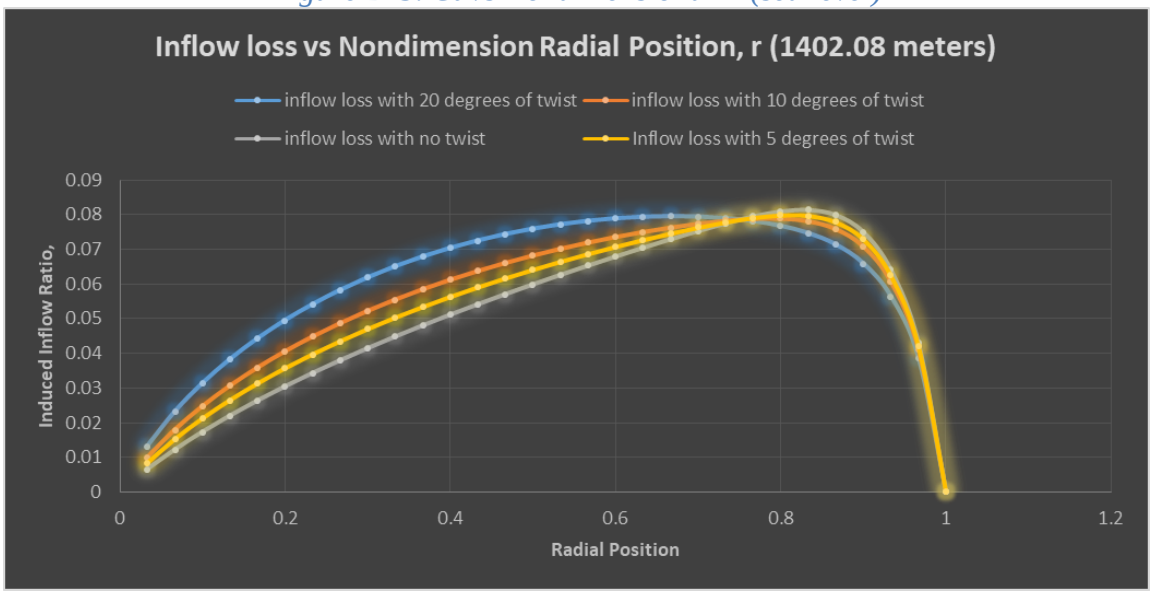

Figure D-4. inflow loss vs nondimensional r (1402.08)

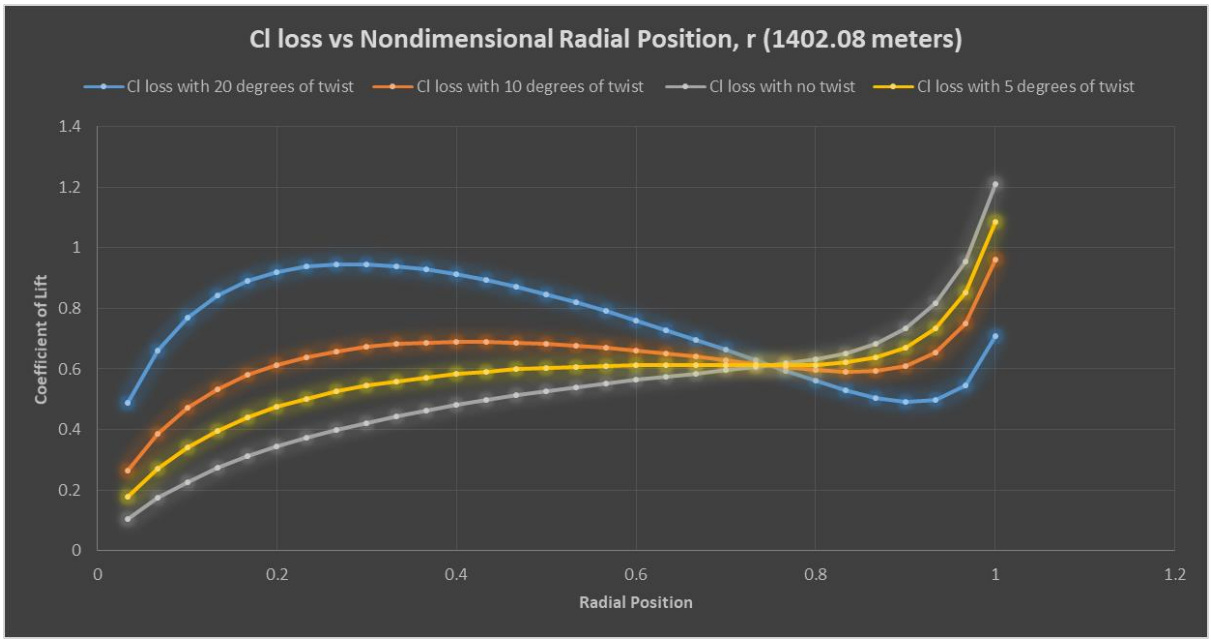

Figure D-5 Cl Loss vs Non-dimensional Radial Position, r (1402.08 meters)

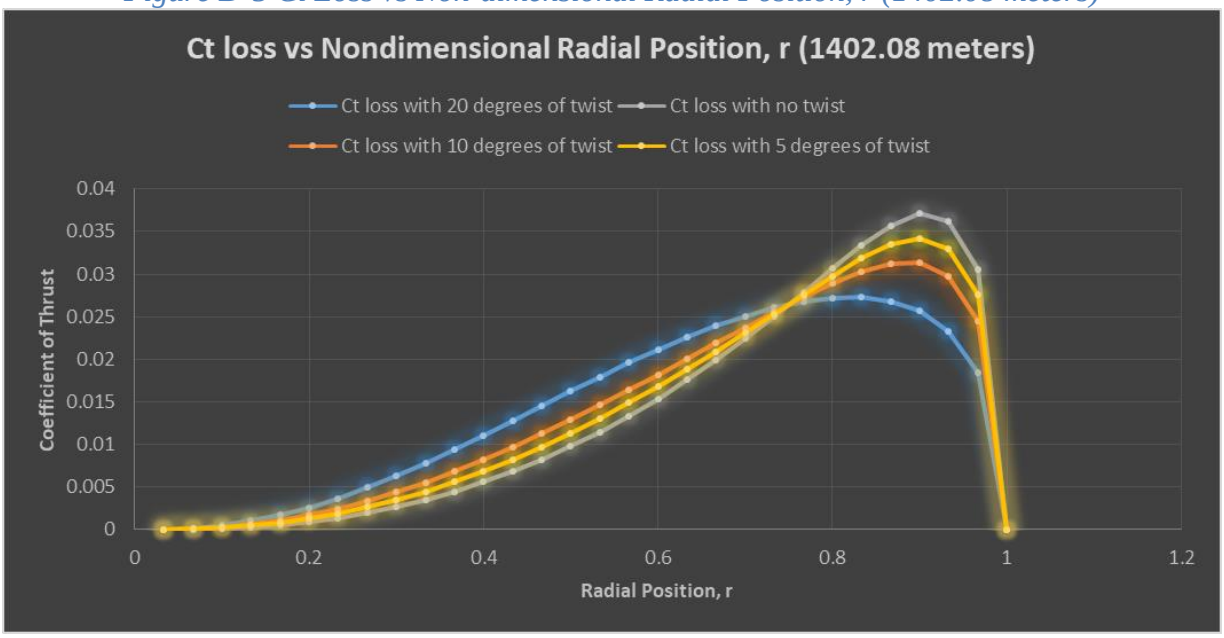

Figure D-6 Ct Loss vs Non-dimensional Radial Position, r (1402.08 meters)

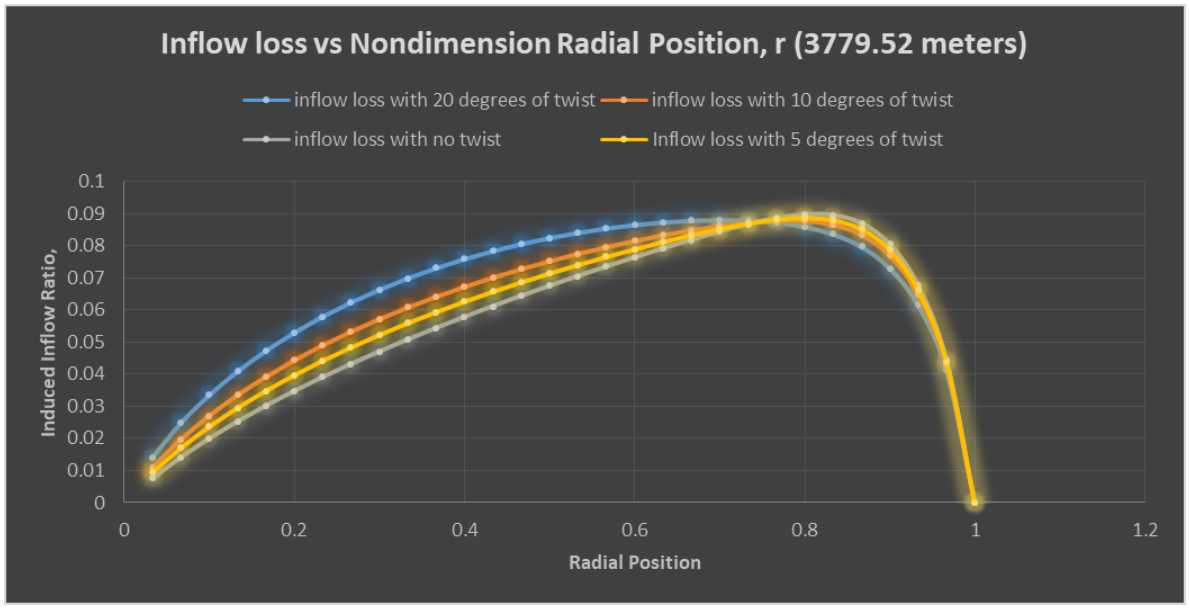

Figure D-7 Inflow Loss vs Non-dimensional Radial Position, r (3779.52 meters)

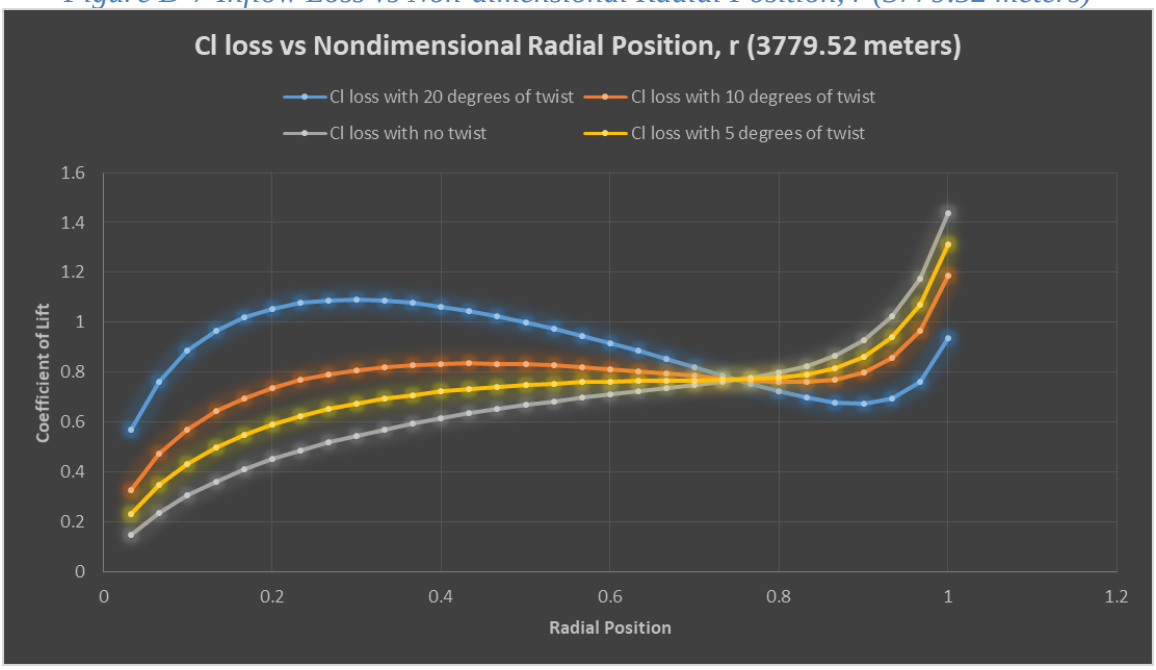

Figure D-8 Cl Loss vs Non-dimensional Radial Position, r (3779.52 meters)

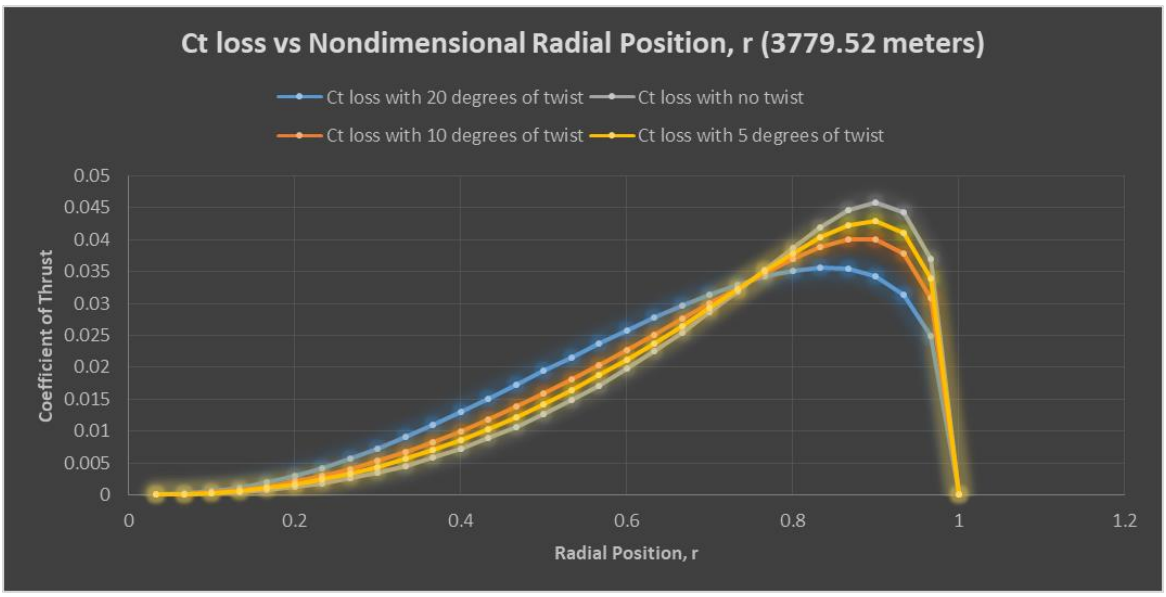

Figure D-9 Ct Loss vs Non-dimensional Radial Position, r (3779.52 meters)

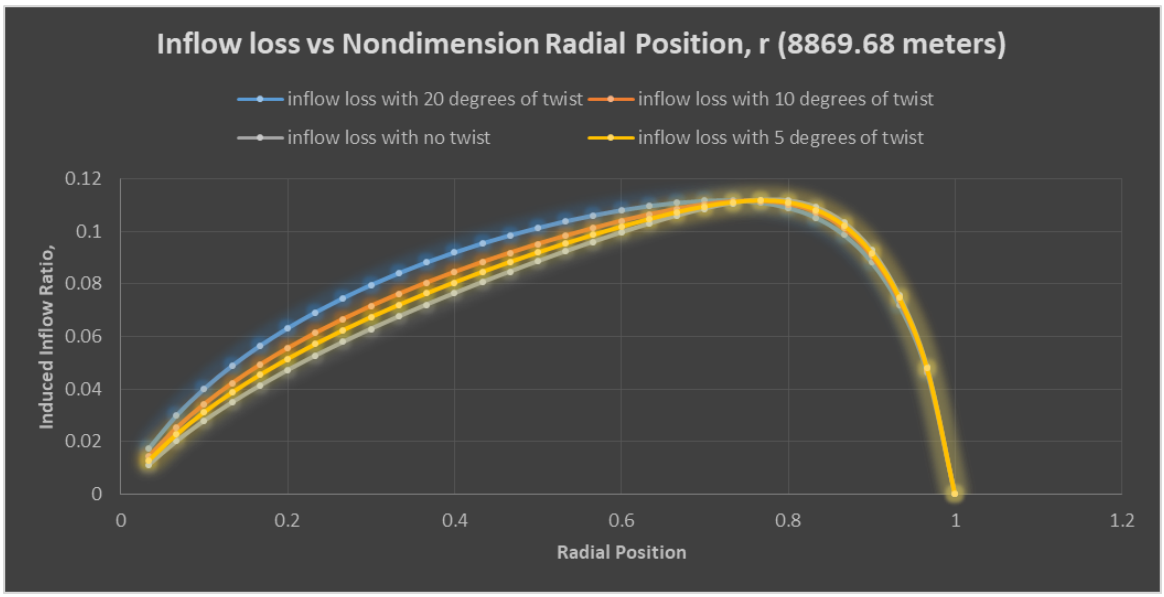

Figure D-10 Inflow Loss vs Non-dimensional Radial Position, r (8869.68 meters)

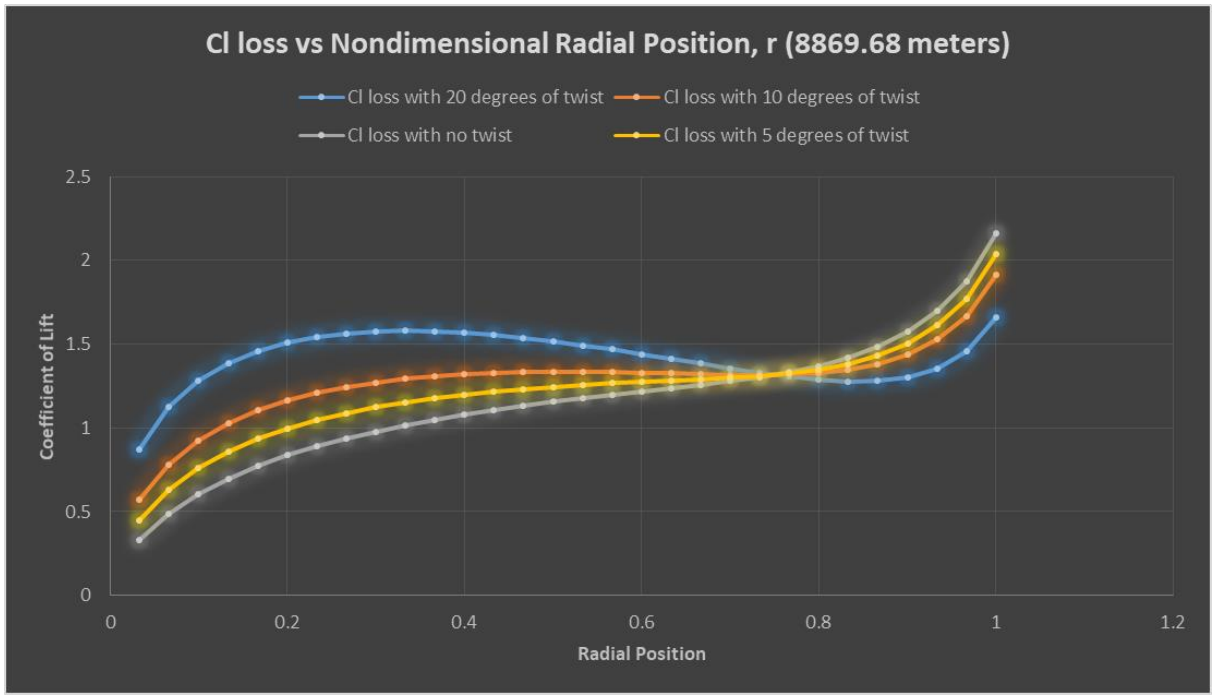

Figure D-11 Cl Loss vs Non-dimensional Radial Position, r (8869.68 meters)

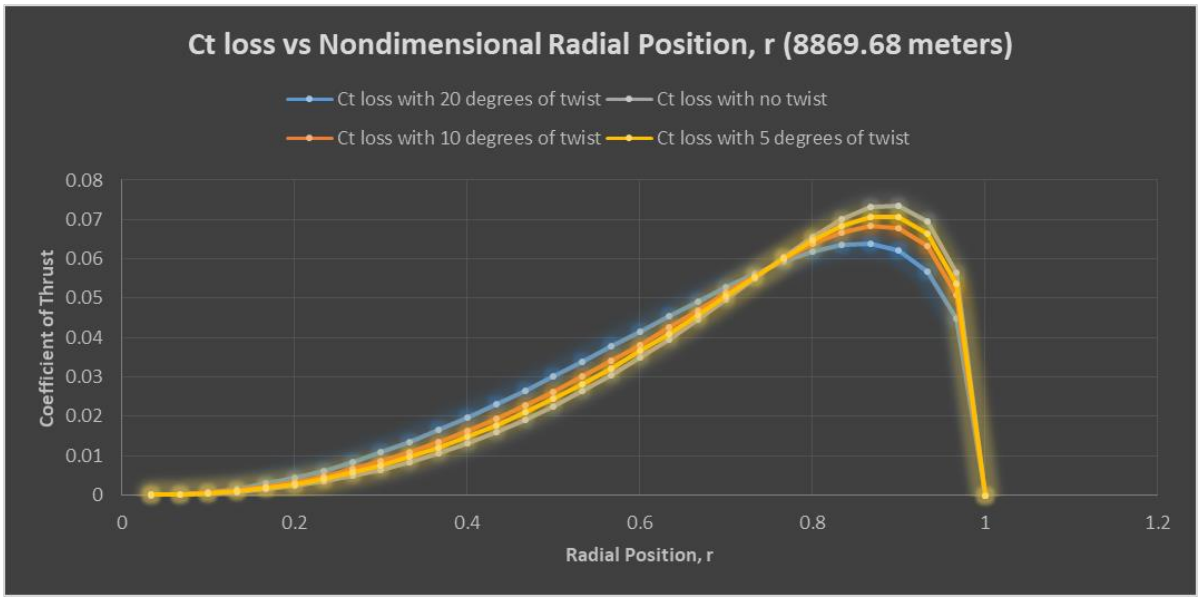

Figure D-12 Ct Loss vs Non-dimensional Radial Position, r (8869.68 meters)

Blade Design Two

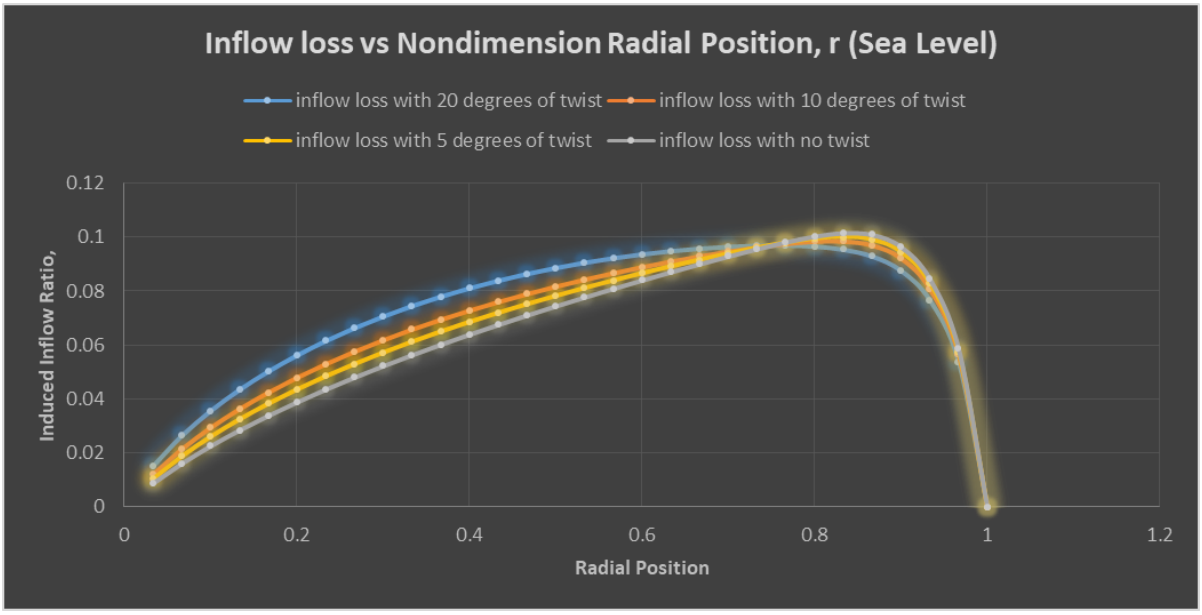

Figure D-13 Inflow Loss vs Non-dimensional Radial Position, r (Sea Level)

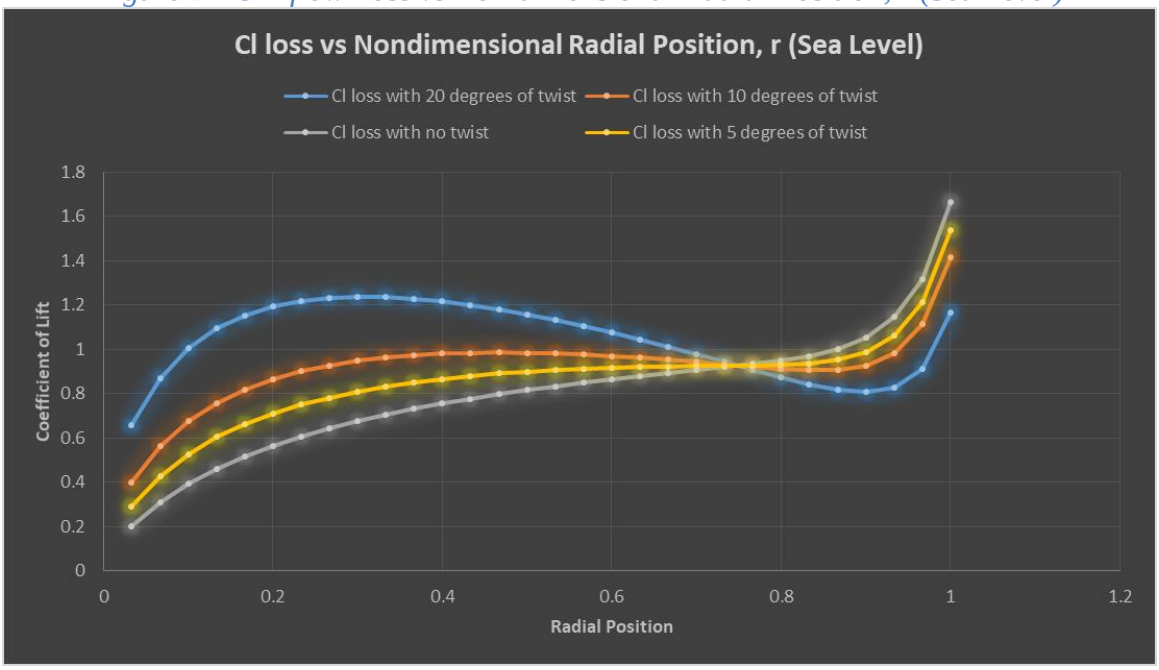

Figure D-14 Cl Loss vs Non-dimensional Radial Position, r (Sea Level)

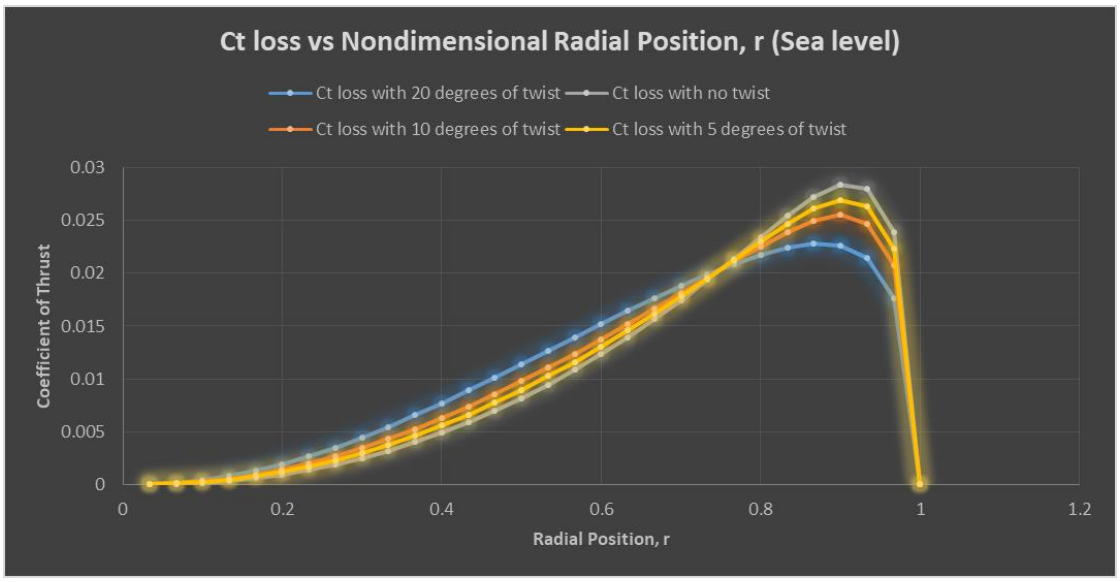

Figure D-15 Ct Loss vs Non-dimensional Radial Position, r (Sea Level)

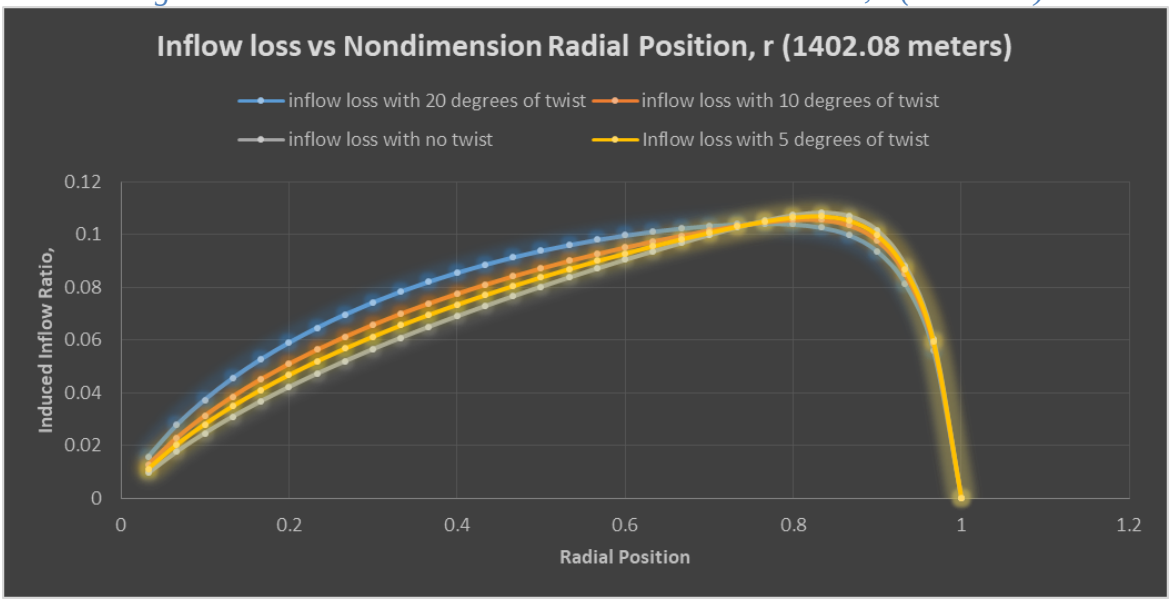

Figure D-16 Inflow Loss vs Non-dimensional Radial Position, r (1402.08 meters)

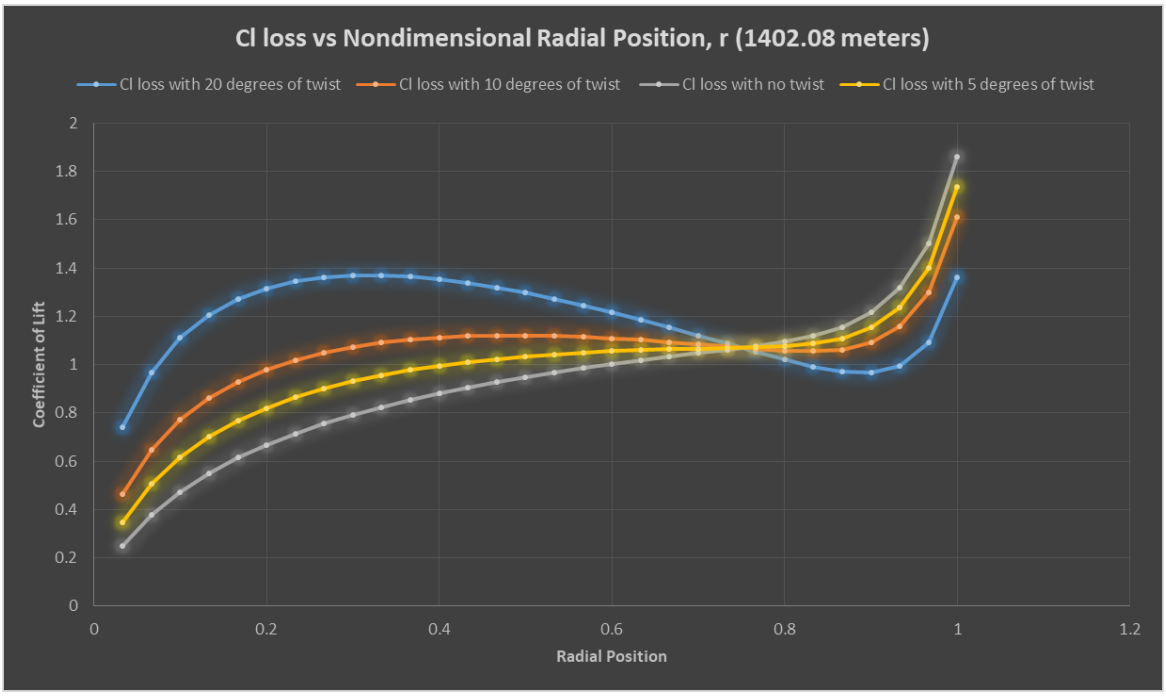

Figure D-17 Cl Loss vs Non-dimensional Radial Position, r (1402.08 meters)

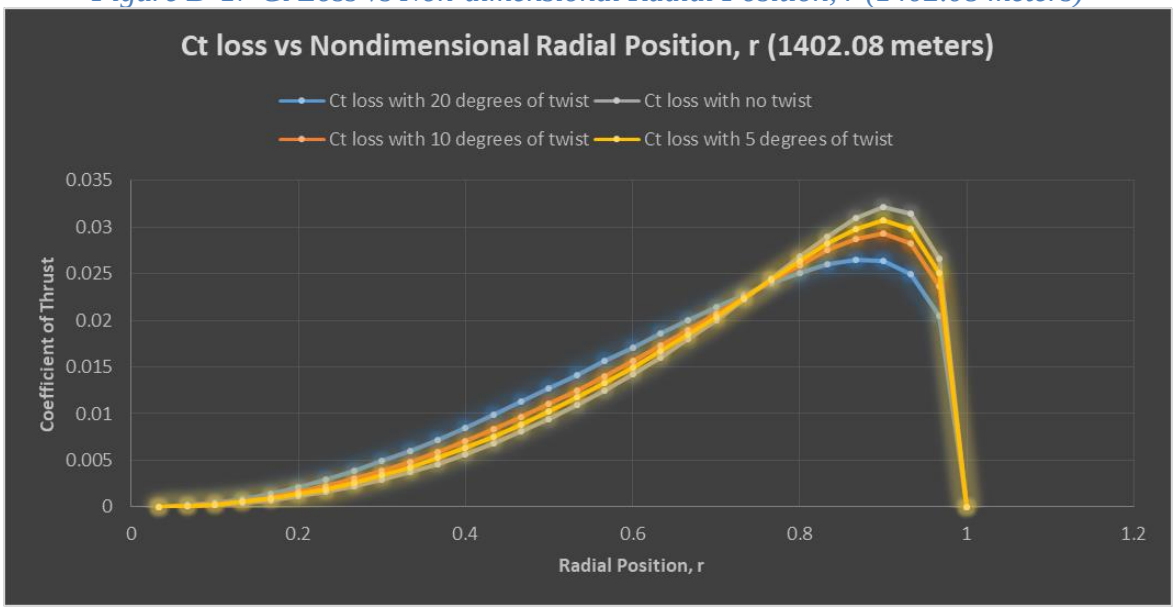

Figure D-18 Ct Loss vs Non-dimensional Radial Position, r (1402.08 meters)

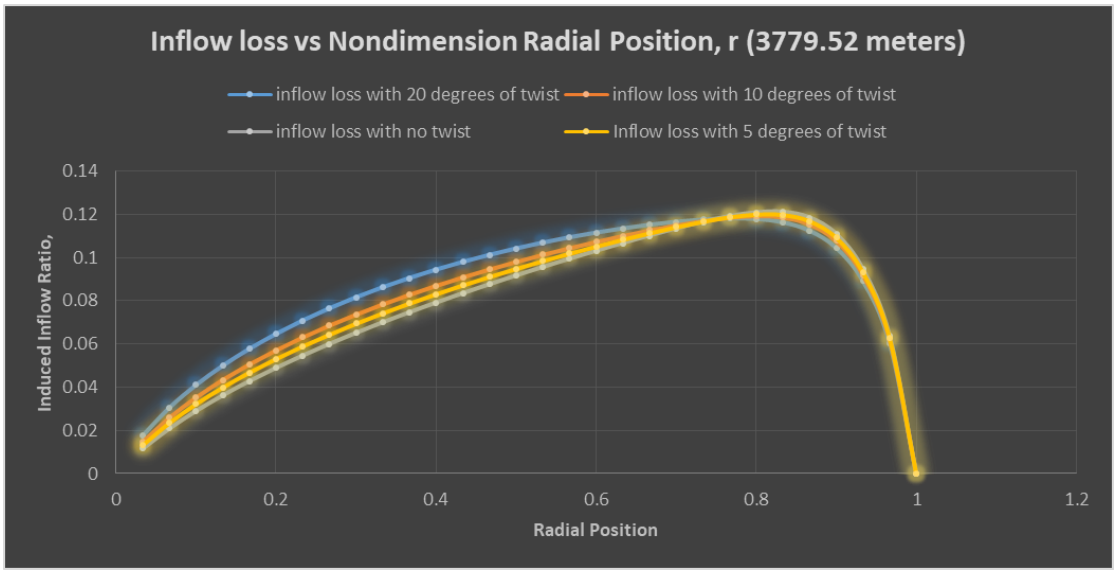

Figure D-19 Inflow Loss vs Non-dimensional Radial Position, r (3779.52 meters)

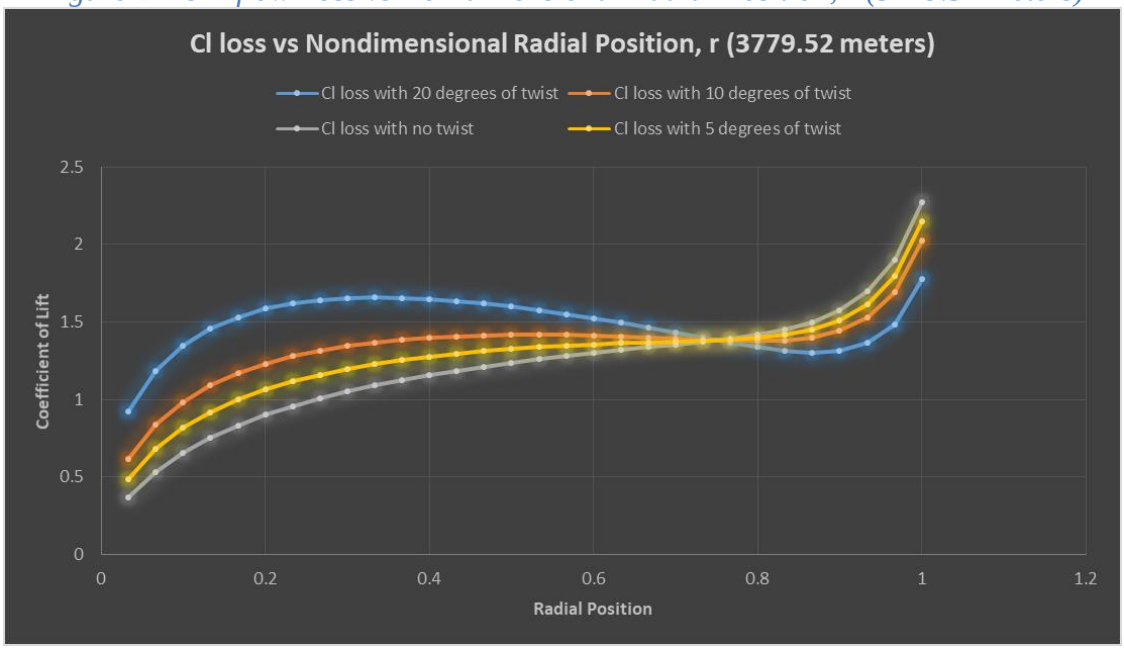

Figure D-20 Cl Loss vs Non-dimensional Radial Position, r (3779.52 meters)

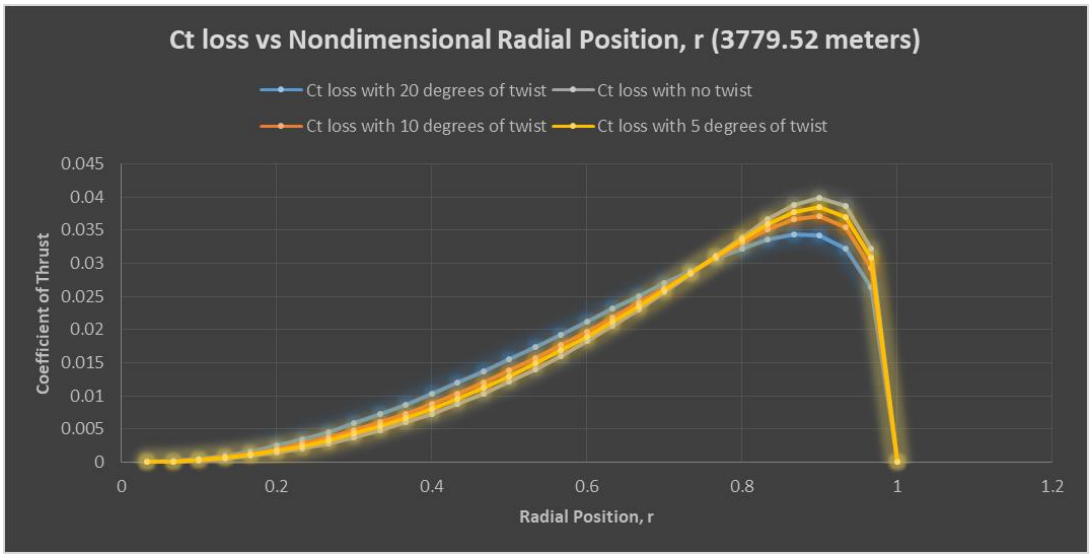

Figure D-21 Ct Loss vs Non-dimensional Radial Position, r (3779.52 meters)

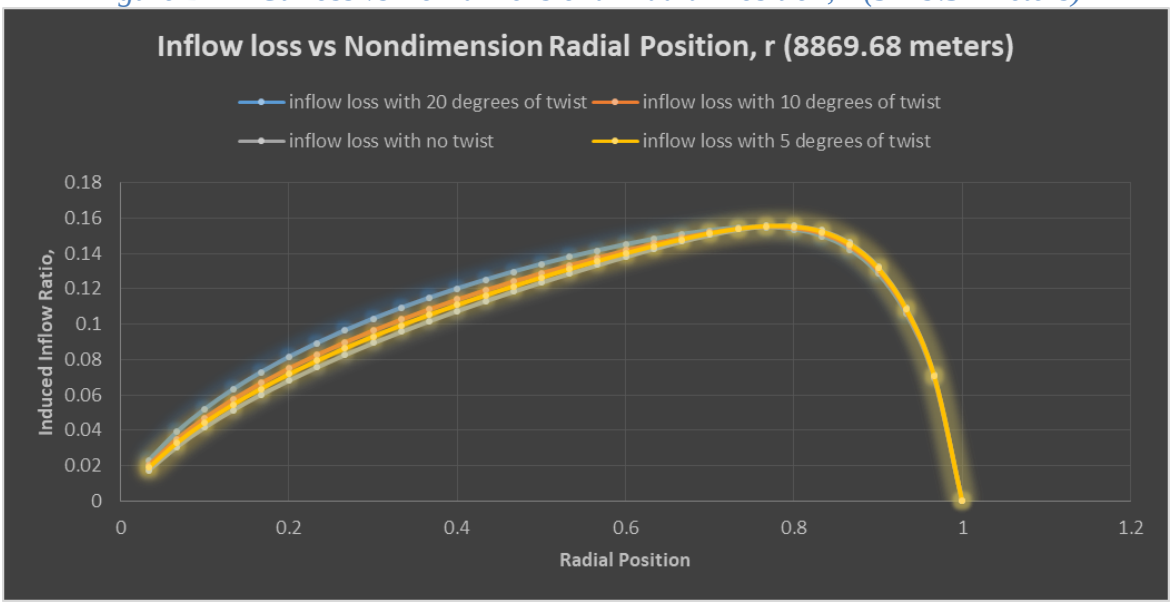

Figure D-22 Inflow Loss vs Non-dimensional Radial Position, r (8869.68 meters)

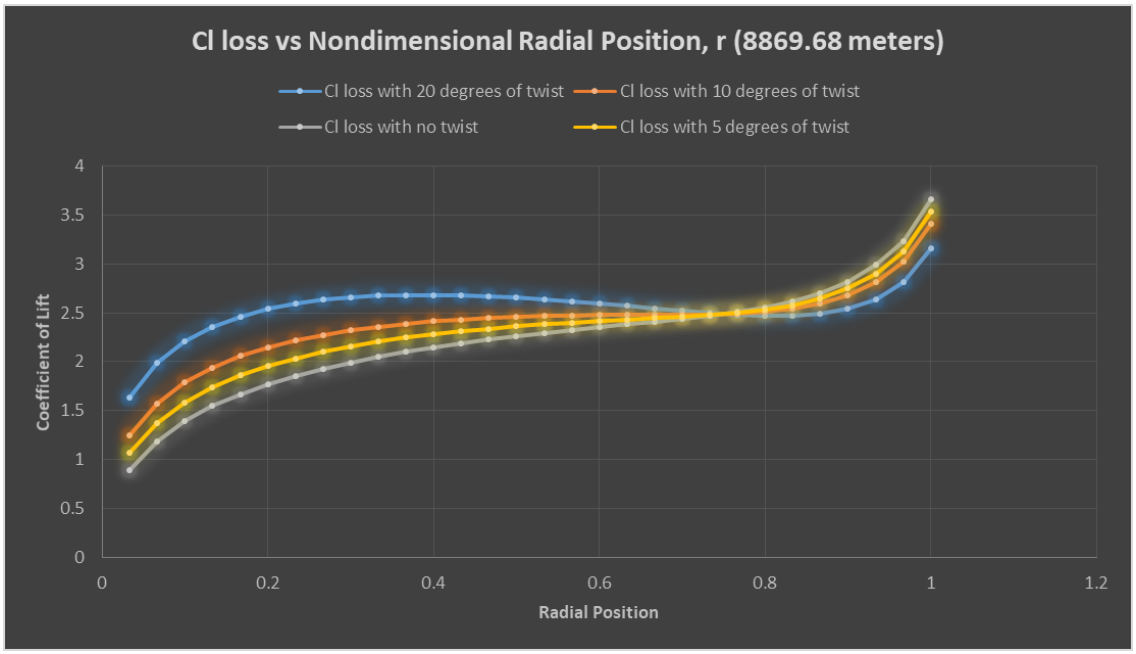

Figure D-23 Cl Loss vs Non-dimensional Radial Position, r (8869.68 meters)

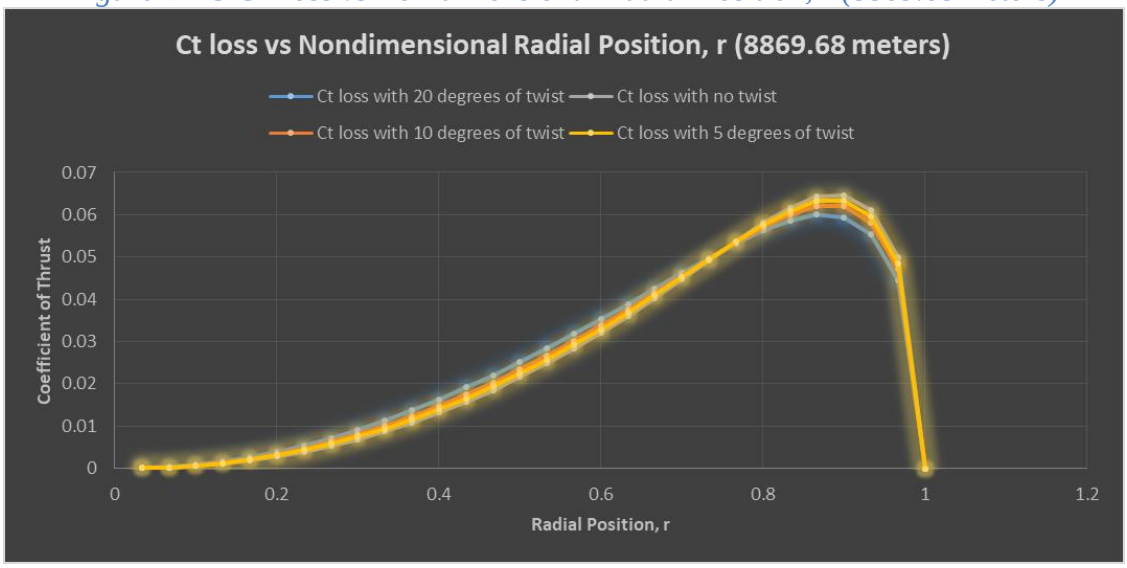

Figure D-24 Ct Loss vs Non-dimensional Radial Position, r (8869.68 meters)

Blade Design Three

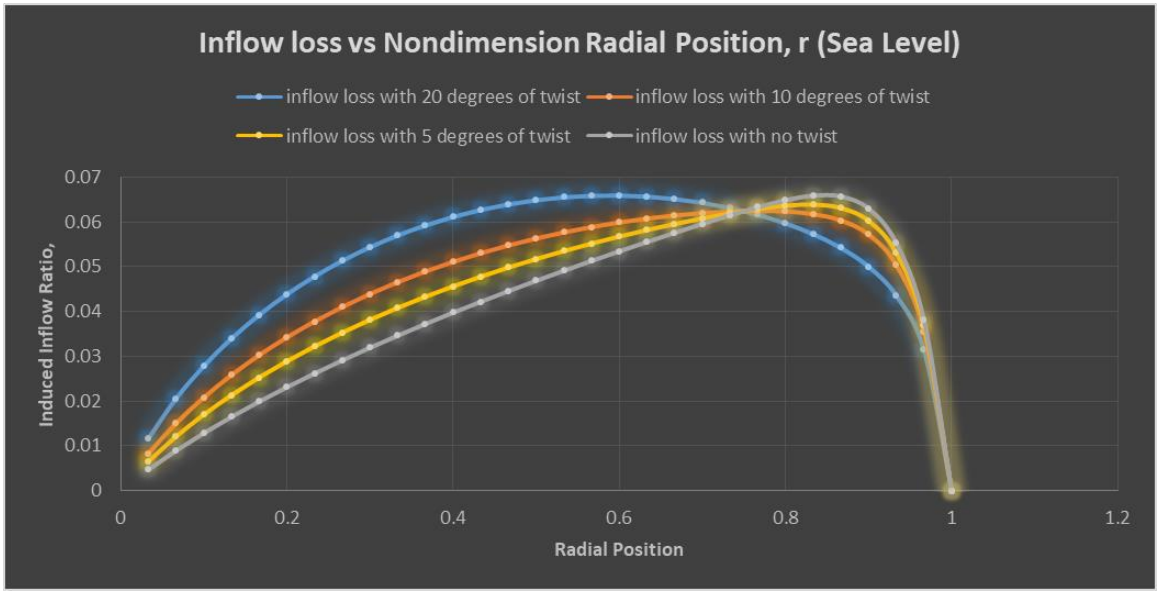

Figure D-25 Inflow Loss vs Non-dimensional Radial Position, r (Sea Level)

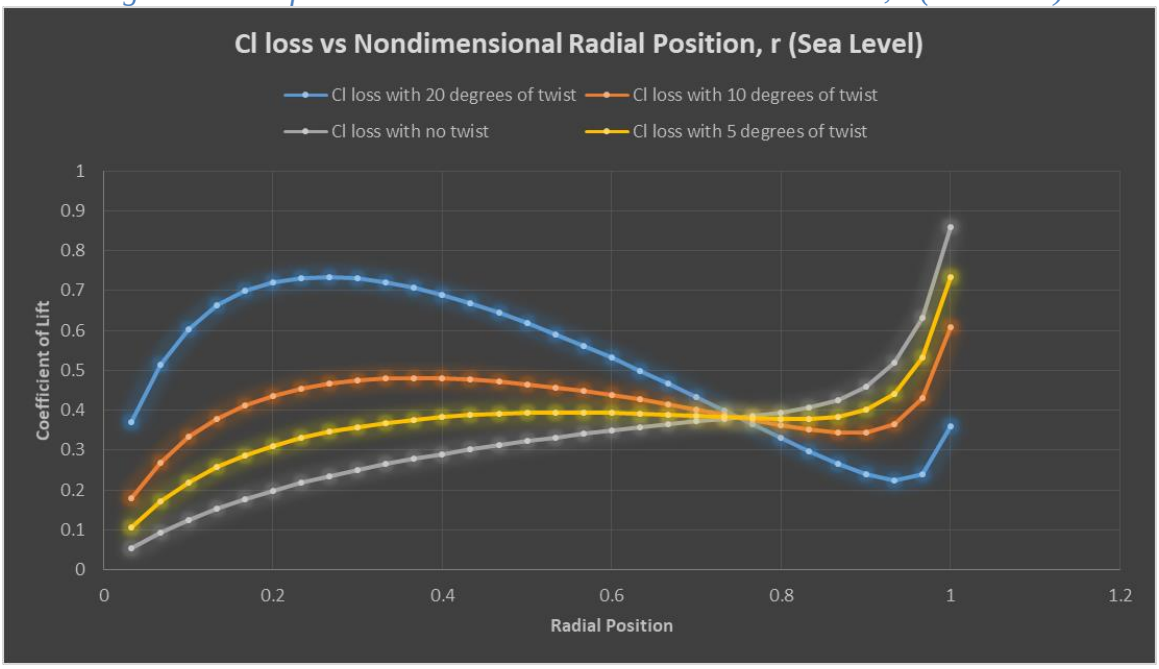

Figure D-26 Cl Loss vs Non-dimensional Radial Position, r (Sea Level)

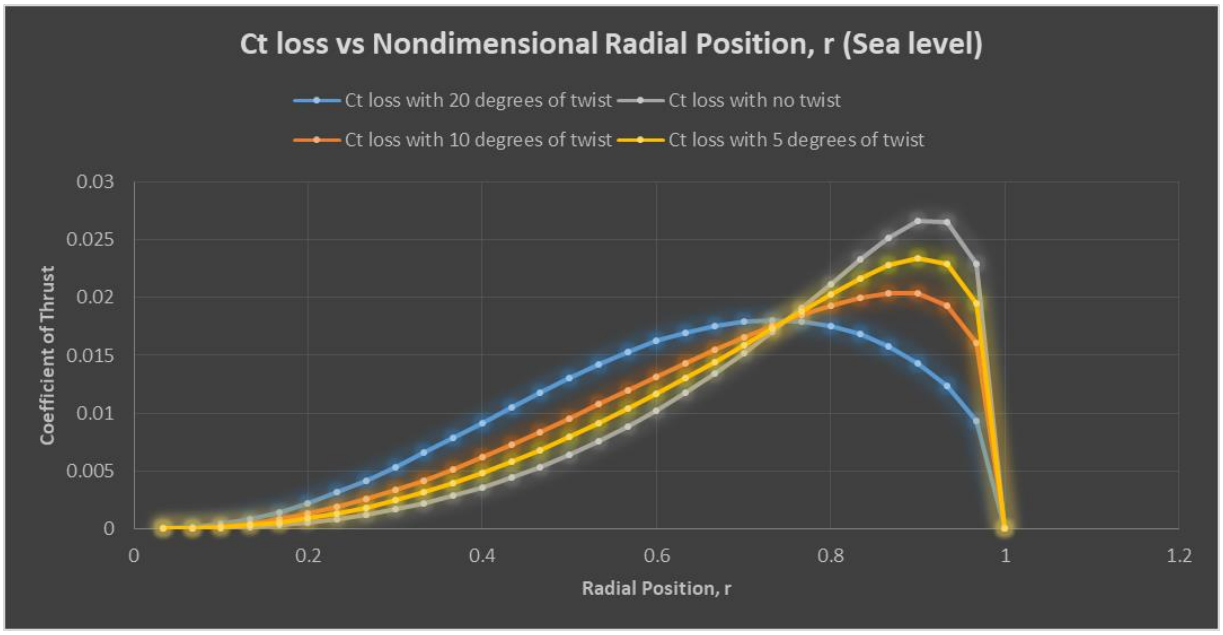

Figure D-27 Ct Loss vs Non-dimensional Radial Position, r (Sea Level)

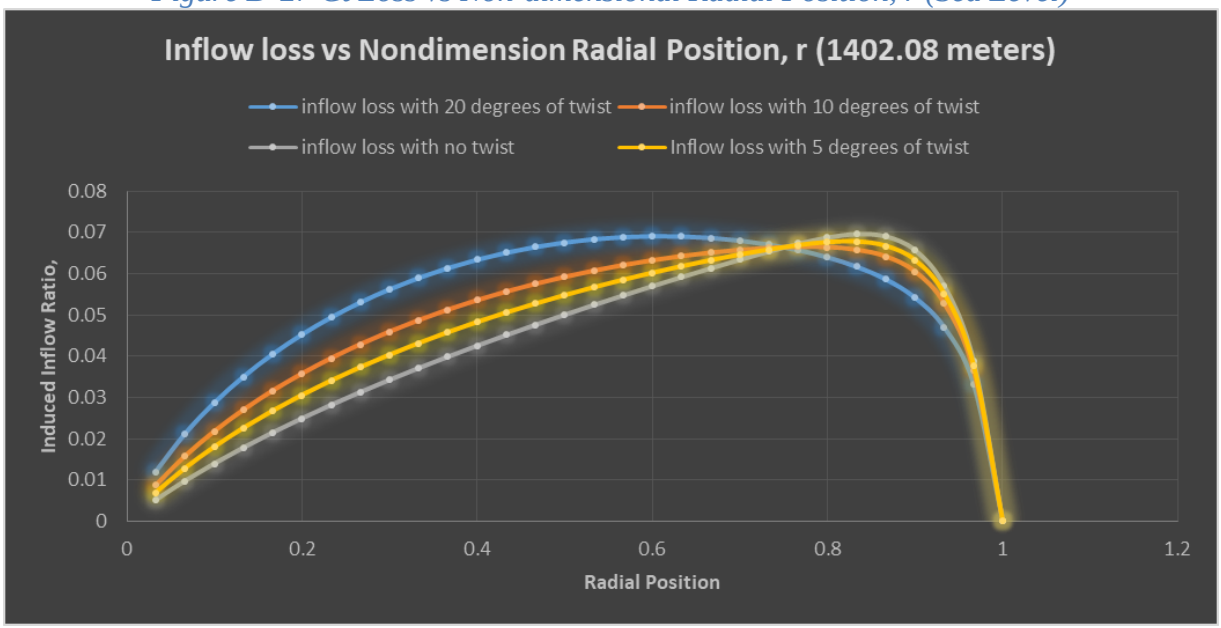

Figure D-28 Inflow Loss vs Non-dimensional Radial Position, r (1402.08 meters)

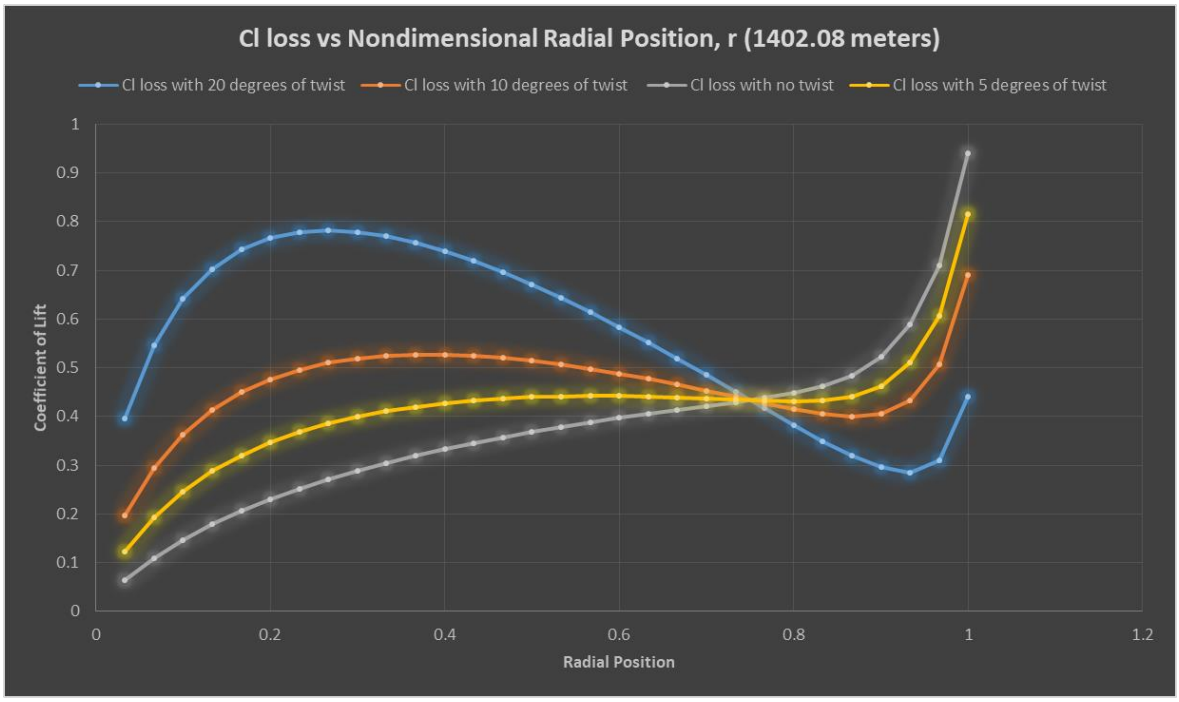

Figure D-29 Cl Loss vs Non-dimensional Radial Position, r (1402.08 meters)

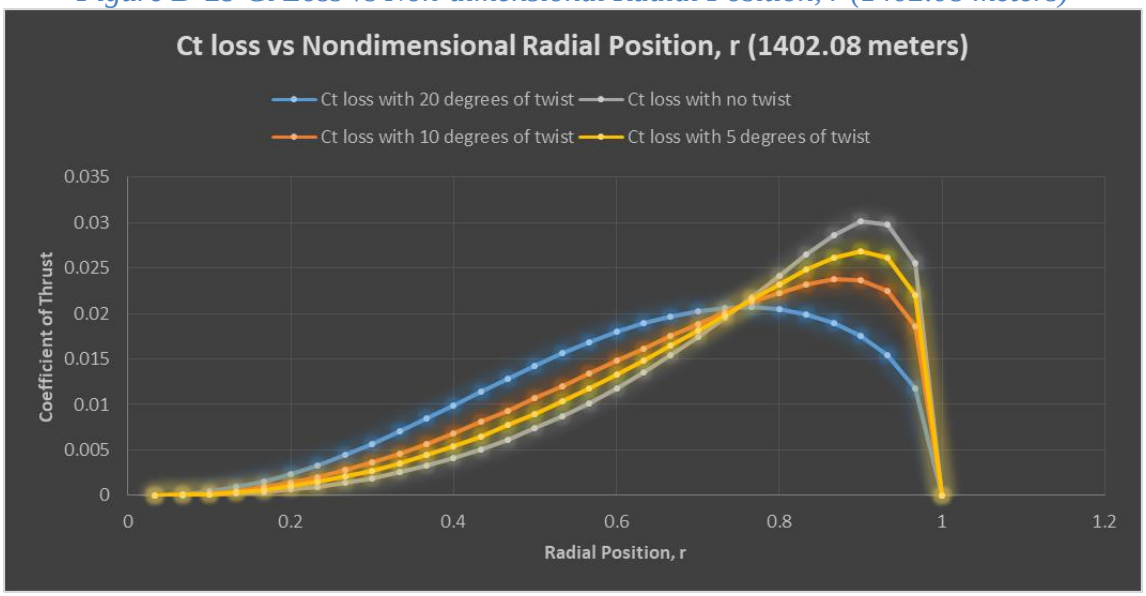

Figure D-30 Ct Loss vs Non-dimensional Radial Position, r (1402.08 meters)

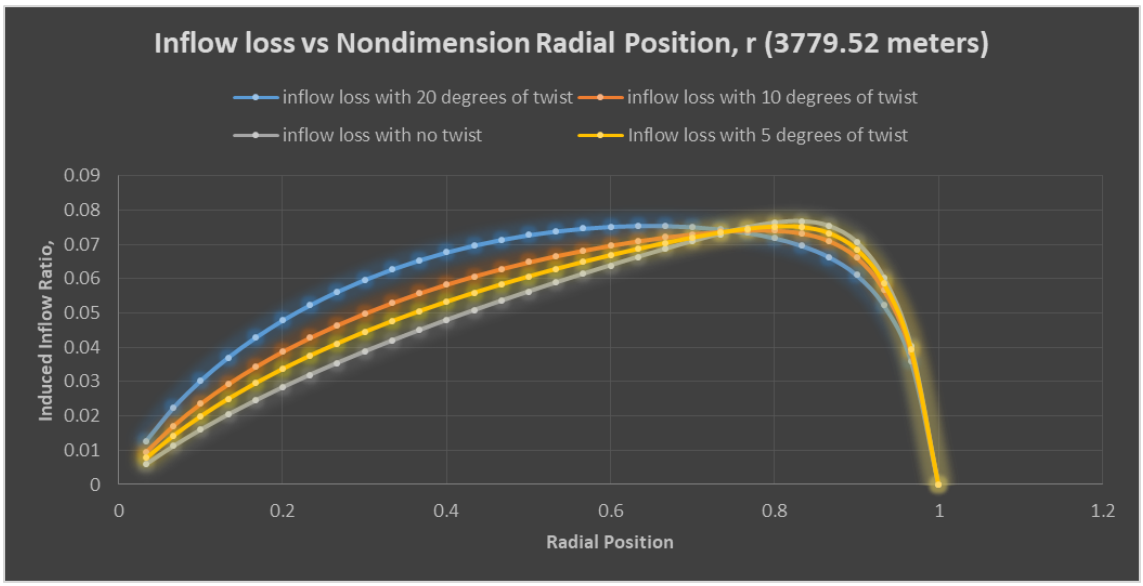

Figure D-31 Inflow Loss vs Non-dimensional Radial Position, r (3779.52 meters)

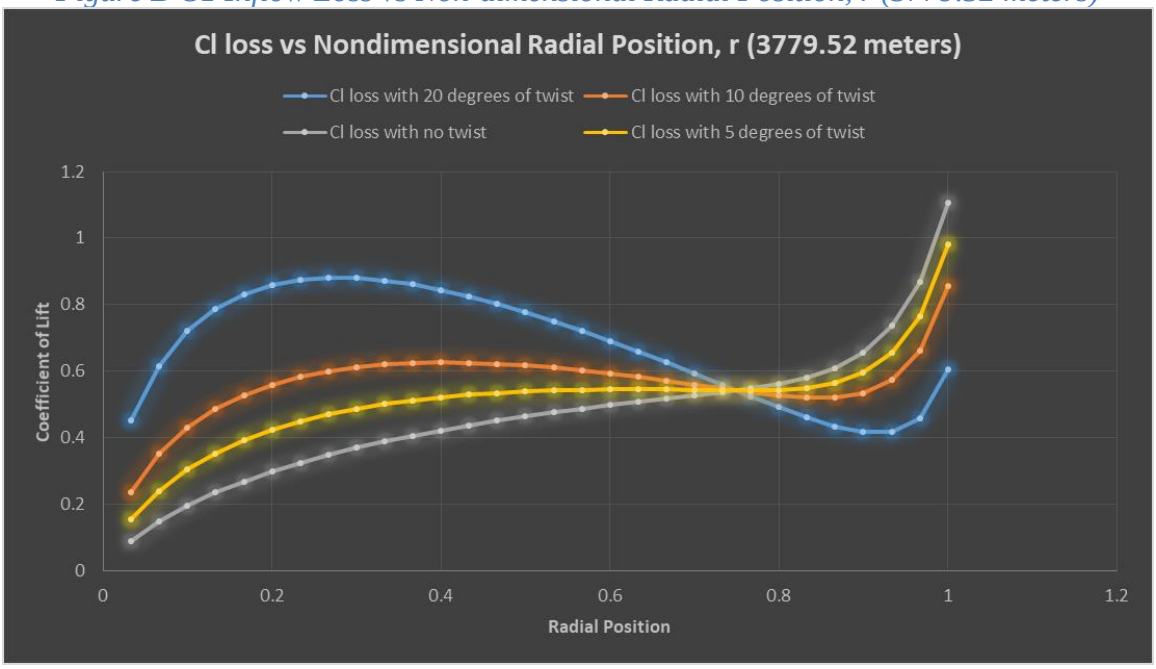

Figure D-32 Cl Loss vs Non-dimensional Radial Position, r (3779.52 meters)

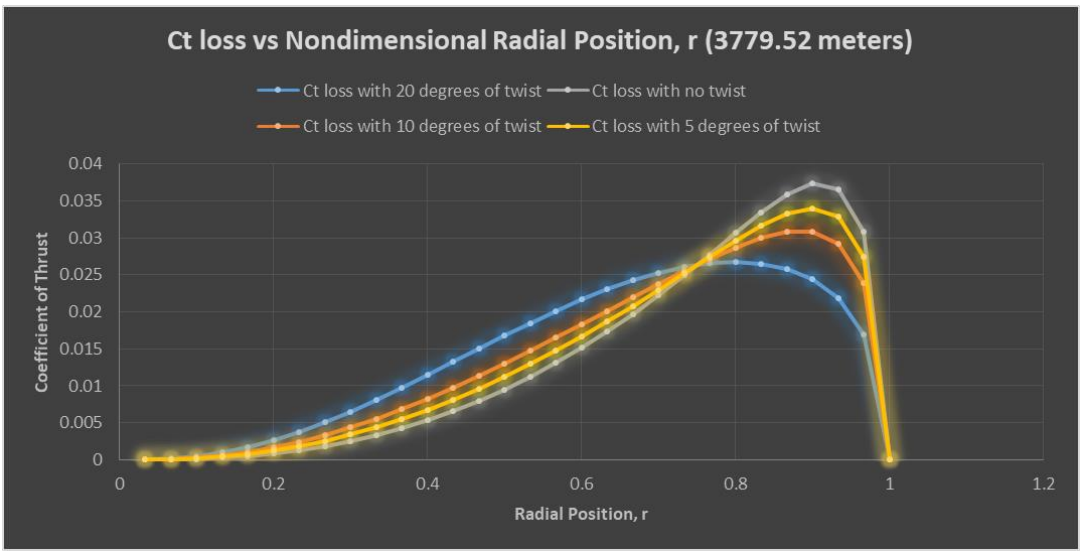

Figure D-33 Ct Loss vs Non-dimensional Radial Position, r (3779.52 meters)

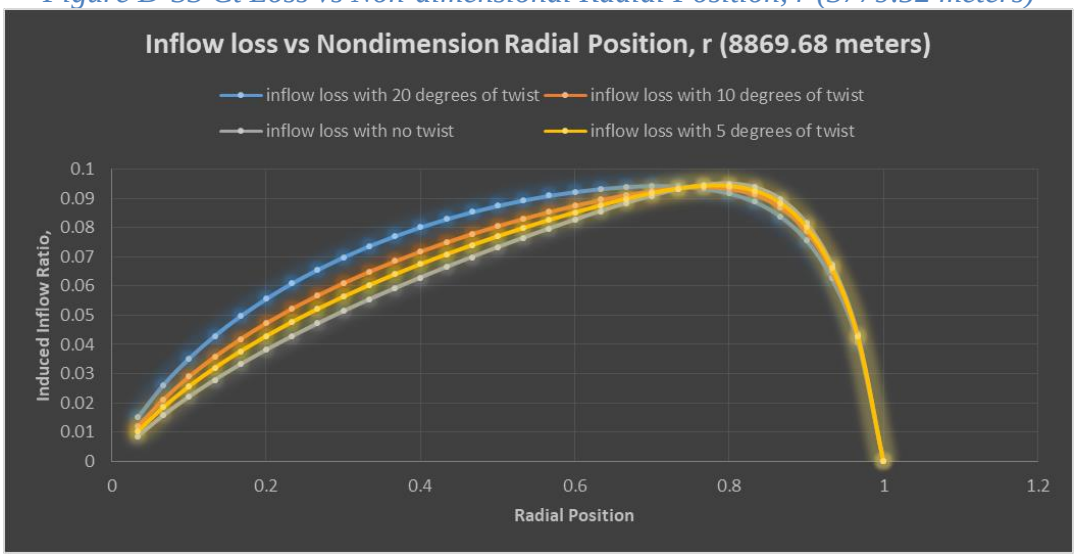

Figure D-34 Inflow Loss vs Non-dimensional Radial Position, r (8869.68 meters)

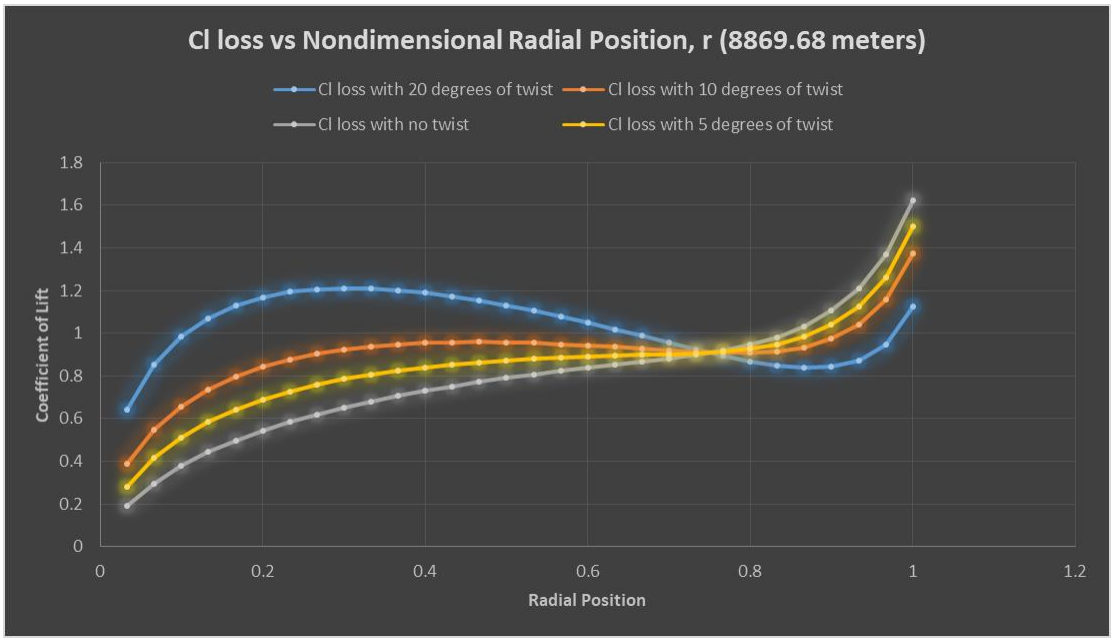

Figure D-35 Cl Loss vs Non-dimensional Radial Position, r (8869.68 meters)

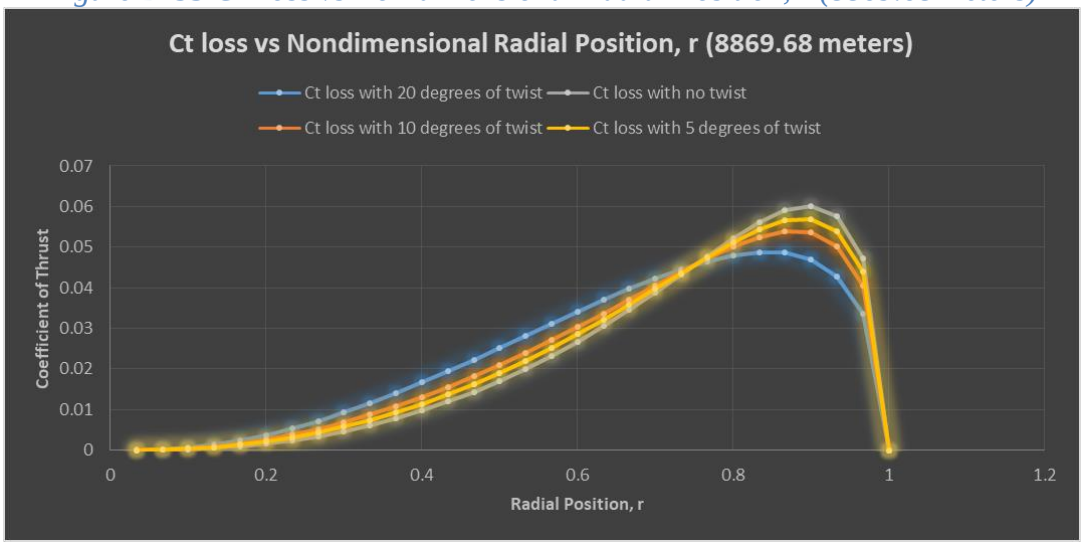

Figure D-36 Ct Loss vs Non-dimensional Radial Position, r (8869.68 meters)

Appendix E: Airfoil Graphs

Sikorsky SC 2110

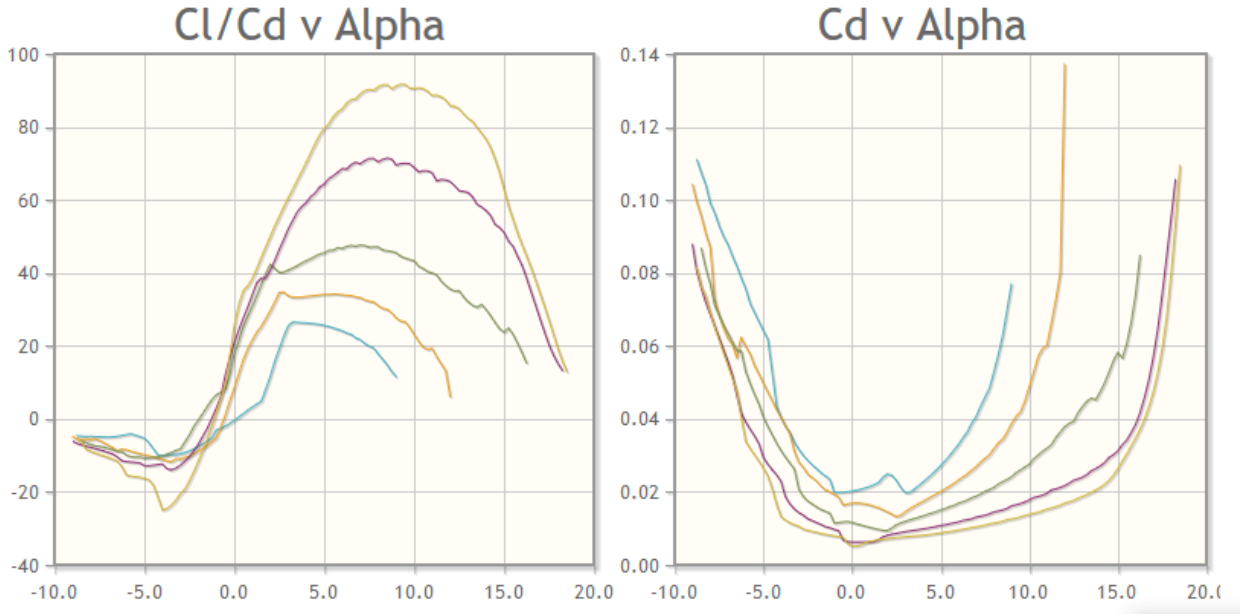

Figure E-37. Cl/Cd vs Alpha and Cd vs Alpha

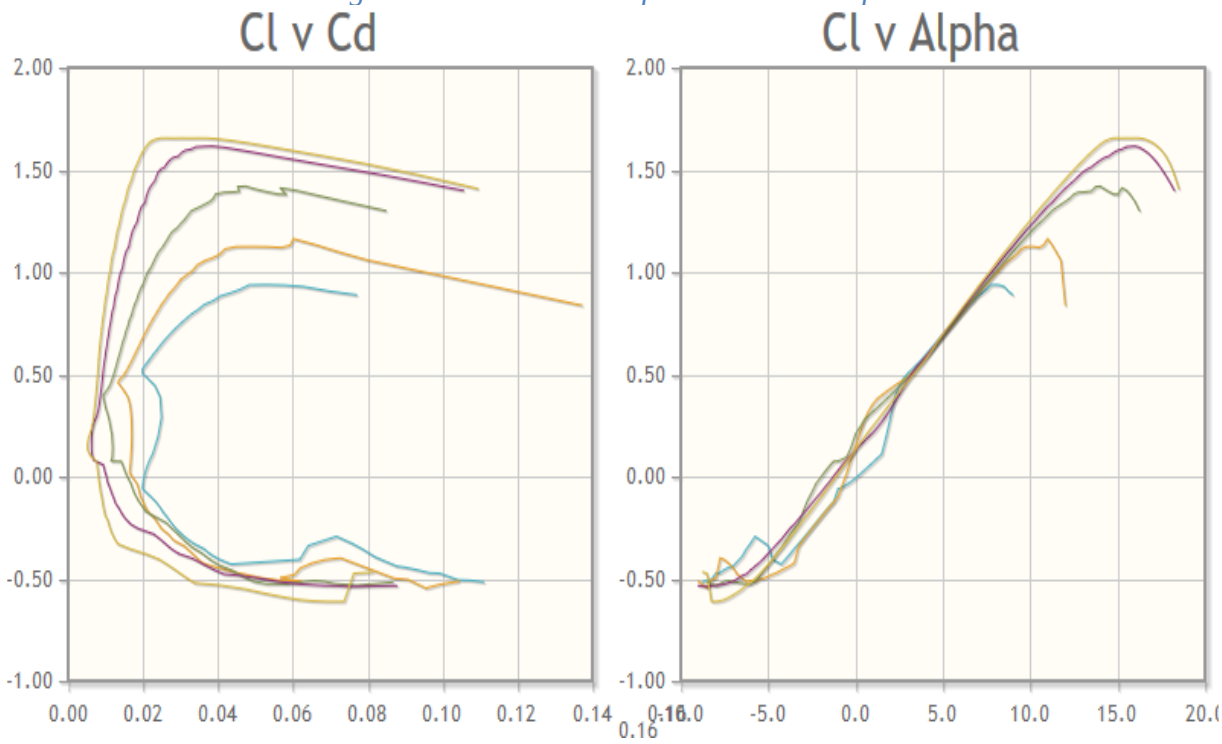

Figure E-38. Cl v Cd and Cl v Alpha

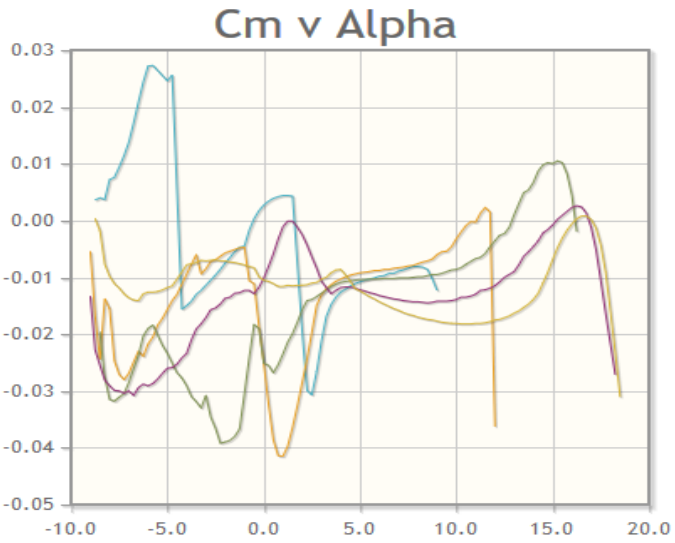

Figure E-39. Cm v alpha

Onera OA209

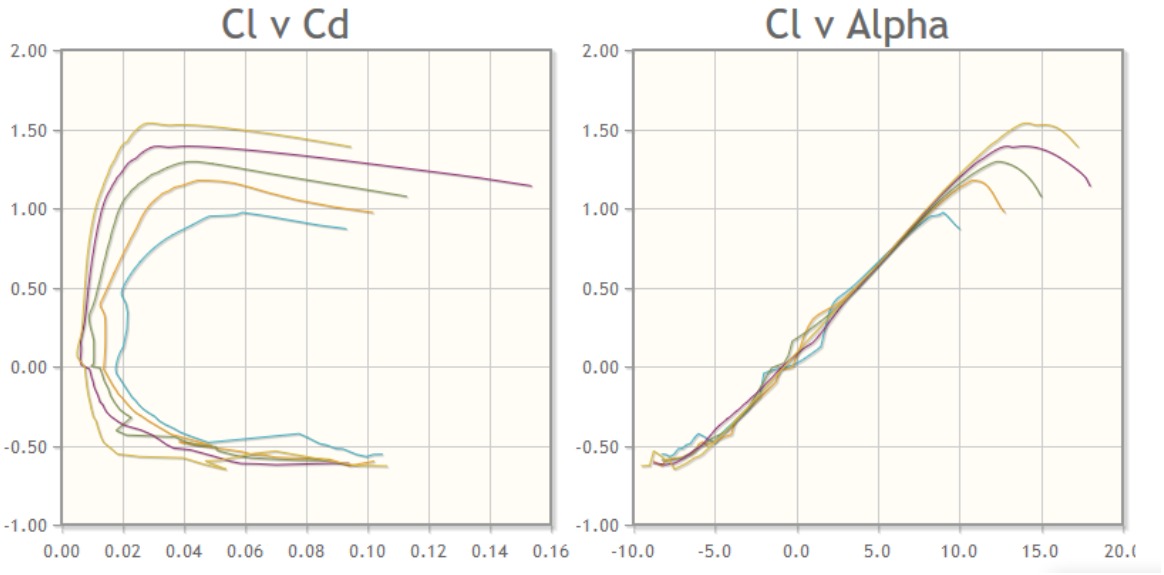

Figure E-40. Cl v Cd and Cl v alpha

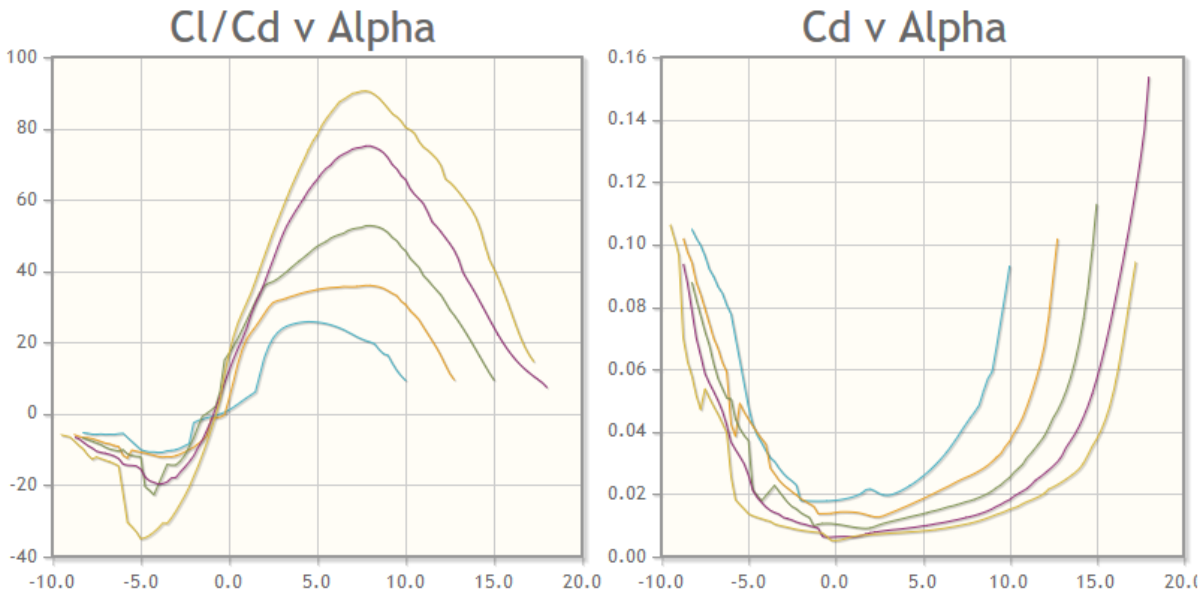

Figure E-41. Cl/Cd v Alpha and Cd v alpha

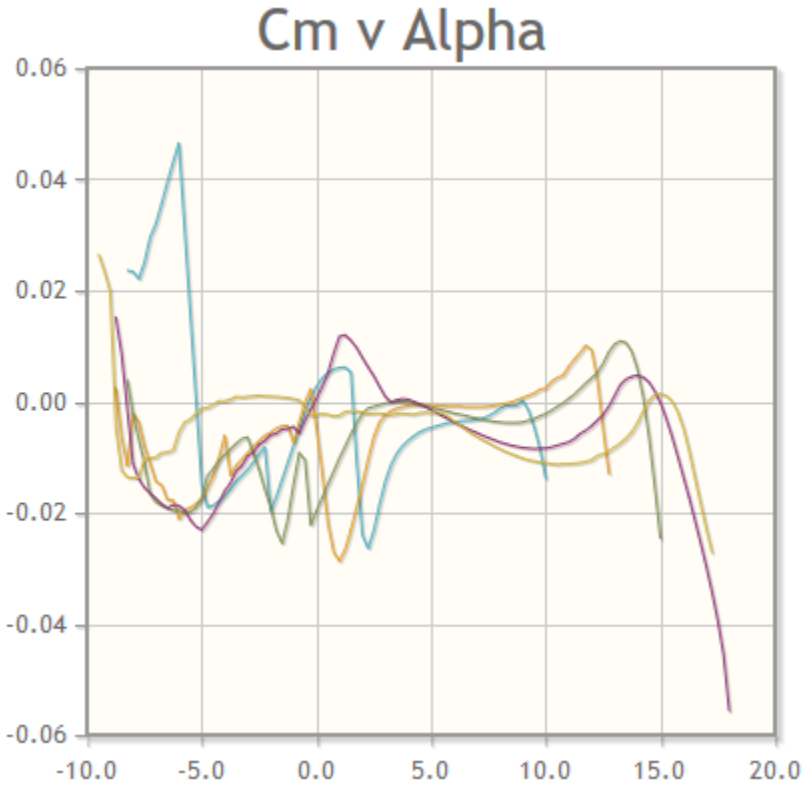

Figure E-42. Cm v alpha

NACA 63-015A

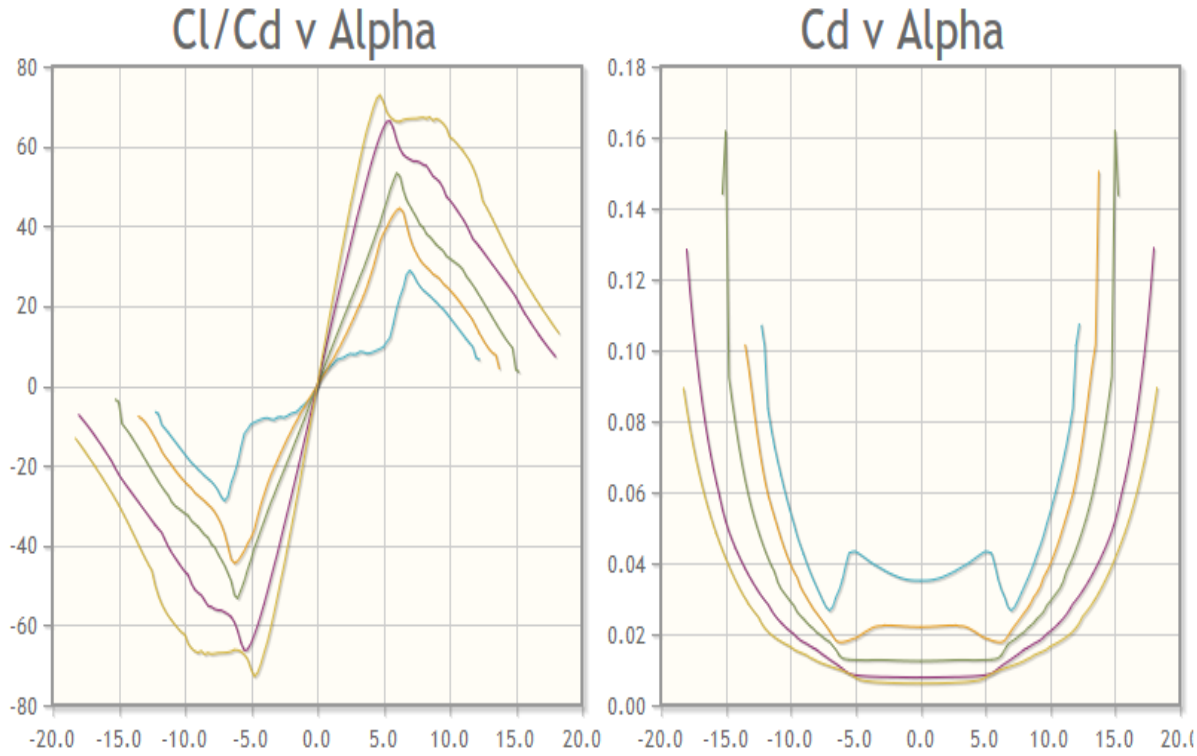

Figure E-43. Cl/Cd v Alpha and Cd v alpha

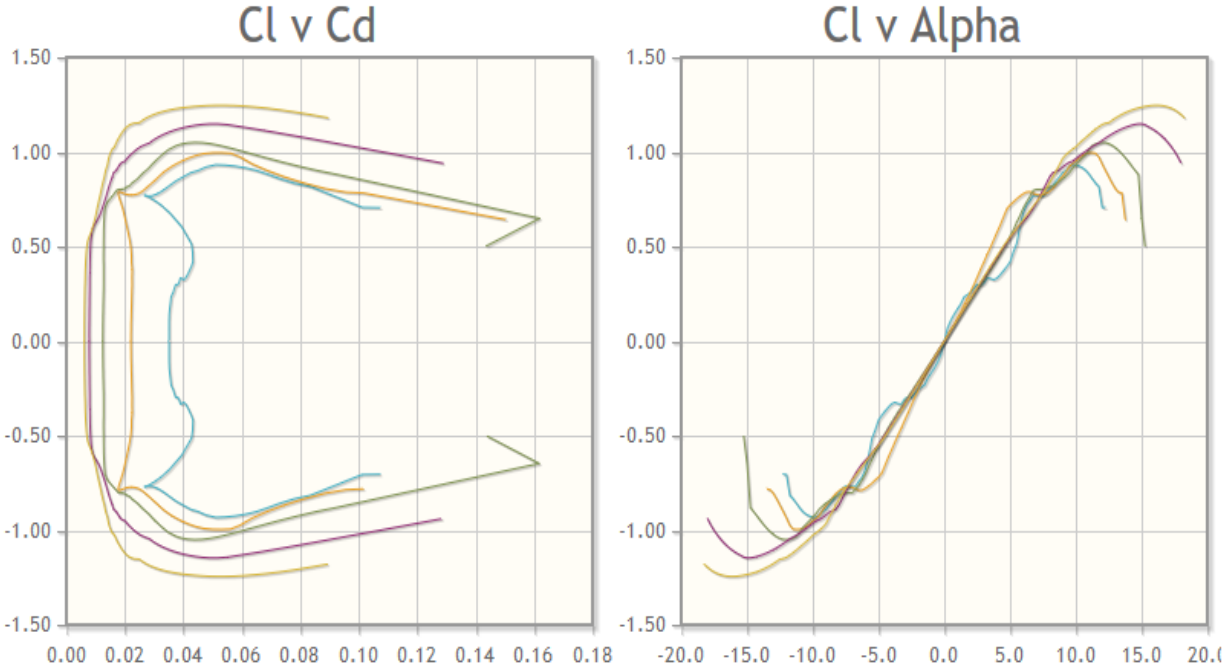

Figure E-44. Cl v Cd and Cl v alpha

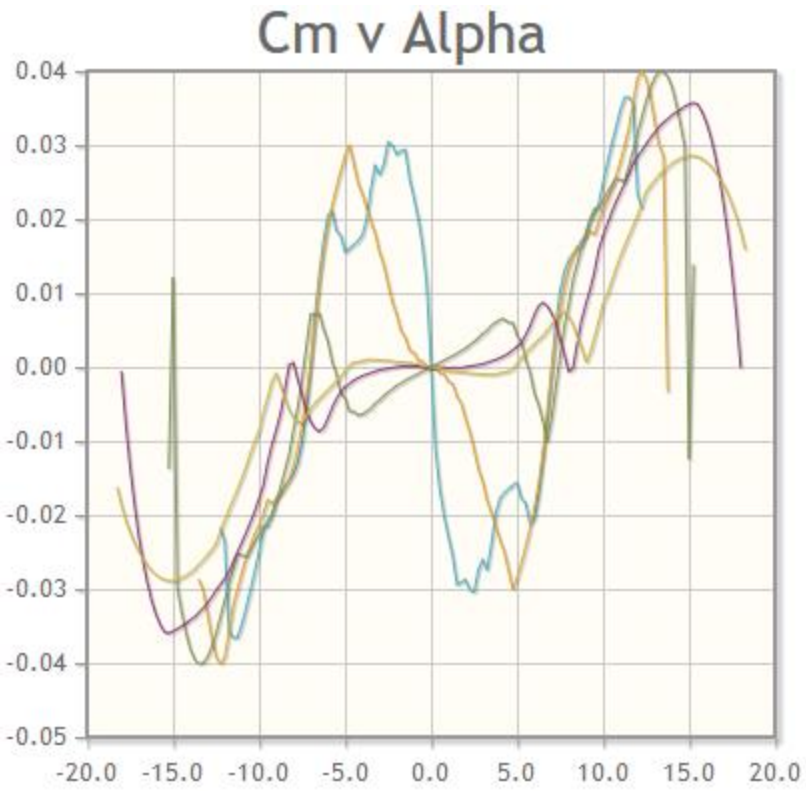

Figure E-45. Cm v alpha

Appendix F: Other Graphs and Figures

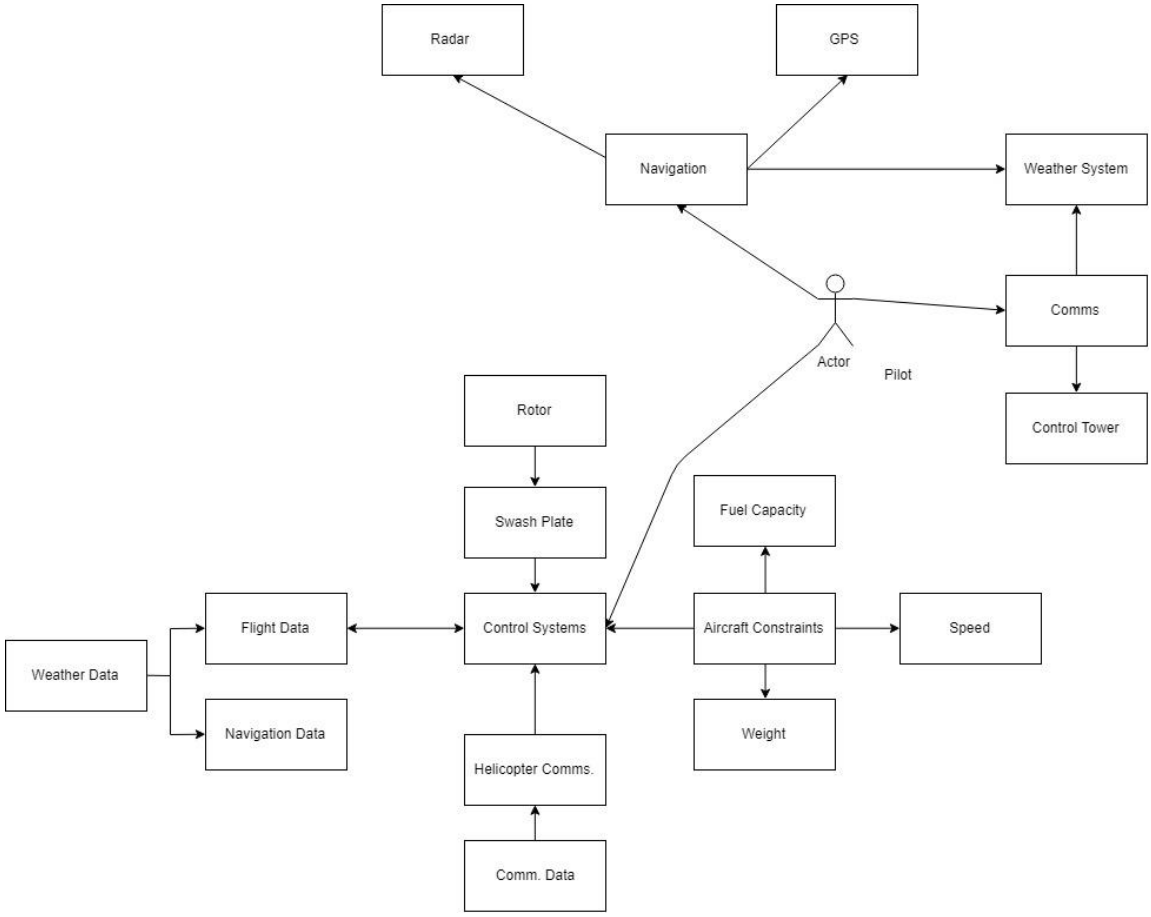

Figure F-46 UML Case Diagram